

https://dspace.org/

The generation of bone in nonhuman primates: experimental studies on the baboon

2015
http://hdl.handle.net/10539/19206

Downloaded from a DSpace repository. https://dspace.org/

THE GENERATION OF BONE IN NONHUMAN PRIMATES. EXPERIMENTAL STUDIES ON THE BABOON (*Papio ursinus*)

Ugo Ripamonti

A thesis submitted to the Faculty of Medicine, University of the Witwatersrand, Johannesburg, for the degree of Doctor of Philosophy

Johannesburg, 1993

TABLE OF CONTENTS

	Page
TABLE OF CONTENTS	i
DECLARATION	v
ACKNOWLEDGEMENTS	vi
PREFACE	ix
PUBLICATIONS	xvi
ABSTRACT	xvii

SECTION I

INTRODUCTION

1.	INTRODUCTION	1
2.	POSTFOETAL OSTEOGENESIS: BIOLOGICAL MECHANISMS OF BONE REPAIR AND REGENERATION	3
	2.1 The Induction of Bone and the Postfoetal Bone Differentiation Model: A Developmental Cascade	3
	2.2 Porous Hydroxyapatite as Alternative to Autogenous Bone Grafts	12
	2.3 Osteogenic Composites	17
	2.3 Calvarial Repair in Primates and Other Animals	20
3.	AIMS OF STUDY	30

SECTION II

MATERIALS AND METHODS

4. THE EXPERIMENTAL ANIMAL: THE BABOON (*Papio ursinus*) 33

4.1 Introduction 33

4.2 Selection of the Animals 34

4.3 Housing Conditions and Diets 35

5. THE HETEROTOPIC MODEL IN THE BABOON 37

5.1 Introduction 37

5.2 Preparation of the Allogeneic Diaphyseal Bone Matrix 38

5.3 Implants of Porous Hydroxyapatite 39

5.4 Operative Procedures and Intramuscular Implantation 40

5.5 Harvesting of Tissue and Histological Preparations 42

5.5.1 Preparation of Decalcified Sections 43

5.5.2 Preparation of Undecalcified Sections 44

5.6 Histological Analysis 45

5.7 Histomorphometric Analysis 47

5.8 Statistical Analysis 48

6. THE ORTHOTOPIC CALVARIAL MODEL IN THE BABOON 50

6.1 Introduction 50

6.2 Surgical Anatomy of the Adult Male Baboon Calvaria 51

6.3 Preparation of the Allogeneic Calvarial Bone Matrix 52

6.4 Implants of Porous Hydroxyapatite 54

6.5 Operative Procedures and Experimental Design 55

6.6 Harvesting of Tissue and Histological Preparations 57

6.6.1 Perfusion 57

6.6.2 Preparation of Decalcified Sections 58

6.6.3 Preparation of Undecalcified Sections 59

6.7 Histological Analysis 60

6.8 Histomorphometric Analysis 61

6.9 Histomorphometric Analysis of Control Baboon Calvariae 62

6.10 Statistical Analysis 64

SECTION III

RESULTS

7. THE HETEROTOPIC INTRAMUSCULAR STUDY 65

7.1 Morphology 65

7.2 Histomorphometry 74

8. THE ORTHOTOPIC CALVARIAL STUDY 77

8.1 Morphology of Calvarial Repair 77

8.1.1 Untreated Calvarial Defects 77

8.1.2 Autogenous Bone Grafts 77

8.1.3 Allogeneic Calvarial Bone Matrix 78

8.1.4 Porous Hydroxyapatite Implants 79

8.2 Histomorphometry 80

9. FIGURES 85

10. TABLES 137

SECTION IV

DISCUSSION

11. THE HETEROTOPIC INTRAMUSCULAR STUDY 150

11.1 The Induction of Bone with Autolysed Antigen-Extracted Allogeneic Bone Matrix 150

11.2 The Hydroxyapatite-Induced Osteogenesis Model 157

11.3 The Induction of Bone in Osteogenic Composites of Bone Matrix and Porous Hydroxyapatite 170

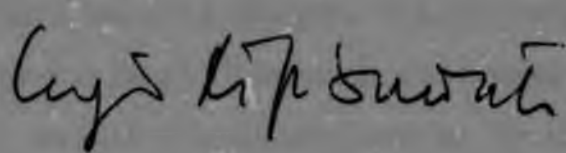
12. THE ORTHOTOPIC CALVARIAL STUDY 175

LIST OF REFERENCES 193

DECLARATION

I, Ugo Ripamonti, hereby declare that this thesis is my own work and has not been presented for any degree of another university.

The work reported in this thesis was performed while I was recipient of a Medical Research Council Scholarship for Visiting Foreign Scientists and then while I was employed by the South African Medical Research Council as Chief Medical Researcher in the Dental Research Institute.



Ugo Ripamonti

AKCNOWLEDGEMENTS

The following persons have been instrumental in the generation of this thesis:

Professor Peter Cleaton-Jones, Director of the Dental Research Institute, who, as supervisor and mentor in the past years, has made available tc me the right environment for my research studies, and has provided continuous support, invaluable critical advice and inspirational scientific insight.

Professor Christine Schnitzler, Head, Department of Orthopaedic Surgery, Baragwanath Hospital, who, as co-supervisor of this thesis, has provided me with invaluable teaching, critical advice and new insights into the bone-bone marrow organ.

Miss Barbara van den Heever, Senior Medical Technologist, Dental Research Institute, for her patience, skills and determination in the preparation of outstanding decalcified and undecalcified sections, as well as continuous help during animal experimentation.

Professor Paul Fatti, Head, Department of Statistics and Actuarial Science, University of the Witwatersrand, Johannesburg, for his expert advice on the experimental design and statistical analysis.

Doctor Maeve Coogan, Department of Oral Pathology, University of the Witwatersrand, Johannesburg, for her continuous support and invaluable help with equipment and the microbiological analysis.

Sisters Ilsa van den Merwe and Janet Willemberg, Central Animal Service, Medical School, University of the Witwatersrand, Johannesburg, for their professional help with the animal experiments.

Miss Janice van Wyk, Senior Medical Technologist, Dental Research Institute, for her constant help with biochemistry, photography and numerous other tasks.

Doctor Edwin Shors, Vice-President, Research and Development, Interpore International, California, for the preparation of the porous hydroxyapatite implants.

Special thanks go to Doctor A. Hari Reddi, Professor of Biological Chemistry and Director, Laboratory of Musculoskeletal Cell Biology, the Johns Hopkins University School of Medicine, for the many hours spent in different parts of the world discussing together bone induction and many other topics.

This research was possible through the financial support of the following granting bodies:

The South African Medical Research Council,
the University of the Witwatersrand, Johannesburg,
the Medical Faculty Research Endowment Fund,
and Elida-Gibbs (South Africa) Pty. Ltd.

PREFACE

Over decades of interest in bone physiology, no single concept has captured the imagination to a greater degree than the phenomenon of bone formation by induction. For the material presented in this thesis is also the result of the writer's passion for this fascinating aspect of bone cell biology.

The origins of this research lie in the studies of Huggins, Urist, Reddi and others who first used biological assays to study the bone inductive properties of the extracellular matrix of bone and other tissues, including tooth matrix and uroepithelium, and then stimulated many groups to contribute a continuous growing knowledge of the cellular and molecular signals involved in endochondral bone differentiation.

A critical issue that prompted this study in 1986 was the desire to gather information concerning bone induction in adult primates as a prerequisite for potential therapeutic applications in man. The material presented in this thesis must now be viewed in historical perspective, since in the past 4 years we have witnessed an explosion of information on the molecular and cellular basis of bone induction. The fundamental work of Urist and Reddi has provided evidence for the existance of a bone morphogenetic protein complex within the bone matrix [1-5]. Until recently, however, it was unclear whether the bone forming activity in demineralized bone matrix was due to the combined action of several factors known to be present in bone, or to a separate protein, or family of proteins, as yet to be characterized and sequenced.

Since the beginning of this study, native bone morphogenetic proteins (BMPs) were firstly isolated from bovine bone matrix, and purified in sufficient quantity and purity to provide amino acid sequence information [6-8]. Based on these data, full-length complementary DNA (cDNA's) clones were isolated, encoding the human equivalent of seven BMPs [9-11]. Expression of the recombinant human proteins with confirmation of their osteogenic activity in the

ectopic bioassay has now been obtained for BMP-2 through BMP-7 [12-14]. This has laid the foundation for the cellular and molecular dissection of bone development, and has dramatically confirmed, as Marshall Urist once wrote, the "Reality of a Nebulous Enigmatic Myth".

Yet, the activity of BMPs is not merely confined to bone development. Significantly, the BMPs are members of an extensive family of highly conserved, secreted proteins that have potent effects on differentiation, axis formation, growth control, and sexual development in many organisms (the transforming growth factor-ß [TGF-ß] gene superfamily). Of the seven BMPs that have been characterized, six show sequence homology with other members of the TGF-ß superfamily [9-11], including, amongst others, the decapentaplegic (*dpp*) and *60A* genes of *Drosophila melanogaster*, involved in dorsal-ventral specification.

The striking evolutionary conservation of the BMP genes indicates that they are critical in the normal development and function of animals. Thus, in addition to postfoetal osteogenesis, the BMPs play multiple roles in embryonic development, including skeletogenesis, and are involved in inductive events unrelated to bone induction that control pattern formation during embryonic organogenesis [15-21]. This suggests that a phylogenetically ancient signalling process, used in dorsal-ventral patterning in the fly, may also operate to produce an unique vertebrate trait such as bone differentiation [22].

The fact that BMP-2 through -7 singly initiate *de novo* endochondral bone formation raises an important question about the biological relevance of this redundancy. Moreover, the high levels of homology between *dpp* and *60A* genes in *Drosophila* with human BMP-2, -4, and BMP-5, -6, and -7 respectively, raises further questions about the primordial role of BMPs during the emergence and development of invertebrates. Because of a possible evolutionary and functional conservation of these genes, they might have retained common developmental roles [23]. This is supported by the results of an elegant study showing that human BMP-4 sequences can rescue and confer normal dorsal-ventral patterning in the *Drosophila* embryo in lieu of the *dpp* gene product [24]. Perhaps the most compelling evidence that

these genes have been conserved for at least 600 million years is the exciting observation that recombinant *Drosophila* proteins, DPP and 60A, have the capacity to induce endochondral bone formation in mammals using the rat subcutaneous assay [25].

The data which originated from this thesis have been published in previous years. Clearly, the methodology reported in this thesis to achieve bone induction in nonhuman primates is now technologically surpassed. The merit of this research effort, however, was the creation of a primate model that proved to be reproducible and invaluable for further investigations using increasingly purified BMP preparations [26-29]. This continuous research effort to study bone induction in primates has culminated in the use of the model to test the efficacy of osteogenin, a bone morphogenetic protein (BMP-3), purified to apparent homogeneity from baboon bone matrix, and one of the human recombinant BMPs. The results of these studies have clearly indicated that novel bone replacement therapies are now close at hand for clinical trials.

The discovery of bone formation in porous hydroxyapatites implanted extraskeletally in adult baboons, as described in this thesis, has indicated that BMPs may be circulating or locally produced. This has stimulated further studies using the same animal model to investigate potential porous carriers as delivery system for BMPs. This body of work has suggested that this endogenously regulated mechanism of bone formation may be exploited to construct delivery systems with defined geometries and surface characteristics for bone replacement therapies [30-34].

It was during a warm African night almost 7 years ago that the writer spoke on a long distance phone call with Doctor Marshall Urist, discussing with him bone induction in baboons. To the writer, these years spent investigating the induction of bone in primates have been the source of an unforgettable experience: for the privilege of having known and discussed this fascinating field with world authorities, and for the privilege of having worked on nonhuman primates.

References

1. Urist MR. Bone: Formation by autoinduction. Science 159: 893, 1965

2. Urist MR, Strates BS. Bone morphogenetic protein. J Dent Res (suppl 6) 50: 1392, 1971

3. Urist MR, Huo Y-K, Brownell AG, Hohl WM, Buyske J, Lietze A, Tempst P, Hunkapiller M, DeLange RJ. Purification of bone morphogenetic protein by hydroxyapatite chromatography. Proc Natl Acad Sci USA 81: 371, 1984

4. Reddi AH, Huggins CB. Biochemical sequences in the transformation of normal fibroblasts in adolescent rats. Proc Natl Acad Sci USA 69: 1601, 1972

5. Sampath TK, Reddi AH. Dissociative extraction and reconstitution of extracellular matrix components involved in local bone differentiation. Proc Natl Acad Sci USA 78: 7599, 1981

6. Wang EA, Rosen V, Cordes P, Hewick RM, Kriz MJ, Luxenberg DP, Sibley BS, Wozney JM. Purification and characterization of other distinct bone-inducing factors. Proc Natl Acad Sci USA 85: 9484, 1988

7. Luyten FP, Cunningham NS, Ma S, Muthukumaran N, Hammonds RG, Nevins WB, Wood WI, Reddi AH. Purification and partial amino acid sequence of osteogenin, a protein initiating bone differentiation. J Biol Chem 264: 13377, 1989

8. Sampath TK, Coughlin JE, Whetstone RM, Banach D, Corbett C, Ridge RJ, Ozkaynak E, Oppermann H, Rueger DC. Bovine osteogenic protein is composed of dimers of OP-1 and BMP-2A, two members of the transforming growth factor β superfamily. J Biol Chem 265: 13198, 1990

9. Wozney JM, Rosen V, Celeste AJ, Mitsock LM, Whitters, MJ, Kriz RW, Hewick RM, Wang EA. Novel regulators of bone formation: Molecular clones and activities. Science 242: 1528, 1988

10. Ozkaynak E. Rueger DC, Drier EA, Corbett C, Ridge RJ, Sampath TK, Oppermann H. OP-1 cDNA encodes an osteogenic protein in the TGF-ß family. EMBO J. 9: 2085, 1990

11. Celeste AJ, Iannazzi JM, Taylor, RC, Hewick RM, Rosen V, Wang EA, Wozney JM. Identification of transforming growth factor ß family members present in bone-inductive protein purified from bovine bone. Proc Natl Acad Sci USA 87: 9843, 1990

12. Wang EA, Rosen V, D'Alessandro JS, Bauduy M, Cordes P, Harada T, Israel D, Hewick RM, Kerns K, LaPan P, Luxenberg DP, McQuaid D, Moutsatsos I, Nove J, Wozney JM. Recombinant human bone morphogenetic protein induces bone formation. Proc Natl Acad Sci USA 87: 2220, 1990

13. Hammonds RG, Schwall R, Dudley A, Berkemeier L, Lai C, Lee J, Cunningham N, Reddi AH, Wood WI, Mason AJ. Bone inducing activity of mature BMP-2b produced from a hybrid BMP-2a/2b precursor. Mol Endocrinol 5: 149, 1991

14. Sampath TK, Maliakal JC, Hauschka PV, Jones WK, Sasak A, Tucker RF, White KH, Coughlin JE, Tucker MM, Pang RHL, Corbett C, Ozkaynak E, Oppermann E, Rueger DC. Recombinant human osteogenic protein-1 (hOP-1) induces new bone formation in vivo with a specific activity comparable with natural bovine osteogenic protein and stimulates osteoblast proliferation and differentiation in vivo. J Biol Chem 267: 20352, 1992

15. Lyons KM, Pelton RW, Hogan BLM. Patterns of expression of murine Vgr-1 and BMP-2a RNA suggest that transforming growth factor-ß-like genes coordinately regulate aspects of embryonic development. Genes Dev 3: 1657, 1989

16. Lyons KM, Pelton RW, Hogan BLM. Organogenesis and pattern formation in the mouse: RNA distribution patterns suggest a role for bone morphogenetic protein-2A (BMP-2A). Development 109: 833, 1990

17. Jones MC, Lyons KM, Hogan BLM. Involvement of Bone Morphogenetic Protein-4 (BMP-4) and Vgr-1 in morphogenesis and neurogenesis in the mouse Development 111: 531, 1991

18. Dale L. Howes G, Price BMJ, Smith JC. Bone morphogenetic protein 4: a ventralizing factor in Xenopus development. Development 115: 573, 1992

19. Vukicevic S, Paralkar VM, Cunningham NS, Gutkind JS, Reddi AH. Autoradiographic localization of osteogenin binding sites in cartilage and bone during rat embryonic development. Dev Biol 140: 209, 1990

20. Paralkar VM, Weeks BS, Yu MY, Kleinman HK, Reddi AH. Recombinant human bone morphogenetic protein 2B: Stimulation of neuronal differentiation in PC12 cells and modulation by binding to type IV collagen. J Cell Biol 119: 1721, 1992

21. Kingsley DM, Bland AE, Grubber JM, Marker PC, Russell LB, Copeland NG, Jenkins NA. The mouse short ear skeletal morphogenesis locus is associated with defects in a bone morphogenetic member of the TGF-ß superfamily. Cell 71: 399, 1992

22. Shimell MJ, Ferguson EL, Childs SR, O'Connor MB. The drosophila dorsal-ventral patterning gene tolloid is related to human bone morphogenetic protein 1. Cell 67: 469, 1991

23. Wharton KA, Thomsen GH, Gelbart WM. Drosophila 60A gene, another transforming growth factor ß family member, is closely related to human bone morphogenetic proteins. Proc Natl Acad Sci USA 88: 9214, 1991

24. Padgett RW, Wozney JM, Gelbart WM. Human BMP sequences can confer normal dorsal-ventral patterning in the drosophila embryo. Proc Natl Acad Sci USA 90: 2905, 1993

25. Sampath TK, Rashka KE, Doctor JS, Tucker RF, Hoffmann FM. Drosophila TGF-ß superfamily proteins induce endochondral bone formation in mammals. Proc Natl Acad Sci USA 1993, in press

26. Ripamonti U, Magan A, Ma S, van den Heever B, Moehl T, Reddi AH. Xenogeneic osteogenin, a bone morphogenetic protein, and demineralized bone matrices, including human, induce bone differentiation in athymic rats and baboons. Matrix 11: 404, 1991

27. Ripamonti U, Ma S, van den Heever B, Reddi AH. Osteogenin, a bone morphogenetic protein, adsorbed on porous hydroxyapatite substrata induces rapid bone differentiation in calvarial defects of adult primates. Plast Reconstr Surg 90: 382, 1992

28. Ripamonti U, Ma S, Cunningham N, Yeates L, Reddi AH. Reconstruction of the bone-bone marrow organ by osteogenin, a bone morhogenetic protein, and demineralized bone matrix in calvarial defects of adult primates. Plast Reconstr Surg 91: 27, 1993

29. Ripamonti U, Ma S, Cunningham N, Yeates L, Reddi AH. Initiation of bone regeneration in adult baboons by osteogenin, a bone morphogenetic protein. Matrix 12: 369, 1992

30. Ripamonti U, Ma S, Reddi AH. Induction of bone in composites of osteogenin and porous hydroxyapatite in baboons. Plast Reconstr Surg 89: 731, 1992

31. Ripamonti U, Ma S, Reddi AH. The critical role of geometry of porous hydroxyapatite delivery system in induction of bone by osteogenin, a bone morphogenetic protein. Matrix 12: 202, 1992

32. Ripamonti U, Yeates L, van den Heever B. Initiation of heterotopic osteogenesis in primates after chromatographic adsorption of osteogenin, a bone morphogenetic protein, onto porous hydroxyapatite. Biochem Biophys Res Commun 193: 509, 1993

33. Ripamonti U, van den Heever B, van Wyk J. Expression of the osteogenic phenotype in porous hydroxyapatite implanted extraskeletally in baboons. Matrix 1993, in press

34. van Eeden S, Ripamonti U. Bone differentiation in porous hydroxyapatite in baboons is regulated by the geometry of the substratum: Implications for reconstructive craniofacial surgery. Plast Reconstr Surg 1993, in press

The following publications have arisen from material presented in this thesis:

Ripamonti U. Bone induction in nonhuman primates. An experimental study on the baboon (*Papio ursinus*). Clinical Orthopaedics and Related Research 269: 284-294, 1991

Ripamonti U. The morphogenesis of bone in replicas of porous hydroxyapatite obtained from conversion of calcium carbonate exoskeletons of coral. Journal of Bone and Joint Surgery 73-A: 692-703, 1991

Ripamonti U. The induction of bone in osteogenic composites of bone matrix and porous hydroxyapatite replicas: An experimental study on the baboon (*Papio ursinus*). Journal of Oral and Maxillofacial Surgery 49: 817-830, 1991

Ripamonti U. Inductive bone matrix and porous hydroxyapatite composites in rodents and nonhuman primates. In Handbook of Bioactive Ceramics, Volume II: Calcium Phosphate and Hydroxylapatite Ceramics. T Yamamuro, J Wilson-Hench, LL Hench, Eds., CRC Press, Boca Raton, Florida, 1990; pp 245-253

Ripamonti U. Calvarial regeneration in primates with autolyzed antigen extracted allogeneic bone. Clinical Orthopaedics and Related Research 282: 293-303, 1992

Ripamonti U, Reddi AH. Growth and morphogenetic factors related to bone induction. Role of osteogenin and related bone morphogenetic proteins in craniofacial and periodontal bone repair. CRC Critical Reviews in Oral Biology and Medicine 3: 1-14, 1992

Ripamonti U. Primate model: evaluation of bone substitutes in craniofacial reconstruction. In Bone Grafts and Bone Substitutes, MB Habal, AH Reddi, Eds., WB Saunders, Philadelphia, 1992; pp 235-240

Ripamonti U. Calvarial reconstruction in baboons with porous hydroxyapatite. Journal of Craniofacial Surgery 3: 149-159, 1992

ABSTRACT

Information concerning bone induction in primates is a prerequisite for the exploration of potential therapeutic applications for the regeneration of bone in humans. Twenty-four recipient adult Chacma baboons (*Papio ursinus*) were used to study bone repair and regeneration initiated and promoted by osteoinductive and osteoconductive bone substitutes implanted in heterotopic intramuscular sites and in orthotopic calvarial sites.

Diaphyseal bone was harvested from 10 male baboons and chemosterilized to obtain autolyzed, antigen-extracted allogeneic (AAA) bone preserving bone morphogenetic protein activity essential for osteoinduction. AAA bone cylinders were implanted intramuscularly in 24 adult male baboons and harvested at 3, 6 and 9 months. Histological analysis on undecalcified and decalcified sections showed that the matrix had undergone considerable resorption, particularly at 6 and 9 months. Numerous specimens showed extensive bone formation, which persisted in association with remnants of the matrix for as long as 9 months. Bone formation was confirmed by intravital double tetracycline labelling of the mineralization fronts.

Rods of a porous hydroxyapatite, obtained after hydrothermal conversion of the calcium carbonate exoskeleton of coral (genus Goniopora) with pores averaging 600 μm and pore interconnections averaging 260 μm in diameter, and a void fraction of 70 percent, were implanted intramuscularly in 24 adult baboons. Histological examination of the whole material showed remarkable and unexpected differentiation of bone within the porous spaces of the hydroxyapatite. Serial sections, prepared from specimens harvested at 3, 6 and 9 months, showed that he morphogenesis of bone was intimately associated with the differentiation of connective tissue condensations at the hydroxyapatite interfaces. Bone formed without an intervening endochondral phase. Although the amount of bone varied considerably, in several specimens extensive bone had developed, filling large portions of the porous spaces and culminating in total bone penetration within the implants. Histomorphometry showed that the amount of bone in the porous spaces increased significantly with time.

Osteogenic composites were prepared by inserting rods of the porous hydroxyapatite into the endosteal canals of AAA bone cylinders and in 24 adult baboons. Undecalcified and decalcified sections prepared at 3, 6

and 9 months showed bone differentiation by induction along the endosteal surfaces of the chemosterilized matrix and within the porous spaces of the hydroxyapatite substratum. Bone formation was often extensive, culminating in complete penetration of the porous spaces, merging with the newly formed bone originating from the AAA bone matrix envelope. Histomorphometry showed that bone in the porous spaces of the hydroxyapatite increased significantly with time. Bone formation was confirmed by fluorescence microscopy of the mineralization fronts after intravital double tetracycline labelling.

Ninety-six anterior and posterior calvarial defects, 25 mm in diameter, were prepared in 24 adult male baboons. In each animal, one defect was implanted with a disc of chemosterilized autolyzed, antigen-extracted allogeneic (AAA) bone. AAA bone implants were prepared from donor baboon calvariae and processed so as to retain bone morphogenetic protein activity in the bone matrix. Another defect was implanted with a disc of porous hydroxyapatite obtained after hydrothermal conversion of the calcium carbonate exoskeleton of coral (genus Goniopora). A third defect was grafted with a disc of autogenous cortico-cancellous bone harvested from the iliac crest. The fourth defect was left ungrafted and used as control. Histology and histomorphometry on

undecalcified and decalcified sections prepared from specimens harvested at 3, 6 and 9 months after surgery, showed superior osteogenesis in AAA bone implants when compared with autogenous bone grafts and untreated defects ($P<0.04$ and $P<0.01$ at 3 months). The superior osteogenesis in AAA bone implants appeared consistent with extensive osteoconductive invasion from the open diploic and endosteal spaces of the recipient calvariae. In addition, the finding of trabecular-like bone, appositional to the central areas of the implanted matrix, suggests that AAA bone implants might also have acted as inductive substratum for bone differentiation by induction.

Substantial bone growth had occurred in the implants of hydroxyapatite ($P<0.01$ vs bone grafts and $P<0.001$ vs untreated defects at 3 months), culminating in complete penetration by bone of the porous spaces. Anterior untreated defects showed greater amounts of bone when compared to posterior defects. The extent of osteogenesis in AAA bone and hydroxyapatite implants, however, appeared to be independent of the site of surgical implantation. This suggests that bone formation was a function of the implanted substrata rather than the healing potential of specific regions within the calvaria.

The results obtained in this calvarial primate model indicate that AAA bone matrix and porous hydroxyapatite implants may be a valid alternative to autogenous bone grafts for craniofacial reconstruction in humans.

The unequivocal demonstration of bone formation by induction in a large series of adult nonhuman primates provides evidence that long-lived higher vertebrates retain bone morphogenetic proteins in the extracellular matrix of bone and the crucial set of responding mesenchymal cells capable of transformation and differentiation into osteoblastic cell lines.

The extraskeletal morphogenesis of bone in porous hydroxyapatite is a new observation which may have important biomedical implications. The hydroxyapatite substratum may have acted a solid state matrix for adsorption, storage and controlled release of bone morphogenetic proteins which locally initiated bone formation. This hydroxyapatite-induced osteogenesis model may help to design appropriate delivery systems for bone morphogenetic proteins for the therapeutic initiation of bone formation.

SECTION I

INTRODUCTION

1. INTRODUCTION

One of the most exciting achievements in bone cell biology has been the recognition of the extracellular matrix of bone as a multifactorial repository of locally active growth and morphogenetic factors which modulate the function of bone cells (Mark and Popoff, 1988; Reddi, 1982, 1984; Urist et al., 1983a; Vukicevic et al., 1993 for reviews). While in most cases their role *in vivo* remains to be established definitively, it is clear that growth and morphogenetic factors isolated from the extracellular matrix of bone are potential molecular mediators of bone differentiation, maintenance and repair. A remarkable example of inductive interactions between the extracellular matrix of bone and responding cells is the phenomenon of bone formation by induction (Urist, 1965; Urist et al., 1967, 1968, 1969). Intramuscular and subcutaneous implantation of demineralized bone matrix results in a developmental cascade of biochemical and morphogenetic events culminating in local differentiation of endochondral bone (Reddi,

1981; Reddi and Huggins, 1972a; Urist, 1965; Urist et al., 1967). The origins of this research lie in the studies of Charles Huggins, Marshall Urist, Hari Reddi and others who first used biological assays to study the bone inductive properties of the extracellular matrix of bone and other tissues, including tooth matrix and uroepithelium (Huggins, 1931), and then stimulated many groups to contribute to a continuous growth of knowledge about the molecular and cellular signals involved in endochondral bone differentiation.

The growing appreciation that the extracellular matrix of bone is a rich source of cellular modulators underlies the increasing interest in their role in repair and regeneration of the bone-bone marrow organ. These developments have arisen from a desire to understand fundamental developmental processes: the control of cell differentiation, and the generation of form. One expectation of this research is the discovery of new forms of regulatory agents with novel biological and therapeutic potential.

2. POSTFOETAL OSTEOGENESIS: BIOLOGICAL MECHANISMS OF BONE REPAIR AND REGENERATION

2.1 The Induction of Bone and the Postfoetal Bone Differentiation Model: A Developmental Cascade

There is a relationship between growth and differentiation processes in early development and regeneration processes; fracture repair may be considered to recapitulate events that occur in the normal course of embryonic bone development. The tissue response elicited by subcutaneous or intramuscular implantation of demineralized bone matrix is reminiscent of embryonic bone development (Reddi, 1984, 1985; Urist et al., 1983a). However, unlike the epiphyseal growth plate, where a continuum of cartilage and bone differentiation is observed, in the matrix-induced implants a single cycle of endochondral bone formation is evident (Reddi, 1981; Reddi and Huggins, 1972a; Urist, 1965; Urist et al., 1983a). The developmental cascade includes: activation and migration of undifferentiated mesenchymal cells by chemotaxis, anchorage-dependent cell attachment to the matrix *via* fibronectin, mitosis and proliferation of mesenchymal cells, differentiation of cartilage,

mineralization of the cartilage, vascular invasion and chondrolysis, differentiation of osteoblasts and deposition of bone matrix, and finally mineralization of bone and differentiation of hemopoietic marrow in the newly developed ossicle (Rath and Reddi, 1979; Reddi, 1981; Reddi and Huggins, 1972a; Reddi and Huggins, 1975; Reddi and Kuettner, 1981; Urist, 1965; Urist et al., 1967, 1968, 1969, 1983a; Weiss and Reddi, 1980, 1981a, 1981b).

Which are the molecular signals that initiate the cascade of bone differentiation? Identification of osteogenic proteins in mammalian bone has been a difficult task due to the relative inaccessibility of small quantities of proteins tightly bound to the organic and inorganic components of the extracellular matrix of bone (Sampath and Reddi, 1984b; Urist et al., 1979, 1987a).

The observation that demineralized bone matrix could be dissociatively extracted (Mizutani and Urist, 1982; Urist et al., 1979, 1982, 1983b) and inactivated with chaotropic agents (such as 4 M guanidine-HCl or 6 M urea), and the osteogenic activity restored by reconstituting the inactive residue (mainly insoluble collagenous matrix) with solubilized protein fractions (Sampath and Reddi, 1981), confirmed the existance of

bone morphogenetic proteins (Sampath et al., 1987; Urist, 1971; Urist et al., 1983a, 1984a), and triggered a race for their purification. It is noteworthy that by themselves, neither the solubilized proteins nor the insoluble collagenous matrix were active: however a combination of the two restored the osteoinductive activity in an extraskeletal bioassay in rodents (Sampath and Reddi, 1981, 1983). The operational reconstitution of the soluble signal with an insoluble substratum was a key experiment that provided a bioassay for *bona fide* initiators of cartilage and bone differentiation (Reddi, 1992; Urist, 1992 for reviews). This functional bioassay provided the starting point for the purification of native bone morphogenetic proteins (BMPs), which was followed by molecular cloning and expression of the recombinant human proteins.

This explosive progress has been aided by four important technical developments: the development of a functional bioassay using extraskeletal sites of rodents to monitor the specific biological activity of osteogenic proteins (Sampath and Reddi, 1981, 1983; Urist et al., 1970, 1983a); the development of specific purification schemes involving hydroxyapatite and heparin affinity chromatography (Sampath et al., 1987; Urist et al., 1984a); the use of electroendosmotic

elution techniques after preparative sodium dodecyl sulfate gel electrophoresis to achieve final purification to homogeneity (Luyten et al., 1989; Sampath et al., 1990); and finally, the use of recombinant DNA methodologies for the cloning and expression of several members of the bone morphogenetic protein family (Wozney et al., 1988).

One of the bone morphogenetic proteins, osteogenin, was isolated from bovine bone matrix by heparin affinity chromatography, and purified to homogeneity by electroendosmotic elution after preparative sodium dodecyl sulfate gel electrophoresis (Luyten et al., 1989). The amino acid sequence of the tryptic peptides of osteogenin revealed an unique primary structure, identical to the amino acid sequence deduced from the cDNA clones of one of the recently characterized human bone morphogenetic proteins, BMP-3, cloned and expressed independently by Wozney et al. (1988). Later, native osteogenin was also isolated and purified to apparent homogeneity from baboon bone matrix (Ripamonti et al., 1992a). Since the identification by molecular cloning approaches of human BMP-2a (now known as BMP-2), BMP-3 (osteogenin) and BMP-2b (now known as BMP-4) (Wozney et al., 1988), several other BMPs, also called osteogenic proteins (OPs), have been identified, cloned, and expressed (Celeste et al., 1990; Ozkaynak

et al., 1990, Sampath et al., 1990).

Native and recombinant human (rh) BMPs induce local endochondral bone formation in conjunction with the insoluble collagenous bone matrix, the inactive residue obtained after dissociative extraction of the bone matrix with 4 M guanidine-HCl (Hammonds et al., 1991; Sampath et al., 1990, 1992; Luyten et al., 1989; Wang et al., 1988, 1990). The bone morphogenetic proteins show sequence homologies with members of the transforming growth factor-ß (TGF-ß) family (Celeste et al., 1990; Ozkaynak et al. 1990; Wozney et al., 1988), widely distributed in vertebrates and invertebrates (Sporn and Roberts, 1990). The TGF-ß family encompasses a group of structurally related proteins affecting a wide range of differentiation processes during embryonic development (Heine et al., 1989; Lyons et al., 1989a; Rosa et al., 1988). The bone morphogenetic proteins including osteogenin (BMP-3) are related to developmentally critical regulatory genes such as decapentaplegic (*dpp*) in *Drosophila*, which is implicated in dorsal-ventral specification (Ferguson and Anderson, 1992; Padgett et al., 1987), *60A* gene also in *Drosophila*, the expression pattern of which suggests a role in embryonic mesoderm and ectoderm determination (Doctor et al., 1992; Wharton et al., 1991), and vegetal (*Vg-1*) in *Xenopus* (Weeks and

Melton, 1987), and the Vg-1 related murine protein Vgr-1 (Lyons et al., 1989b).

The reproducible initiation of cartilage and bone in the rat extraskeletal site using demineralized bone matrix or bone morphogenetic protein preparations has permitted the study of the first wave of endochondral bone development and mineralization, and enabled a systematic study of endogenous and exogenous growth factors in bone development by the operational dissection of the major steps in the developmental cascade (Foidart and Reddi, 1980; Reddi, 1982, 1985, Reddi and Huggins, 1975, 1976; Reddi and Anderson, 1976; Reddi and Sullivan, 1980; Reddi and Kuettner, 1981; Reddi et al., 1977, 1978; Urist et al., 1983a; Weiss and Reddi, 1980).

Bone induction is the result of the combinatorial action of bone morphogenetic proteins and a complementary substratum to which responding mesenchymal cells can attach, proliferate and differentiate (Reddi, 1992; Reddi et al., 1989; Urist, 1989, 1992; Urist et al., 1983a). It is likely, however, that after the initiation of the first wave of bone differentiation by bone morphogenetic proteins, including the commitment and the clonal expansion of osteoprogenitor stem cells, the osteogenic cascade may

be promoted and mantained by a variety of growth factors including TGF-ß (Reddi et al., 1989). Indeed, TGF-ß was detected from day 9 onwards after subcutaneous implantation of bone matrix in rats (Carrington et al., 1988). The increased concentration correlated with the onset of angiogenesis and calcification of cartilage. TGF-ß appeared to b' compartmentalized in the mineral phase of the newly formed bone matrix and this may be a mechanism for storage of the latent form of the growth factor (Carrington et al., 1988; Seyedin et al., 1987).

It is noteworthy that TGF-$ß_1$ either purified from human platelets or expressed by recombinant techniques does not initiate endochondral bone formation in the *in vivo* bioassay (Hammonds et al., 1991; Sampath et al., 1987). It has been pointed out that considerable confusion exists in the literature on *initiation of bone formation* by certain growth factors (Reddi, 1992; Urist, 1992). Since the *in vivo* bioassay in rodents is highly discriminatory, the term initiation (or induction) of endochondral bone should be reserved for a phenomenon elicited by specific proteins, osteogenic in the ectopic bioassay in rodents. Thus, a more pertinent term to describe the *in vivo* effects of growth factors, including TGF-ß (not osteoinductive in the rodent bioassay), would be modulation or

stimulation of determined osteoprogenitor cells in pre-existing orthotopic sites, such as the periosteum end endosteum, into cartilage and bone.

Although mammalian bone may retain a considerable repair capacity, as often shown by the formation of an exuberant fracture callus, in general, regeneration of bone appears to diminish inversely with the experimental animal's position on the phylogenetic scale (Schmitz and Hollinger, 1986; Urist et al., 1989). Thus, the advantages that primates might have gained in the evolutionary process have been accompanied by loss of the capacity to regenerate severe skeletal discontinuities. If bone induction is to be applied to therapeutic use in humans, there must be an unequivocal demonstration of heterotopic bone differentiation after implantation of demineralized bone matrix or purified bone morphogenetic proteins in adult primates. The extensive evidence available from rodent models indicates that regulatory factors within the extracellular matrix of bone initiate postfoetal endochondral bone differentiation in these species. Can the same be said for primates? While Hosny and Sharawy (1985) reported limited bone formation by induction in adult rhesus monkeys, Aspenberg et al. (1988) found no evidence of heterotopic bone formation after implantation of demineralized bone in adult squirrel

monkeys. It is noteworthy, however, that bone morphogenetic protein preparations solubilized from the extracellular matrix of monkey and human bones induced bone formation in the rodent ectopic bioassay (Sampath and Reddi, 1983; Urist et al., 1983b).

The present study addresses the challenging problem of bone formation by induction in primates, and provides evidence that long-lived higher vertebrates do retain bone morphogenetic proteins in the extracellular matrix of bone as well as the crucial set of responding mesenchymal cells capable of transformation and differentiation into osteoblastic cell lines.

2.1 Porous Hydroxyapatite as Alternative to Autogenous Bone Grafts

The architectural and functional reconstruction of complex osseous mutilations in the craniofacial and axial skeletons are formidable challenges to modern surgery. Despite advances in biological knowledge and technique, large skeletal defects resulting from disease, resective surgery or traumatic mutilations, continue to defy predictable replacement by conventional autotransplantation or allotransplantation (Friedlaender et al., 1983; Habal and Reddi, 1992).

The biological superiority of autogenous bone grafts in reconstructive craniofacial and orthopaedic surgery rests on the grafted non-immunogenic matrix of bone which partially retains viability of its cellular and molecular components (Bassett, 1972; Burchardt, 1983, 1987; Burwell, 1966; Friedlaender, 1987; Heiple et al., 1983). Autogenous bone grafts, however, face several disadvantages: donor site morbidity, limited donor bone supply, grafting in heterotopic skeletal sites for which they are often anatomically and structurally unsuitable, high infection rate, and, most importantly, high resorption during healing and incorporation

(Burchardt, 1983, 1987; Habal, 1992; Lance, 1985; Prolo and Rodrigo, 1985).

The use of inorganic, biocompatible and nonimmunogenic bone substitutes is an important goal for reconstructive surgeons. This may reduce the need for surgical harvest of autogenous bone and the associated morbidity. While the replication of the living cellular and extracellular matrix of bone is, at the moment, unattainable, a major advance in biomaterial science has been the recognition of the importance of porosity in biomaterial design and development (Hulbert et al., 1970).

In orthotopic implantation, the porosity of bone substitutes is essential for optimal implant incorporation and osteoconductivity. Biologically, porous biomaterials, as opposed to monolithic nonporous implants, exploit the potential for bone regeneration by ingrowth of osteogenic and osteoprogenitor cells from the endosteal and marrow spaces of the recipient viable bone interface. Centripetal fibrovascular and osseous growth into a porous biomaterial depends on the availability of freely interconnected porosities of a minimum diameter of 100 μm (Hulbert et al., 1970; Klawitter et al., 1976; Spector et al., 1976). Interconnectivity is essential for osteoconductivity

because constrictions between pores and isolated or dead-end porous spaces limit vascular support to ingrowing tissue. Limited vascular penetration will result in failure of the implant and fibrous union at the interfaces.

Considerable interest has been focused in recent years on the osteoconductive property of a porous hydroxyapatite substratum obtained after hydrothermal conversion of the calcium carbonate exoskeletal microstructure of the scleractinian reef-building corals of both genera Porites and Goniopora (Chiroff et al., 1975; Roy and Linnehan, 1972; White et al., 1975). The hydroxyapatite is characterized by a relatively uniform network of interconnected channels and pores, similar to the microstructure of cancellous bone (Chiroff et al., 1975; Holmes, 1979; White et al., 1975). Because the hydroxyapatite is derived from the exoskeletons of corals, genera Porites and Goniopora (Wells, 1956), its porous spaces and interconnectivity are dictated genetically by the coral. This ensures the presence of interconnected porous spaces after conversion of the original calcium carbonate exoskeleton of coral into hydroxyapatite (Tencer et al., 1990; White and Shors, 1986; White et al., 1975).

Several lines of evidence have established the osteoconductive properties of the porous hydroxyapatite when implanted in orthotopic sites. Hydroxyapatite implants prepared from coral exoskeletons of the genus Porites (Wells, 1956), with an average porosity of 200 μm, have been used experimentally in a variety of reconstructive operations, particularly craniofacial procedures, as an alternative to autogenous bone grafts (Holmes, 1979; Holmes and Hagler, 1987, 1988a; Holmes et al., 1987; Piecuch et al., 1983). Previous studies have shown that the implantation in extraskeletal sites results in penetration of fibrovascular tissue, without bone formation, indicating that the porous hydroxyapatite does not act as a bone-inducing substratum (Piecuch, 1982). Bone growth into the porous spaces is dependent on close apposition of the implant to viable bone at the interfaces of the material (Holmes, 1979; Piecuch, 1982; White and Shors, 1986).

Comparatively limited material has been presented, however, using the 600 μm specification (Holmes et al., 1986), obtained from the exoskeleton of coral of the genus Goniopora (Wells, 1956) (Interpore 500). Morphometric comparison of its structure with that of bone harvested from human iliac crests, showed a remarkable degree of morphological similarity (Holmes et al., 1986; White and Shors, 1986).

Hydroxyapatite implants obtained from coral exoskeletons of the genus Porites (200 μm pore size) have been implanted extraskeletally in rodent and canine models (Piecuch, 1982; White and Shors, 1986). No data were available on the biological incorporation of any kind of porous hydroxyapatite implanted extraskeletally in nonhuman primates. Similarly, while Holmes and Hagler have recently examined the 200 μm porous hydroxyapatite in a canine cranial model (Holmes and Hagler, 1988b) no data were available on the incorporation of any porous hydroxyapatite in calvarial defects of adult nonhuman primates.

2.3 Osteogenic Composites

In recent years, the quest for a suitable implant to initiate and promote bone regeneration has led to the development of composites of bone inductive preparations and porous biomaterials as biological alternatives to autogenous bone grafts. Thus, a rational approach to bone regeneration is the creation of *osteogenic composites* of porous biomaterials and inductive bone matrix preparations (Vanderteenhoven and Spector, 1983).

The bone inductive potential of osteogenic composites must be tested by implantation in extraskeletal sites of recipient animals. The heterotopic implantation permits the histological and biochemical investigation of bone formation by induction, avoiding the possible ambiguities of the orthotopic site (Reddi, 1985, 1992; Urist, 1992; Urist et al., 1983a). A variety of biomaterials have been used in combination with demineralized bone matrix or solubilized bone morphogenetic protein fractions. Biomaterial carriers included polysulfone implants (Vanderteenhoven and Spector, 1983), collagenous preparations (Deatherage and Miller, 1987; Nathan et al., 1988), ß-tricalcium phosphate (Urist et al., 1984b), and sintered porous

hydroxyapatite (Kawamura et al., 1987).

Porous hydroxyapatites, by exploiting the biological principle of centripetal mesenchymal tissue ingrowth (Hulbert et al., 1970) appear to be well suited for the creation of osteogenic composites. It was noteworty, however, that crude extracts of rabbit bone matrix did not induce bone formation within the porous spaces of the hydroxyapatite. Bone was found only at the periphery of the implanted composite of hydroxyapatite and bone matrix proteins (Kawamura et al., 1987).

The need for having viable bone in direct contact with the porous hydroxyapatite to ensure adequate bone ingrowth *via* osteoconduction may limit the use of porous hydroxyapatite as a bone substitute in large skeletal discontinuities. Bone growth into the interconnected channels and pores may be confined to the peripheral regions of the implant only. By using an inductive substratum, heterotopic bone induction and bone growth within the porous spaces of the hydroxyapatite, in tissue lacking viable bone, may be achieved by the preparation of an osteogenic composite of porous hydroxyapatite and allogeneic demineralized bone matrix. In the present study, osteogenic composite implants were constructed by inserting porous hydroxyaptite rods into chemically processed and

surface-demineralized diaphyseal cylinders. The morphogenetic potential of the composite was investigated after implantation in intramuscular sites of the baboon (*Papio ursinus*).

2.4 Calvarial Repair in Primates and Other Animals

Large defects in the calvaria of adult mammals do not heal spontaneously (Prolo et al., 1982). The limited regenerative capacity of the membranous calvarial bones provides an ideal model to study the biocompatibility, incorporation, remodeling and the osteogenic potential of bone substitutes designed for reconstructive craniofacial and orthopaedic surgery (Hollinger and Kleinschmidt, 1990; Schmitz and Hollinger, 1986, for reviews).

Friedenberg and Lawrence (1962), while studying the regeneration of bone in calvarial defects of varying size, have outlined an important concept in experimental osteogenesis using surgically created defects:

If the capacity of the animal to fill a defect of known size and its inability to lay down sufficient bone to fill a larger defect are established, it is possible to alter the experimental conditions in an effort to increase the regenerative capacity.

Thus, the validity of an osseous defect as a model for

evaluating the osteogenic potential of bone substitutes is subjected to its limited capacity of spontaneous repair. Only in this situation, the osteogenic potential of a bone substitute may be considered unequivocal.

These early observations in experimental osteogenesis helped to formulate the concept of a *critical-size defect* in experimental skeletal nonunions (Hollinger and Kleinschmidt, 1990; Schmitz and Hollinger, 1986):

> *A critical size-defect may be defined as the smallest size intraosseous wound in a particular bone and species of animal that will not heal spontaneously during the life time of the animal. Attempted repair of a critical size-defect results in the formation of fibrous connective tissue rather than bone.*

A critical size-defect will thus require a graft of viable bone or alternative substitutes to heal. The use of calvarial defects to evaluate the osteogenic potential of bone substitutes is particularly appealing for potential craniofacial applications. Anatomically, the calvaria consists of two cortical plates separated by intervening cancellous bone and marrow, similar to the structure of the mandible. Embryologically, the calvaria develops *via* membranous ossification,

similar to the membranous bones of the facial skeleton (Bruce, 1941; Moss, 1954).

The limited osteogenesis in calvarial defects of adult mammals has been attributed to a limited blood supply, and a relative deficiency of bone marrow (Oklund et al., 1986; Prolo et al., 1982). Thus, a stringent test for bone substitutes is their implantation in calvarial defects. Because of this, a variety of animal models have been developed in the past decades aiming at the creation of standardized calvarial defects to study the biology of incorporation and the healing potential of bone grafts and bone substitutes (Schmitz and Hollinger, 1986).

Burger et al. (1962) found that calvarial defects of 2 mm in diameter in adult albino rats healed after 9 weeks. Superior osteogenesis was observed, however, when demineralized bone matrix, in comjunction with chondroitin sulfate, was implanted into the defects (Burger et al., 1962). Ray and Holloway (1957), after preparing defects of 4 mm in diameter in adult Wistar rats, showed superior osteogenesis in implants of demineralized bone matrix when compared with frozen homogenous (allogeneic) and deproteinized bone matrix implants (Ray and Holloway, 1957). Mulliken and Glowacki (1980) and Glowacki et al. (1981a) determined

that a defect of 4 mm in diameter in the parietal bone of 28-day-old Charles River rats was a critical size-defect of the rat calvaria. In the same model, superior osteogenesis was achieved by particulate demineralized bone matrix when compared to untreated controls (Mulliken and Glowacki, 1980). Takagi and Urist (1982) used calvarial defects of 8 mm in diameter prepared in adult Sprague-Dawley rats to test the efficacy of bovine bone morphogenetic protein fractions compared with allogeneic demineralized bone matrix. The results showed that bone morphogenetic protein fractions induced complete repair of the craniotomies. Moreover, bone morphogenetic protein fractions induced greater amounts of bone when compared with implants of demineralized bone matrix. In addition, osteogenesis was proportional to the dose of implanted bone morphogenetic protein preprations (Takagi and Urist, 1982). Using calvarial defects of 4 mm in diameter, Deporter et al. (1988) showed that a reconstituted bovine skin collagen enhanced bone regeneration in calvarial defects of adult Wistar rats. Minimal osteogenesis was observed in untreated defects (Deporter et al., 1988). Using insoluble collagenous matrix as carrier for osteogenin fractions, Mark et al. (1990) found superior osteogenesis in rat calvarial defects of 8 mm in diameter when compared to untreated craniotomies. It was noteworthy that intact

demineralized bone matrix often induced complete regeneration of the defects (Mark et al., 1990). More recently, a composite of bioerodible polyorthoester and demineralized bone matrix was found to regenerate calvarial defects of 4 mm in diameter prepared in adult Wistar rats (Solheim et al., 1992).

In rabbits, calvarial defects of 8 mm in diameter showed substantial bone regeneration, though the regenerated bone never achieved the thickness of the original calvaria (Kramer et al., 1968). In this latter study, bone deposition in control defects hindered a comparison with defects treated with anorganic bovine cancellous bone (Kramer et al., 1968). Similar results were obtained by Young (1964) using calvarial defects of 5 mm in diameter prepared in adult rabbits. Schmitz and Hollinger (1988) studied osteogenesis in calvarial defects of 15 mm in diameter surgically prepared in adult rabbits. The results showed minimal spontaneous healing in untreated defects. A biodegradable copolymer of polylactide-polyglycolide combined with allogeneic demineralized bone matrix showed superior osteogenesis when compared with untreated controls (Schmitz and Hollinger, 1988). In other studies using the rabbit model, Hollinger et al. (1989a) compared biodegradable ß-tricalcium phosphate of two configurations with untreated defects, 15 mm in diameter. Omnidirectional

tricalcium phosphate discs showed superior incorporation and greater amounts of bone when compared with unidirectional tricalcium phosphate implants. It was noteworthy, however, that greater amounts of bone formed in untreated defects when compared with unidirectional tricalcium phosphate discs (Hollinger et al., 1989a). In an identical rabbit model, Moore et al. (1990) showed superior osteogenesis in calvarial defects of 15 mm in diameter treated with guanidine-extracted protein fractions when compared with untreated defects. In this study, inductive proteins were delivered at site of surgical implantation after co-precipitation with purified bovine type I collagen (Moore et al., 1990).

In a canine model, Friedenberg and Lawrence (1962) studied the regeneration of calvarial bone in defects of varying size. They reported that, at 20 weeks after surgery, a residual defect of 60 percent or more was present in craniotomies of 17 and 20 mm in diameter. Dogs kept for the same period with 12 mm defects showed an average residual defect of 40 percent; dogs with 9 mm craniotomies a residual defect of 30 percent, and dogs with 7 mm craniotomies showed a residual defect of 14 percent (Friedenberg and Lawrence, 1962). Prolo et al. (1982) and Oklund et al. (1986) in a series of investigations on the healing potential of autogenous

bone grafts, processed autogenous bone and chemically processed allogeneic implants showed minimal spontaneous bone regeneration in calvarial defects of 18 and 20 mm in diameter in dogs. In the same model, chemosterilized, autolyzed antigen-extracted allogeneic (AAA) bone implants, processed so as to retain bone morphogenetic protein activity within the bone matrix (Urist et al., 1975), failed to regenerate calvarial defects (Oklund et al., 1986). Remodeling and incorporation of the chemosterilized matrix appeared to be consistent with osteoconductive invasion as opposed to osteoinductive mechanisms stimulated by bone morphogenetic protein activity (Oklund et al., 1986). Bovine bone morphogenetic protein fractions induced regeneration almost as completely as in autogenous bone grafts when implanted in calvarial defects of 14 mm in diameter of adult dogs (Sato and Urist, 1985). It was noteworthy that complete regeneration was achieved by a combination of bone morphogenetic protein fractions and bone marrow. This suggested that calvarial bone regeneration is bone marrow-dependent for a supply of responding mesenchymal cells (Sato and Urist, 1985). Bovine bone morphogenetic protein fractions also induced repair of calvarial defects of 18 and 20 mm in diameter in sheep (Lindholm et al., 1988). Interestingly, however, identical preparations of bovine bone morphogenetic protein fractions did not

induce heterotopic bone formation in sheep intramuscular sites (Lindholm et al., 1988). A canine model has been used to test bone regeneration using a composite of bone morphogenetic protein fractions precipitated onto resorbable ß-tricalcium phosphate and implanted in calvarial defects of 14 mm in diameter (Urist et al., 1987b). Rectangular defects (15 x 20 mm) prepared in the calvaria of adult dogs were used to study the growth of bone into porous hydroxyapatites with an average porosity of 200 µm (Interpore 200) (Holmes and Hagler, 1988b). At 6, 12, 24 and 48 months after implantation, the fractional volume of bone in the hydroxyapatite specimens was 15.2, 19.6, 23.8 and 18.5 respectively (Holmes and Hagler, 1988b).

The foregoing review shows that experimental repair and regeneration of calvarial defects has been essentially investigated in rodent and canine models. A review of the accessible literature at the outset of this investigation showed no previous data on calvarial defects of nonhuman primates, nor any investigation using bone morphogenetic preparations or porous hydroxyapatites implanted in calvarial defects of adult primates. Information concerning bone induction in primates is a prerequisite for potential therapeutic applications in man. There is a growing interest in novel bone substitutes incorporating bone morphogenetic

proteins for craniofacial and orthopaedic reconstructive procedures in an effort to reduce the harvest of autogenous bone and related morbidity. The creation of a calvarial primate model, using species comparable to man with respect to bone regulatory mechanisms and bone remodelling (Frost, 1973; Urist, 1989), would closely approximate bone repair and the biological fate of bone substitutes in man, accelerating the pace of clinical trials.

Since the beginning of this investigation, a limited number of studies using nonhuman primates have been published. In a preliminary report, Ferguson et al. (1987) prepared calvarial defects of 14 and 20 mm in diameter in 3 Rhesus monkeys (*Macaca speciosa*). Defects were implanted with 100-200 mg of partially purified bone morphogenetic protein fractions, and the animals were killed at 8, 10 and 16 weeks after implantation. The results showed superior osteogenesis, as assessed by radiomorphometry, when compared with untreated defects (Ferguson et al., 1987). In another study in primates, 9 skeletally mature male and female baboons of undetermined species, were used to test the efficacy of partially purified osteogenin fractions in regenerating calvarial defects of 15 mm in diameter (Hollinger et al., 1989b). Approximately 10 mg of partially purified bovine protein fractions were

implanted in conjunction with insoluble collagenous matrix prepared from Rhesus monkeys (*Macaca mulatta*). The results showed that xenogeneic osteogenin fractions induced 1.7 times more bone when compared with untreated defects. This reported limited osteogenesis could be related to the use of a xenogeneic collagenous matrix carrier, which was prepared from bone matrix of *Macaca mulatta* and used for reconstitution of bovine protein fractions for implantation in baboons (Hollinger et al., 1989b). In addition, the defect of 15 mm in diameter was found not to be a critical size-defect of the baboon calvar[illegible] (Hollinger and Kleinschmidt, 1990; Hollinger et al., 1989b). In more recent experiments, Hollinger et al. (1990) prepared calvarial defects of 20 and 24 mm in diameter in cynomolgus monkey (*Macaca fascicularis*), establishing a critical size-defect of the adult monkey calvaria. Nonhealing defects were treated with particulate human autolyzed antigen-extracted (AA) bone, and with bovine bone morphogenetic protein fractions in conjunction with a biodegradable polylactide coglycolide carrier. Histomorphometry showed partial healing with particulate AA bone matrix, but minimal regeneration using bone morphogenetic protein fractions-copolymer composite when compared to autogenous bone grafts (Hollinger et al., 1990).

3. AIMS OF STUDY

Against this introductory background, it was anticipated that the knowledge gained from a systematic nonhuman primate study would provide data pertinent to craniofacial repair and reconstructive skeletal surgery in man.

Twenty-four recipient adult Chacma baboons (*Papio ursinus*) were used to study bone repair and regeneration initiated and promoted by osteoinductive and osteoconductive bone substitutes.

The specific aims of these studies were set as follws:

1. To create a nonhuman primate model with surgically prepared calvarial defects which may closely approximate bone repair in the human: This model would allow qualitative and quantitative comparisons of various bone substitutes predicting their biological fate in the human;

2. To devise quantitative methods of evaluation to assess osteogenesis in untreated and treated calvarial defects;

3. To evaluate the spontaneous regenerative capacity of the adult baboon calvaria, and to establish a critical size-defect of the adult baboon calvaria;

4. To evaluate histologically and histomorphometrically the healing, remodelling and incorporation of autogenous cortico-cancellous iliac bone grafts transplanted into calvarial defects of adult baboons;

5. To evaluate histologically and histomorphometrically the healing, remodelling and incorporation of chemosterilized autolyzed antigen-extracted allogeneic (AAA) bone implants as a possible alternative to autogenous bone grafts;

6. To evaluate histologically and histomorphometrically the incorporation and the growth of bone into a porous hydroxyapatite as a suitable osteoconductive bone substitute for craniofacial reconstruction;

7. To compare histologically and histomorphometrically osteogenesis in autogenous bone grafts, AAA bone matrix implants and porous hydroxyapatite implants;

8. To study the bone induction properties of chemosterilized autolyzed antigen-extracted allogeneic

(AAA) bone matrix when implanted in intramuscular sites of the baboon;

9. To study the biology of incorporation and mesenchymal tissue growth into porous hydroxypatites after implantation in intramuscular sites of the baboon;

10. To construct an osteogenic composite by inserting the porous hydroxyapatite into AAA bone matrix implants, and to study its morphogenetic and induction properties after implantation in intramusculr sites of the baboon.

SECTION II

MATERIALS AND METHODS

4. THE EXPERIMENTAL ANIMAL: THE BABOON (*Papio ursinus*)

4.1 Introduction

The genus Papio (superfamily Cercopithecoidea, family Cercopithecidae, subfamily Cercopithecinae) includes five species of which the Chacma baboon (*Papio ursinus*) is a natural inhabitant of major vegetational zones of Southern Africa. They are large, heavily-built quadrupeds, with a characteristic long face with a prominent muzzle, the tip of which protrudes beyond the plane of the upper lip (Napier and Napier, 1985). A considerable sexual dimorphism exists in the species, the adult males being almost twice the size of the females. The formidable canines which are more strongly developed in the male than in the female baboon, are slashing and cutting devices (Napier and Napier, 1985). They have also an intimidatory function, and are used in aggressive display, as is often seen when approaching the cage of an adult male baboon. In

males, puberty is reached at 4 to 6 years, and the life span is 30 to 40 years (Napier and Napier, 1985). The ready availability of adult male individuals housed in the facilities of the University of the Witwatersrand, Johannesburg, and the convenient 'surgical' handling size determined the Chacma baboon the primate of choice for the present investigations. More importantly, comparative static histomorphometric studies between iliac crest bone biopsies of humans (Schnitzler et al., 1990) and baboons showed a remarkable degree of similarity (Schnitzler et al., 1993). This makes the adult male baboon ideally suited for the study of comparative bone physiology and repair with relevance to man (Schnitzler et al., 1993).

4.2 Selection of the Animals

Recipient animals. Twenty-four clinically healthy outbred adult male Chacma baboons with a mean weight of 27.8 ± 3.3 kg (range 22.4 - 36 kg), were selected from the primate colony of the University of the Witwatersrand, Johannesburg, 1800 metres above sea level. Criteria for selection were normal haematological and biochemical profiles (Melton and Melton, 1982) and skeletal maturity, confirmed by radiographic evidence of closure of the distal

epiphyseal plate of the radius and ulna. Their adult status was also confirmed by the presence of variable wear of the occlusal surfaces of the third molars.

Donor animals. Ten sub-adult male baboons with a mean weight of 13.9 ± 3.5 kg (range 10.9 - 22 kg), were selected as donors of diaphyseal and calvarial bone for the preparation of the allogeneic bone matrix to be implanted in the recipient animals. The sub-adult status of the donor animals was judged by the radiographic presence of the distal epiphyseal growth plate of the radius and ulna.

4.3 Housing Conditions and Diets

Following standard quarantine procedures, the animals were housed individually in suspended wire-mesh cages in the primate unit of the Central Animal Service of the university. Animals were caged in rooms kept under slight negative pressure (-25 kPa) with controlled ventilation (18 filtered air changes per hour), temperature (22 ± 2 degrees C), humidity (40 ± 10 percent) and photoperiod (lights on 0600 to 1800 hours). The diet of the baboons consisted of a balanced protein-fat-carbohydrate diet with vitamins (thiamine, riboflavin and nicotinic acid) and mineral supplements

(Ca:P= 1.2:1), and a soft dietary intake of sweet potatoes, pumpkins and oranges mixed in a ratio of 3:1 with a protein-vitamin-mineral (PVM) dietary supplement (Dreyer and Du Bruyn, 1968). The baboons had access to tap water in unlimited quantities. Before experimentation, the research protocols were approved by the Animal Ethics Screening Committee of the University (AEC No. 86/66/5).

5. THE HETEROTOPIC MODEL IN THE BABOON

5.1 Introduction

The demonstration of bone formation by induction must be obtained after implantation of inductive matrix preparations in extraskeletal sites. The rodent intramuscular (Urist, 1965; Urist et al., 1983a) or subcutaneous (Reddi, 1981; Reddi and Huggins, 1972a) sites are the established models to investigate bone induction by allogeneic demineralized bone matrices.

If bone induction is to be applied to therapeutic use in humans, there must be an unequivocal demonstration of heterotopic bone differentiation after implantation of demineralized bone matrix or purified bone morphogenetic proteins in adult primates. Conflicting reports emerged from the sparse literature on bone differentiation in primates. While Hosny and Sharawy (1985) reported limited subcutaneous bone formation by induction in adult rhesus monkeys, Aspenberg et al. (1988) found no evidence of heterotopic bone formation after intramuscular implantation of demineralized bone matrix in adult squirrel monkeys. The present study addresses the challenging problem of bone formation by

induction in primates using an intramuscular heterctopic model in adult baboons.

5.2 Preparation of the Allogeneic Diaphyseal Bone Matrix

The ten sub-adult baboons, immobilized by intramuscular phencyclidine hydrochloride (1 mg/kg of body weight), were killed by an intracardiac overdose of sodium pentobarbitone and used as source of donor bone tissue. After standard surgical preparation of the extremities, the long bones were exposed and the diaphyses were aseptically harvested after sectioning at metaphyseal level using a reciprocating saw while cooling with sterile deionized water. Muscular tissue, periosteum, and marrow were mechanically removed, and cylinders 20 mm in length were prepared by sectioning the cleaned diaphyses. The external diameter of the diaphyseal cylinders ranged from approximately 13 to 18 mm. Diaphyseal cylinders were sequentially extracted and chemosterilized to obtain autolyzed antigen-extracted allogeneic (AAA) bone (Table 5.1) in accordance with protocols devised by Urist et al. (1975) and Urist (1980, 1983). The sequential extraction preserves the bone morphogenetic protein activity in the bone matrix by adding chemical inhibitors of putative bone

morphogenetic proteases and lowers the alloantigenic load of the donor tissue (Urist et al., 1975). All solutions (with the exception of chloroform and methanol) were sterilized by filtration using Millipore filters (Millipore Corporation, Bedford, MA, USA), 0.2 µm pore size. Solution changes and bone handling were performed in a laminar flow cabinet. After incubation, the diaphyseal cylinders were washed twice in pre-chilled 7 mM sodium azide (4 degrees C), and vigorously stirred in deionized water to remove retained chemicals. The bone matrix was snap-frozen in liquid nitrogen and stored at -60 degrees C in sterile glass vials until implantation.

In accordance with protocols designed for human bone allografts (Friedlander, 1983; Tomford, 1983), swabs for microbiological analysis were taken before and after surgical preparation of the skin, after bone exposure, at resection lines, after chemosterilization and freezing, and before surgical implantation of the allogeneic bone.

5.3 Implants of Porous Hydroxyapatite

Implants of porous hydroxyapatite were prepared by Interpore International (Irvine, CA, USA). A

hydrothermal chemical exchange with phosphate converted the original calcium carbonate exoskeleton of the coral of the genus Goniopora (Wells, 1956) into an inorganic replica consisting of hydroxyapatite (Roy and Linnehan, 1974; White et al. 1975). Implants consisted of rods of porous hydroxyapatite, 20 mm in length and 7 or 5 mm in diameter. The solid trabeculae of the framework averaged 130 μm in diameter and their interconnections average 220 μm in diameter. The average porosity was 600 μm and their interconnections averaged 260 μm in diameter, while the void fraction averaged 70 percent (Interpore 500, Fig. 5.1)(Holmes et al. 1986; White and Shors, 1986). Conversion to hydroxyapatite was confirmed by X-ray diffraction pattern which showed that implants were composed of 90 percent hydroxyapatite and 10 percent tricalcium phosphate. Before implantation, the rods of hydroxyapatite were sterilized in an autoclave at 115 degrees C for 20 minutes.

5.4. Operative Procedures and Intramuscular Implantation

Food was withdrawn from the 24 recipient animals on the evening before surgery but there was continued access to water *ad libitum*. On the day of surgery, the

animals were immobilized by intramuscular phencyclidine hydrochloride (1 mg/kg) or ketamine hydrochloride (8 mg/kg) and anaesthetized with intravenous thiopentone sodium (15 mg/kg). Anaesthesia was maintained by halothane vapor in 100 percent oxygen after orotracheal intubation. After skin preparation and sterile draping, 48 AAA bone cylinders, 48 hydroxyapatite rods, and 48 AAA bone-hydroxyapatite composites were implanted in ventral and dorsal intramuscular pouches created by sharp and blunt dissection in the rectus abdominis and in the latissimus or longissimus dorsi after partial reflection of the trapezius, 6 implants per animal: 2 hydroxyapatite rods, 2 AAA bone cylinders, and 2 AAA bone-hydroxyapatite composites. Implants were equally distributed between the ventral and dorsal sites of implantation. Composite implants were prepared by inserting the hydroxyapatite rods into the medullary canals of the AAA bone cylinders (Fig. 5.2). An equal number of hydroxyapatite rods of 7 and 5 mm in diameter were distributed between both sites of surgical implantation. After implantation, the pouches were closed by repairing, in layers, the fasciae and the superficial tissues with atraumatic resorbable sutures (Vicryl, Ethicon, NJ, USA). Individually housed animals were kept under daily clinical observation and fed as previously described (Section 4.3). Ten animals (two at

3 months and eight at 9 months) received intravital double tetracycline labeling (Oxytetracycline, Terramycin, Pfizer Laboratories, 20 mg/kg of body weight) as follows: 1st label, on the 12th and 11th day before scheduled harvesting, and after a six days interval without tetracycline administration, the 2nd label, on the 4th and 3rd day before killing. Both labels were administered by intramuscular injections at 0900 hours. Clinically, healing was uneventful in all instances with no evidence of infection.

5.5 Harvesting of Tissue and Histological Preparations

The experiment was terminated at 3, 6 and 9 months after surgery, with eight animals per observation period. Immobilized animals were anaesthetized with intravenous thiopentone sodium (15 mg/kg) and prepared for perfusion of the head to optimize recovery of the calvarial specimens (see 6.6.1: Perfusion). During perfusion of the head, specimens implanted in the ventral and dorsal musculature were dissected free of adhering soft tissue and subjected to two different histological processings. Histological and histomorphometric analyses were carried out on decalcified and undecalcified sections as illustrated

in Figure 5.3.

5.5.1 Preparation of Decalcified Sections

Implants of AAA bone matrix and composites of AAA bone-hydroxyapatite harvested from the rectus abdominis were fixed in 10 percent neutral buffered formaldehyde. Implants of hydroxyapatite harvested from both ventral and dorsal musculature were also fixed by immersion in 10 percent formaldehyde and processed to obtain decalcified sections. Formaldehyde-fixed specimens were decalcified by immersion in a formic-hydrochloric acid mixture (Molnar, 1975). The acid mixture was changed every 24 hours, at which interval the specimens were radiographed to monitor the progression of decalcification. Decalcified specimens were double-embedded in celloidin and paraffin wax (Bancroft and Stevens, 1992) using an automatic tissue processor. Specimen blocks were sectioned manually on a Reichert-Jung 2040 microtome (Reichert-Jung, Germany) using a wedge-shaped (profile C) knife at a clearance angle of 5 degrees. The blocks were first trimmed for approximately 5 mm. Serial sections, cut at 5 μm, were floated out on a distilled water bath at a temperature of 42 degrees C. Microscope slides were coated with a gelatine-formaldehyde adhesive to minimize section

detachment during staining. The sections were stained with 0.1 percent toluidine blue in 30 percent ethanol. Sections were cut in a plane perpendicular to the long axis of the specimens (Fig. 5.3).

5.5.2 Preparation of Undecalcified Sections

Implants of AAA bone matrix and composites of AAA bone-hydroxyapatite harvested from the dorsal musculature were fixed by immersion in 70 percent ethanol, dehydrated in ascending concentrations of ethanol and cleared in toluene. A plastic-embedding system for light microscopy based on a methylmethacrylate resin (Medim K-Plast, Germany) was used for processing the undecalcified specimens. Specimen blocks, processed manually in individual glass bottles, were infiltrated with the methylmethacrylate monomer under vacuum for 21 days. After infiltration, specimen blocks were embedded in teflon moulds (4 cm x 4 cm x 4 cm) to which the K-Plast embedding and polymerizing solution was added (Fig. 5.4). Moulds were designed and created in collaboration with the Department of Physics of the University. Polymerization was carried out at 35 degrees C. Specimen blocks were then trimmed for approximately 5 mm in a plane perpendicular to the long axis of the specimens using a

Kent MK2 lapping and polishing machine. Blocks were cut in automatic mode on a Reichert-Jung 2050 Supercut microtome (Reichert-Jung, Germany) using a tungsten-carbide (profile D) knife at a clearance angle of 0 degrees. Blocks were moistened between each stroke with 70 percent ethanol. Sections were cut at 7 μm and stored in 30 percent ethanol. Floating sections were then stained with the Goldner's trichrome stain for undecalcified bone (Goldner, 1938). Adjacent sections were mounted unstained for fluorescent microscopy (Fig. 5.3). Sections were cut in a plane perpendicular to the long axis of the specimens.

5.6 Histological Analysis

From each specimen, a minimum of four sections, approximately 50 to 150 μm apart, were available for analysis. Bone formation by induction was identified using the presence of the following morphological features: osteoid seams lined by contiguous osteoblasts, newly formed highly cellular bone structures and bone marrow, contrasting with the uniform acellularity of the chemosterilized matrix. Undecalcified and stained sections prepared from tetracycline-labeled specimens were examined and compared with unstained sections to confirm bone

formation by induction as evidenced by the presence of tetracycline labels. Unstained sections were analyzed at a magnification of 200x using a microscope equipped with incident UV light (episcopic fluorescence Labophot, Nikon, Japan).

For the purpose of a semiquantitative histological analysis, the amount of induced bone generated by the bone matrix in both AAA bone and AAA bone-hydroxyapatite specimens was graded using values from 0 to 3 (Ripamonti et al., 1989): 0, none; 1, minimal amounts of induced bone within the matrix and/or lining the external or internal surfaces of the diaphyseal cylinders; 2, moderate amounts of induced bone scattered throughout the matrix or lining the internal and external surfaces of the cylinders; 3, well defined bone formation within the matrix and invading the interior of the cylinders.

The amount of dissolution and resorption of the implanted matrix was estimated by superimposing each histological section on a star-shaped symmetric grid comprising four cross hairs arranged radially printed on an acetate film placed over the stage of a Wild M 420 macroscope (Wild Heerbrugg, Switzerland) and examined at a magnification of x6.3 (Fig. 5.5). By

positioning the endosteal canal of the diaphyseal cylinders centrally, the grid divided the cross-sectional area of the matrix into eight fields, each representing 12.5 percent of matrix area. The percentage of matrix resorption was recorded by examining each of the eight fields delineated by the intersections of the radial cross hairs with the circumference of the implanted cylinders (Fig. 5.5).

5.7 Histomorphometric Analysis

Sections representing the area of the hydroxyapatite implants (either with or without the enveloping AAA bone matrix) were subjected to histomorphometric analysis (Fig. 5.3). Histological examination of the hydroxyapatite specimens implanted without AAA bone matrix showed remarkable and unexpected differentiation of bone within the porous spaces of the hydroxyapatite (see 7.1: Morphology, Figs. 7.7 and 7.8). A calibrated square Zeiss Integration Platte II (Zeiss, Germany) with 100 lattice points was used to calculate, with the point counting technique (Parfitt, 1983), the fractional volumes (in percent) of each histological component: bone, soft tissue (including fibrovascular and marrow tissues), and the implanted hydroxyapatite matrix. Sections were analyzed in an Univar light

microscope (Reichert AG, Austria) at a magnification of 40x with the Zeiss graticule superimposed over the centre of the specimen. A single and central field of 7.84 mm^2 was analyzed for each section (Fig. 5.6). Histomorphometric analysis was performed on two sections from the same specimen at two different levels, 100 or 150 μm apart. On undecalcified sections, prepared from the AAA bone-hydroxyapatite composites, bone volume was computed by calculating, separately, its mineralized and osteoid components.

5.8 Statistical Analysis

The data were analyzed in an IBM 3083 J24 computer using the Statistical Analysis System (1985). An F test was performed using the General Linear Models procedure for an unbalanced analysis of variance with multiple interactions. For each histologic component, the model design analyzed the effects and interactions of six independent class variables: the treatment, the individual animal response (nested with time), the time period, the site of implantation, the diameter of the hydroxyapatite rods, and the histological levels of the histomorphometric analysis. By including the hydroxyapatite matrix as an independent covariate in the General Linear Models procedure, a linear

regression analysis was performed to estimate the possible effect of the volume fraction of the hydroxyapatite matrix on the extent of bone formation. The Pearson product-moment correlation coefficient was computed for the two variables included in the regression analysis (bone and hydroxyapatite volumes). Comparison of mean values were obtained using Scheffe's multiple comparison procedure on the dependent variables included in the analysis. The critical level of statistical significance chosen was $P<0.05$.

6. THE ORTHOTOPIC CALVARIAL MODEL IN THE BABOON

6.1 Introduction

A review of the accessible literature at the onset of this investigation disclosed no previous work on the surgical preparation of calvarial defects and on the harvesting of autogenous bone from the iliac crest of any kind of nonhuman primates. The creation of the orthotopic calvarial model required a thorough analysis of the adult male baboon calvaria and its surgical anatomy, to establish the feasibility of accomodating four symmetrically located calvarial defects of 25 mm in diameter.

The anatomy of the calvaria was studied on dry skulls of adult male baboons, and the surgical procedure for the creation of the orthotopic model was first performed on one adult male baboon, killed after the termination of unrelated experiments.

For the creation of the model, it was necessary to design two revolving craniotomes (Fig. 6.1), which were constructed in collaboration with the Department of Physics of the University. One craniotome, with an

external diameter of 25 mm. was designed for the preparation of calvarial defects of 25 mm in diameter in the recipient animals. The other craniotome, with an internal diameter of 25 mm, was designed for the harvesting of allogeneic calvarial discs of 25 mm in diameter, and for the preparation of autogenous bone grafts, in disc form, harvested from the iliac crests, and suitable for implantation in the recipient defects.

6.2 Surgical Anatomy of the Adult Male Baboon Calvaria

In the adult male baboon, the cranium represents approximately one third of the whole skull, while the remaining two-thirds consist of the prominent mandibulo-facial skeleton accomodating the formidable canines and the large nasal cavities (Fig. 6.2). The calvaria is characterized by a spherical convexity in the posterior region of the parietal bone, and by a planar convexity in the anterior region at the level of the temporal fossa, accomodating the well developed temporalis muscles (Fig. 6.2). A sagittal crest, originating from a marked external occipital protuberance, characterizes the posterior part of the sagittal suture only. More anteriorly, the crest blends into well developed and diverging temporalis crests,

separating the parietal bones and delineating the temporal and infratemporal fossae at the level of the pronounced post-orbital constriction.

The comparatively large size of the adult male calvaria allows the surgical preparation of four defects each of 25 mm in diameter with intervening calvarial bone of more than 25 mm between ipsilateral defects, and with intervening calvarial bone of more than 40 and 30 mm between contralateral anterior and posterior defects, respectively (Fig. 6.3).

6.3 Preparation of the Allogeneic Calvarial Bone Matrix

The sub-adult baboons used as donors of allogeneic diaphyseal bone, were also used as source of donor calvarial bone matrix after surgical exposure of the calvariae. Using sterile operative techniques, calvarial bone discs, 25 mm in diameter were cut with the craniotome (25 mm of internal diameter) using slow revolution and abundant cooling with sterile deionized water. To prepare discs with the endocranial surface suitable for implantation in different areas of recipient calvariae, each donor animal provided four allogeneic discs, two harvested from the right and left

anterior calvaria (with planar concave endocranial surface), and two harvested from the right and left posterior regions (with spherical endocranial surface). Remaining muscular tissue, periosteum and endosteum were mechanically removed, but no effort was made to remove bone marrow. Calvarial discs were sequentially extracted and chemosterilized to obtain autolyzed antigen-extracted allogeneic (AAA) bone, preserving BMP activity in accordance with protocols devised by Urist et al. (1975), and Urist (1980, 1983), as previously described for baboon diaphyseal bone matrix. Briefly, after extensive washing in 7 mM sodium azide at 4 degrees C, discs were extracted in chloroform-methanol (1:1) at room temperature, surface-demineralized for 24 hours in two changes of 0.6 N HCl at 4 degrees C, and autodigested at 37 degrees C for 48 hours in 0.1 M (PBS), pH 7.4, with 7 mM sodium azide and 7 mM N-ethyl maleimide as protease inhibitor. Solutions (with the exception of chloroform and methanol) were sterilized by filtration using Millipore filters (Millipore Corporation, Bedford, MA, USA), 0.2 μm pore size. Solution changes and bone handling were performed in a laminar flow cabinet. After incubation, the calvarial discs were washed twice in pre-chilled 7 mM sodium azide, vigorously stirred in two changes of deionized water, snap-frozen in liquid nitrogen, and stored at

-60 degrees C in sterile glass vials until implantation.

Swabs for microbiological analysis were taken before and after surgical preparation of the scalp, after exposure of the calvaria, after chemosterilization and before surgical implantation of the allogeneic bone matrix.

6.4 Implants of Porous Hydroxyapatite

The porous hydroxyapatite, obtained after conversion of the calcium carbonate coral exoskeleton of the genus Goniopora (Wells, 1956) was prepared by Interpore International (Irvine, California). Implants consisted of discs of porous hydroxyapatite, 25 mm in diameter, with a minimal thickness at the center of 3 mm. Conversion to hydroxyapatite was confirmed by X-ray diffraction pattern which showed that implants were composed of 90 percent hydroxyapatite and 10 percent tricalcium phosphate. The average porosity of the scleroseptal channels was 600 μm and their fenestrated interconnections was 260 μm, while the void fraction averaged 70 percent (Holmes et al. 1986; White and Shors, 1986). The endocranial aspects of the discs were prepared with either a planar or spherical concave

surface according to the site of implantation in the calvaria. Before implantation, the discs of hydroxyapatite were sterilized in an autoclave at 115 degrees C for 20 minutes.

6.5 Operative Procedures and Experimental Design

After completion of the intramuscular implantations, an intravenous line was established and 800 ml of Ringer's lactate were administered to each animal for the duration of the cranial surgery. After standard surgical preparation of the scalp, a midline antero-posterior incision exposed the temporalis fasciae. After dissection of the fasciae, the underlying muscles were cut 5 mm from the attachment to the temporal crest, and elevated from the calvaria. On each side of the calvaria, two full-thickness defects, 25 mm in diameter, were made with the craniotome (25 mm of external diameter) while cooling with sterile deionized water. The posterior defects were trephined in the posterior convexity of the parietal bone, 5 mm anterior to the lambdoid suture and lateral to the temporal crest (Fig. 6.4). The anterior defects were trephined in the fronto-parietal region of the calvaria, 5 mm lateral to the temporal crest. In each animal, two defects were implanted with a disc of AAA

bone matrix and a disc of hydroxyapatite. A third defect was grafted with a disc of cortico-cancellous autogenous bone, 25 mm in diameter and with a thickness at the margins of 3 to 4 mm. The autogenous grafts were harvested just behind the anterior superior iliac spine after standard exposure of the right iliac crests; this yielded slightly curved discs conforming to the curvature of the baboon calvaria. The fourth defect was left ungrafted to evaluate the spontaneous repair potential of the adult baboon calvaria. Discs were inserted by friction-fit into the defects, and no additional fixation was performed (Fig. 6.5). To determine whether the position of the defects (anterior or posterior) may affect the extent of bone regeneration in the different treatment modalities, a Latin square block design was used to allocate the position of the implants and the ungrafted defect (Fig. 6.6). Spherical concave AAA bone and hydroxyapatite discs were inserted in the posterior defects, and planar concave discs in the anterior defects, conforming to the different radii of curvature of the baboon calvaria. Muscle, fascia, and skin incisions were repaired in layers using atraumatic resorbable sutures, and benethamine and procaine penicillins were administered by intramuscular injection (250.000 IU in 1.5 ml). Postoperative pain was controlled by

intramuscular buprenorphine hydrochloride (0.3 mg, twice daily for 2 days). Individually housed animals were kept under daily clinical observation and fed as previously described. Clinically, healing was uneventful in all instances with no evidence of neurological complication or infection.

6.6 Harvesting of Tissue and Histological Preparations

6.6.1 Perfusion

The experiment was terminated at 3, 6 and 9 months after surgery, with eight animals per observation period. After induction of general anaesthesia (thiopentone sodium, 15 mg/kg, i.v.), the common carotid arteries and internal jugular veins were exposed after standard dissection of the neck. After cannulation of the carotid arteries, the animals were killed with an overdose of intravenous pentobarbitone sodium. After cutting the jugular veins, tissue in the operative site was fixed by bilateral carotid perfusion with two liters of isotonic saline, pH 7.4, followed by two liters of 10 percent neutral buffered formaldehyde. The calvariae were then dissected, leaving a thin layer of muscle over the operative sites and the surrounding

bone. Using a reciprocating saw, the calvariae were cut into halves along the sagittal plane. Two large calvarial blocks, each including the ipsilateral anterior and posterior specimens, were then dissected free and further fixed by immersion in 70 percent ethanol. Specimen blocks with surrounding calvarial bone were radiographed, and cut into halves along the sagittal diameter of the implanted discs or untreated craniotomies. Specimen halves were subjected to two different histologic processings (Fig. 6.7). Histological and histomorphometric analyses were carried out on decalcified and undecalcified sections as outlined in Figure 6.7.

6.6.2 Preparation of Decalcified Sections

One half of each calvarial specimen was further fixed in 10 percent neutral buffered formaldehyde and decalcified by immersion in a formic-hydrochloric acid mixture (Molnar, 1975). The acid mixture was changed every 24 hours, at which interval the specimens were radiographed to monitor the progression of decalcification. Decalcified specimens were double-embedded in celloidin and paraffin wax (Bancroft and Stevens, 1992) using an automatic tissue processor. Specimen blocks were sectioned manually on a

Reichert-Jung 2040 microtome using a wedge-shaped (profile C) knife at a clearance angle of 5 degrees. The blocks were first trimmed for approximately 100 µm. Serial sections, cut at 7 µm, were floated out on a distilled water bath at a temperature of 42 degrees C. Microscope slides were coated with a gelatine-formaldehyde adhesive to minimize section detachment during staining. The sections were stained with 0.1 percent toluidine blue in 30 percent ethanol.

6.6.3 Preparation of Undecalcified Sections

The other half of each calvarial specimen was further fixed by immersion in 70 percent ethanol, dehydrated in ascending volumes of ethanol and cleared in toluene. Specimen blocks, processed manually in individual glass bottles, were infiltrated in methylmethacrylate resin (Medim K-Plast, Germany) as described for specimens harvested from the dorsal musculature. After infiltration, specimen blocks were embedded in rectangular teflon moulds (6 cm x 2 cm x 4 cm) to which the K-Plast embedding solution was added (Fig. 6.8). Polymerization was carried out at 35 degrees C. Specimen blocks were then trimmed using a Kent MK2 lapping and polishing machine until a full section was visible. Blocks were cut in automatic mode on a

Reichert-Jung 2050 Supercut microtome using a tungsten-carbide (profile D) knife at a clearance angle of 0 degrees. Blocks were wet sectioned between each stroke with 70 percent ethanol. Sections, cut at 7 μm, were stored in 70 percent ethanol. Floating sections were then stained with the Goldner's trichrome stain for undecalcified bone (Goldner, 1938). Stained sections were mounted after recording the position of the anterior and posterior interfaces of the craniotomies with their corresponding recipient calvarial margins (Figs. 6.7 and 6.9).

6.7 Histological Analysis

The histological sections were examined with a Univar light microscope (Reichert AG, Austria). On undecalcified sections, newly formed and mineralized bone in untreated defects stained blue with orange-red osteocytes. Osteoid stained orange-red tissue at the bone - bone marrow (or fibrovascular space) interface. Osteoblasts were defined as contiguous cuboidal bone cells directly apposed to osteoid. New bone deposition in craniotomies grafted with autogenous bone was identified by the presence of osteoid seams lined by contiguous osteoblasts, newly mineralized highly cellular and vascularized bone structures, contrasting

with the uniform acellularity, dark-blue stain and compactness of the transplanted cortico-cancellous graft. Newly formed highly cellular bone and osteoid seams also contrasted with the uniform acellularity of the implanted chemosterilized AAA bone matrix.

6.8 Histomorphometric Analysis

A calibrated Zeiss Integration Platte II with 100 lattice points was used to calculate, with the point-counting technique (Parfitt, 1983) the fractional volumes (in percent) of each histological component: newly formed bone, soft tissue (including fibrovascular, muscle and marrow tissues), and the implanted matrix (the implanted scaffolds of the autogenous bone grafts, AAA bone matrix and hydroxyapatite implants). Because of the inherent brittleness of the hydroxyapatite matrix, undecalcified sections prepared from hydroxyapatite specimens showed frequent lifting of the matrix during processing, causing folding of bone within the sections. Volume fraction compositions of hydroxyapatite specimens were therefore calculated examining decalcified sections (Fig. 6.7). Sections were analyzed in the Univar light microscope (Reichert AG, Austria) at a magnification of 40x, superimposing the Zeiss graticule over 7 sources

(Parfitt et al., 1987) selected for histomorphometry and defined as follows: two anterior and posterior interfacial regions (AIF and PIF), two anterior and posterior internal regions (AIN and PIN), a central region (CEN), and the two corresponding anterior and posterior marginal regions of the recipient calvaria (Fig. 6.9). This technique allows the histomorphometric evaluation of the distribution of bone regeneration across untreated and treated defects (Fig. 6.9). The anterior and posterior margins of the recipient calvariae were included in the analysis to estimate the effect of the diploic fraction on the extent of bone deposition in treated and untreated defects. On undecalcified sections, bone values were computed by calculating separately its mineralized and osteoid components. Each source was represented by a field of 7.84 mm^2. Histomorphometry was performed on one section per specimen; sections used for histomorphometry were similarly located in all specimens (Fig. 6.7).

6.9 Histomorphometric Analysis of Control Baboon Calvariae

The osteogenic potential of bone substitutes is conventionally expressed in volume percent of new bone

formed within implants or untreated craniotomies. In a more realistic approach, the amount of new bone in treated or untreated defects could be expressed as a percent of newly formed bone related to the original amount of bone that was present before trephination, i.e., the amount of bone (excluding bone marrow) in the segment of normal calvaria harvested in the form of a disc of 25 mm in diameter. The structural microanatomy of the calvaria is a composition of bone and marrow tissues; therefore, the presence of marrow spaces within the diploe will cause an underestimation of the osteogenic potential of the different treatment modalities. To overcome this problem, twenty control discs were harvested from the anterior and posterior calvariae of an additional five adult male baboons used for other experiments. Discs were cut through the diameter, decalcified in a formic-hydrochloric acid mixture, and double embedded in celloidin and paraffin wax as described. Sagittal serial sections, cut at 7 μm were stained with toluidine blue. The fractional volumes of bone and marrow tissues were calculated on two sections per specimen, approximately 200 μm apart, using five histomorphometric sources across the discs as described above.

6.10 Statistical Analysis

The data were analyzed in an IBM 3083 J24 computer with the Statistical Analysis System (1985). An F test was performed using an analysis of variance (ANOVA) with multiple interactions. For each histologic component, the model design analyzed the effects and interactions of four independent class variables: the treatment, the individual animal response (nested with time), the time periods, and the site of implantation within the calvaria. Comparison of mean values were obtained using Scheffe's multiple-comparison procedure on the dependent variables that were included in the analysis. The critical level of statistical significance chosen was $P<0.05$.

SECTION III

RESULTS

7. THE HETEROTOPIC INTRAMUSCULAR STUDY

Clinically, healing was uncomplicated in all instances with no evidence of implant rejection or infection. The eight animals of the third observation period (9 months), which were reweighed before euthanasia, showed an average weight gain of 4.9 kg (mean weight at harvesting: 36 ± 3.9 kg).

7.1 Morphology

AAA bone specimens

Macroscopic examination immediately after harvesting showed a marked variability in implant resorption, ranging from total disappearance of the matrix to an almost complete preservation of the implant. Eleven implants could not be located owing to complete resorption. One specimen, harvested at 3 months from the ventral musculature, was spoiled during processing, leaving 36 AAA bone specimens for histological

analysis. The number of evaluated specimens at each observation period and the mean values of induced bone in AAA bone implants are summarized in Table 7.1. There was no statistical significant difference between observation periods. The percentage of matrix resorption is presented in Table 7.2, showing that the higher resorption occurred between 3 and 6 months ($P<0.001$, Table 7.2). One AAA bone implant harvested at 3 months had no bone morphogenetic effect.

In the preparation of AAA bone, exposure of the matrix to 0.6 N HCl at 4 degrees C for 24 hours had resulted in demineralization of the external and internal surfaces of the diaphyseal cortex only, leaving a histologically well demarcated intramural ring of mineralized matrix. Bone formed by induction both externally, on exposed mineralized matrix after dissolution of the external demineralized layer, and intramurally, within pre-existing osteonic canals and newly formed resorption lacunae and excavation chambers (Fig. 7.1). At 3 months, vascular invasion and penetration of the matrix by mesenchymal elements were mainly confined to the external and internal regions, whereas at 6 and 9 months a progressive fibrovascular invasion and mesenchymal cell aggregation characterized the majority of the implanted matrices. Substantial

bone formed in several specimens harvested at 3, 6 and 9 months after intramuscular implantation (Figs. 7.1, 7.2, and 7.3). Newly mineralized bone had organized into trabecular-like structures mainly invading the interior of the cylinders (Fig. 7.1). In some specimens, however, woven bone formed at the external surfaces of the implanted matrix. Newly mineralized and highly cellular bone matrix was lined by continuous osteoid seams populated by contiguous osteoblasts (Fig. 7.1). Occasionally, large areas of orange-red nonmineralized woven bone showed the presence of foci of nascent, blue mineralized matrix (Fig 7.3). Nonmineralized new bone was lined by very few isolated plump cells with the morphological features of osteoblasts. Bone marrow was seen within large resorption lacunae of the matrix lined by appositional deposits of new bone, or differentiating between newly formed trabeculae of mineralized bone. Resorption of the matrix proceeded mainly from the external surfaces after partial or complete dissolution of the external demineralized layer, followed by progressive resorption and exposure of the mineralized matrix along multiple surfaces of the external cortical layer.

Under fluorescence microscopy, newly formed bone showed sharp and regular lines, rings or ovals of fluorescence within the implanted matrix (Fig. 7.4). Partly nonmineralized induced woven bone, as described above, was characterized by the absence of tetracycline labelling (Fig. 7.5).

Hydroxyapatite specimens

Macroscopic examination immediately after harvesting showed incorporation of the implants within the recipient muscular tissue without fibrous encapsulation. Three specimens were spoiled during histological preparation leaving 45 implants for histological analysis.

Two distinct histological features characterized the connective tissue that invaded the porous spaces of the hydroxyapatite implants: a vascular component within a cellular but loose connective tissue matrix, and the differentiation of a peculiar pattern of mesenchymal condensation and alignment of connective tissue fibers mostly in direct contact with the hydroxyapatite substratum (Fig. 7.6). Osteocyte-like cells were seen embedded within a tissue which had intermediate features between fibrous connective tissue and bone.

Large vessels had invaded the connective tissue matrix penetrating the porous spaces of the hydroxyapatite (Fig. 7.6). Occasionally, the vascular walls were almost in direct contact with the hydroxyapatite substratum. At 3 months, bone developed in 12 specimens (75 percent), and the amount of bone varied from minimal to florid, mainly occupying the center of the hydroaxyapatite implants. Structural organization varied from lamellar to delicate trabecular-like woven bone differentiating in the highly vascularized connective tissue matrix (Figs. 7.7 and 7.8). Bone was mostly in direct contact with the hydroxyapatite, and osteoblasts lined the newly deposited bone matrix. At 6 and 9 months, morphogenesis of bone occurred in 13 (93 percent) and 15 specimens (100 percent), respectively. Although the amount of bone varied considerably, in several specimens extensive bone had developed, filling large portions of the porous spaces both in the center and at the periphery (Figs. 7.9 and 7.10). Vascular spaces with the features of Haversian canals penetrated osteon-like structures of remodeled bone. Whilst the lamellar bone was mainly localized in the central regions of the specimens, newly developing woven bone was seen extending towards the peripheral porosities, occasionally culminating in total bone penetration (Figs. 7.10). Bone deposition was accompanied by the

differentiation of marrow. Bone remodelling resulted in the formation of large marrow cavities confined by relatively thin trabecular-like bone structures laminating the substratum and which were populated by sparse osteoblast-like cells.

AAA bone-hydroxyapatite composite specimens

Macroscopic examination immediately after harvesting showed a marked variability in matrix resorption, ranging from total disappearance of the matrix to an almost complete preservation of the AAA bone envelope. Two specimens were spoiled during histological preparation leaving 46 specimens for histological analysis.

The structural composition of the composite implants permitted separate evaluation of the morphologic structures that formed after implantation of the two different substrata. These histological features represented two distinct spatially non-related osteogenic mechanisms sustained by their complementary substrata and will be described separately.

AAA bone substratum. Mean values of induced bone in AAA bone-hydroxyapatite composites are summarized in Table 7.1. There was no statistical significant difference between observation periods. The percentage of AAA bone matrix resorption at each observation period is presented in Table 7.2, showing that higher resorption occurred between 3 and 6 months ($P<0.001$). Bone differentiated both internally and intramurally within preexisting osteonic canals and newly formed resorption lacunae and excavation chambers. Florid bone formation was seen in several specimens harvested at 3, 6 and 9 months after intramuscular implantation (Figs. 7.11 and 7.12). Bone had also invaded the interior of the diaphyseal cylinders, occasionally fusing with the bone forming within the porous spaces of the hydroxyapatite (Fig. 7.13). Newly formed and mineralized highly cellular bone was lined by continuous osteoid seams populated by osteoblasts. On undecalcified sections, large areas of orange-red nonmineralized woven bone surrounded small foci of blue mineralized matrix (Figs. 7.11 and 7.12). In the preparation of AAA bone, exposure of the matrix to 0.6 N HCl at 4 degrees C for 24 hours had resulted in demineralization of the external and internal surfaces of the diaphyseal cortex only, leaving histologically a well demarcated intramural ring of mineralized matrix.

Resorption of the matrix proceeded mainly from the external surfaces after partial or complete dissolution of the external demineralized layer, followed by progressive resorption and exposure of the mineralized matrix along multiple surfaces of the external cortical layer. Osteoclastic resorption along the external surfaces led to progressive destruction of the implanted diaphyseal envelope and eventually, in some specimens, its total disappearance at 6 and 9 months. The tissue at the interface between the chemosterilized envelope and the external surfaces of the hydroxyapatite implant was mainly characterized by an intervening collagenous matrix uniting the opposing substrata. The highly cellular and vascularized connective tissue was penetrated by dense clusters of organized collagen fibers, often oriented perpendicularly to the bone matrix. In several specimens, induced bone from the chemosterilized matrix had fused with bone originating from the porous spaces of the hydroxyapatite (Fig. 7.14).

HA substratum. Two distinct histological features characterized the mesenchymal tissue that formed within the porous spaces: a pronounced vascular component surrounded by a relatively loose connective tissue matrix, and the differentiation of mesenchymal

condensation and alignment of connective tissue fibers in direct contact with the hydroxyapatite. Bone had formed within the porous spaces as described previously for hydroxyapatite specimens without the AAA bone envelope. Although the amount of bone varied considerably, in several specimens extensive amounts of bone had developed, filling large portions of the porous spaces both in the centre and at the periphery (Figs. 7.14 and 7.15). Bone deposition was accompanied by the differentiation of marrow. Subsequent bone remodeling resulted in the formation of large marrow cavities confined by relatively thin trabecular-like bone structures which laminated the hydroxyapatite substratum and which were populated by sparse osteoblast-like cells (Fig. 7.15). On undecalcified sections, newly formed mineralized bone was often lined by continuous osteoid seams, which were populated by contiguous osteoblasts (Fig. 7.16).

Under fluorescence microscopy, induced bone revealed sharp and regular lines, rings or ovals of fluorescence, particularly within the AAA bone matrix. A diffuse pattern of tetracycline fluorescence as well as a distinct double tetracycline labelling characterized most of the bone surfaces that formed within the porous spaces of the hydroxyapatite. Partly

nonmineralized induced woven bone and large osteoid seams, as described above, were often characterized by the absence of tetracycline labeling.

7.2 Histomorphometry

Volume fraction compositions of the hydroxyapatite implants of both hydroxyapatite specimens and of AAA bone-hydroxyapatite composite specimens at each observation period are summarized in Table 7.3. Greater amounts of bone were found, on average, in hydroxyapatite specimens without the AAA bone envelope. This difference was found to be statistically significant at 6 months ($P<0.01$, Table 7.3). In hydroxyapatite specimens, the amount of bone increased significantly between 3 and 6 months ($P<0.01$) without further significant increase over 9 months. In AAA bone-hydroxyapatite specimens there was also a significant increase in bone volume between 6 and 9 months ($P<0.01$). Although the response of individual animals nested with time had a significant effect on the amount of bone formation ($P<0.01$), the analysis failed to show any significant interaction (crossed effect) between treatment and the individual animal response nested with time.

Separate analyses for the site of implantation showed that, on average, greater amounts of bone formed in anterior specimens ($P<0.05$). For both treatments, the analysis failed to show any statistical significant difference in bone volume between the two histological levels, 100 or 150 μm apart, used for histomorphometric analysis.

In hydroxyapatite specimens implanted without the AAA bone envelope, the volume fraction of the hydroxyapatite substratum ranged from 23 to 50 percent at 3 months, 23 to 51 percent at 6 months, and from 17 to 46 percent at 9 months. Although a difference existed between mean values, the hydroxyapatite substratum did not change significantly between 3 and 6 months. A significant difference existed, however, between 3 and 9 months ($P<0.01$), indicating biodegradation, although moderate, over time.

The histomorphometric analysis showed a considerable fluctuation in the volume fractions of the hydroxyapatite substratum between different specimens, ranging from 17 to 51 percent. This variation was found to have a significant effect on the amount of bone formation within the porous spaces ($P=0.0001$). The analysis showed a negative correlation (Pearson

correlation coefficient r=-0.58) between hydroxyapatite and bone values. Regression analysis showed that the relationship was linear with a negative slope. Plotting bone against hydroxyapatite values indicated that substantial and reproducible bone generation occurred in hydroxyapatite specimens with volume fractions ranging from 23 to 40 percent.

In AAA bone-hydroxyapatite specimens, the volume fraction of the hydroxyapatite substratum ranged from 25 to 56 percent at 3 months, 24 to 55 percent at 6 months, and from 16 to 52 percent at 9 months. The hydroxyapatite framework did not change significantly between 3 and 6 months. A significant difference existed, however, between 3 and 9 months ($P<0.05$), indicating biodegradation, although minimal, over time. The histomorphometric analysis showed a considerable fluctuation in the volume fractions of the hydroxyapatite between different specimens, ranging from 16 to 56 percent. This variation was found to have a significant effect on the amount of bone formation within the porous spaces ($p=0.0001$). The analysis showed a negative Pearson correlation coefficient ($r=-0.39$) between the hydroxyapatite and bone values.

8. THE ORTHOTOPIC CALVARIAL STUDY

8.1 Morphology of Calvarial Repair

8.1.1 Untreated Calvarial Defects

At 3 months, osteogenesis was limited, and confined to the margins of the craniotomies (Fig. 8.1 A). The newly formed bone was highly cellular and vascularized, and continuous osteoid seams lined newly formed trabeculae of mineralized bone. At 6 and 9 months, newly formed bone was seen to extend in a centripetal pattern from the margins of the defects (Fig. 8.1 B). Posterior specimens showed minimal bone deposition within defects (Fig. 8.1 C). The predominant histological feature was the fusion of the pericranium with the underlying dura following the penetration of the temporalis muscle into the defects (Fig. 8.1 C).

8.1.2. Autogenous Bone Grafts

Autogenous bone grafts provided a scaffold for bone deposition from the margins of the craniotomies. At 3 months, newly formed bone had united the grafts to the recipient calvaria (Fig. 8.2). At 6 and 9 months, the

callus uniting the graft to the recipient calvaria showed considerable remodeling (Fig. 8.3 A). Remodelling was particularly evident at the calvarial-graft interfaces and along the cancellous scaffold, and within pre-existing osteonic canals penetrating the cortices of the grafts. The central regions of the grafts often showed the presence of newly deposited bone in continuity with the callus that had formed at the calvarial interface (Fig. 8.3 A). Four specimens showed fibrous unions at 3 and 6 months (Fig 8.3 B).

8.1.3. Allogeneic Calvarial Bone Matrix Implants

At 3 months, in craniotomy defects implanted with autolyzed antigen-extracted allogeneic (AAA) bone matrix, osteogenesis was prominent at the calvaria-implant interfaces, coupled with dissolution and resorption of the peripheral layers of the chemosterilized matrix (Fig. 8.4). A delicate pattern of newly formed woven bone was seen within the open diploic spaces of the implanted calvarial matrix (Figs. 8.5 and 8.6). Dissolution and resorption of the matrix proceeded mainly from the pericranial surface after partial or complete dissolution of the external demineralized cortical layer (Figs. 8.5 and 8.7).

Vascular invasion and penetration of the matrix by mesenchymal elements was mainly confined to the pericranial and endocranial surfaces. Bone was seen forming in direct apposition to both demineralized and mineralized matrix. Newly mineralized and highly cellular bone was lined by continuous osteoid seams populated by numeruous osteoblasts. At 6 and 9 months, considerable bone remodeling had occurred after continuous appositional growth from the interfacial regions, and dissolution of the external demineralized layer of the implanted matrix (Fig. 8.8). Newly formed bone had invaded the diploic spaces, and extensive bone depositions frequently occurred on the pericranial and endocranial surfaces of the remaining mineralized scaffold of the implanted chemosterilized matrix (Fig. 8.8).

8.1.4. Porous Hydroxyapatite Implants

The majority of hydroxyapatite specimens showed bone growth into the porous spaces in direct apposition to the calvarial margins. Occasionally, however, specimens also showed the presence of substantial bone deposition in the central regions of the implants only (Fig. 8.9 A). This newly formed bone was not in continuity with the calvarial margins, as evaluated on serial sections

500 μm apart. As early as 3 months, and at 6 months, extensive deposition of bone had occurred, culminating in complete bone penetration (Fig. 8.9 B). Five specimens, however, showed the presence of nonunion at the calvarial interface (Fig. 8.9 C). At 9 months, bone was organized in solid blocks of remodelling osteonic bone which delineated the geometric configuration of the implanted hydroxyapatite (Fig. 8.10). On undecalcified sections, osteoid seams were populated by numerous osteoblasts, which lined the newly formed mineralized bone within the porous spaces at 3 months and, often, at 9 months (Fig. 8.11). At 9 months, two hydroxyapatite specimens showed the persistence of nonunion at the interfaces, in spite of extensive bone formation within the centre of the implants (Fig. 8.12).

8.2 Histomorphometry

Volume fraction compositions of untreated defects, bone grafts, allogeneic bone matrix, and hydroxyapatite implants at each observation period are summarized in Table 8.1. On undecalcified sections prepared from specimens of autogenous grafts and allogeneic bone matrix, it was necessary to distinguish the enveloping

reparative callus from the bone of the transplanted matrices. Because of the intimate blend of newly formed bone with the implanted chemosterilized matrix and the transplanted graft, the distinction between newly formed bone and matrix was often ill-defined and difficult to recognize histologically at 6 and 9 months. Volume fraction compositions of bone grafts and allogeneic bone matrix implants at 6 and 9 months, therefore, represent the cumulative percent of newly formed bone and implanted matrices (Table 8.1).

The amount of bone in untreated defects and hydroxyapatite implants increased significantly between 3 and 6 months ($P<0.01$), without further significant increase over 9 months. In 3 specimens of hydroxyapatite, the extent of bone deposition was as high as 59, 72 and 76 percent at 3, 6 and 9 months, respectively. Osteoid volume in untreated defects increased between 3 and 6 months ($P<0.05$) with a significant decrease over 9 months ($P<0.01$). In bone grafts, osteoid volume was greater at 3 months, decreasing significantly at 6 and 9 months ($P<0.01$). In AAA bone matrix implants, osteoid volume was greater at 3 months, decreasing significantly at 9 months ($P<0.01$). At 3 months, the amount of bone was significantly greater in AAA bone matrix implants when

compared to autogenous grafts (04). At 6 and 9 months, osteoid volume was significantly greater in AAA bone implants when compared t autogenous grafts ($P<0.05$). Because of decalcification during histologic processing, osteoid could not be measured in hydroxyapatite specimens.

Separate analysis for the site of craniotomy preparation showed that, on average, greater amounts of bone and osteoid were present in anterior untreated defects ($P<0.01$ at 6 and 9 months, Table 8.2). At 3 months, the analysis of AAA bone matrix implants failed to show any significant difference with regard to bone deposition between anterior and posterior sites. Volume fraction composition of hydroxyapatite specimens related to the site of implantation are presented in Table 8.3. The analysis failed to show any significant difference with regard to bone volume between the anterior and posterior sites. Table 8.4 illustrates the distribution of bone and matrix framework at 3 months in autogenous bone grafts and AAA bone matrix implants within the five sources analyzed by histomorphometry. The data are also presented graphically in Figures 8.13 and 8.14. The data show a reduction of bone volume between the interfacial and the central regions of autogenous grafts ($P<0.05$) and AAA bone matrix implants

($P<0.01$). While the grafted autogenous matrix did not vary significantly across the grafted defects, the implanted chemosterilized matrix at the calvarial interfaces was significantly reduced when compared to the internal and central regions ($P<0.01$, Table 8.4). Table 8.5 illustrates the distribution of bone and soft tissue in untreated defects within the 5 sources examined by histomorphometry. The data are also presented graphically in Figures 8.15 (3 months), 8.16 (6 months) and 8.17 (9 months). Analysis of the recipient calvarial margins showed that a significant correlation existed between the amount of diploe in recipient calvariae and the amount of bone in untreated defects ($P<0.01$). Table 8.6 illustrates the distribution of bone in hydroxyapatite specimens within the five sources analyzed by histomorphometry. The data are also presented graphically in Figures 8.18 (3 months), 8.19 (6 months) and 8.20 (9 months). Although a difference existed between mean values, bone volume did not vary significantly between sources, indicating, on average, a rather uniform bone distribution across the implants as early as 3 months. The hydroxyapatite substratum did not vary between the observation periods, indicating lack of significant biodegradation over time. The histomorphometric analysis showed fluctuation in the volume fraction of the

hydroxyapatite within and between specimens. This variation was found to have a significant effect on the amount of bone formation within the porous spaces of the hydroxyapatite (P=0.0004). The regression analysis showed a negative correlation (Pearson correlation coefficient r=-0.32) between values for hydroxyapatite and those for bone.

Volume fraction compositions of control calvariae are presented in Table 8.7. Table 8.8 shows the percent of newly formed bone in untreated and treated defects related to the site of craniotomy preparation, and expressed as a percent of the original amount of bone found in control calvariae.

9. FIGURES



Figure 5.1

Scanning electron photomacrograph of a rod of porous hydroxyapatite (Interpore 500, x 15). Representative samples were coated with gold-palladium and examined in a Jeol scanning electron microscope JSM-840 at an accelerating voltage of 20 KV.



Figure 5.2

Radiographic image of a composite of AAA bone-hydroxyapatite implanted in the dorsal musculature of an adult male baboon. Note the adaptation of the rod of hydroxyapatite within the chemosterilized diaphyseal bone cylinder.

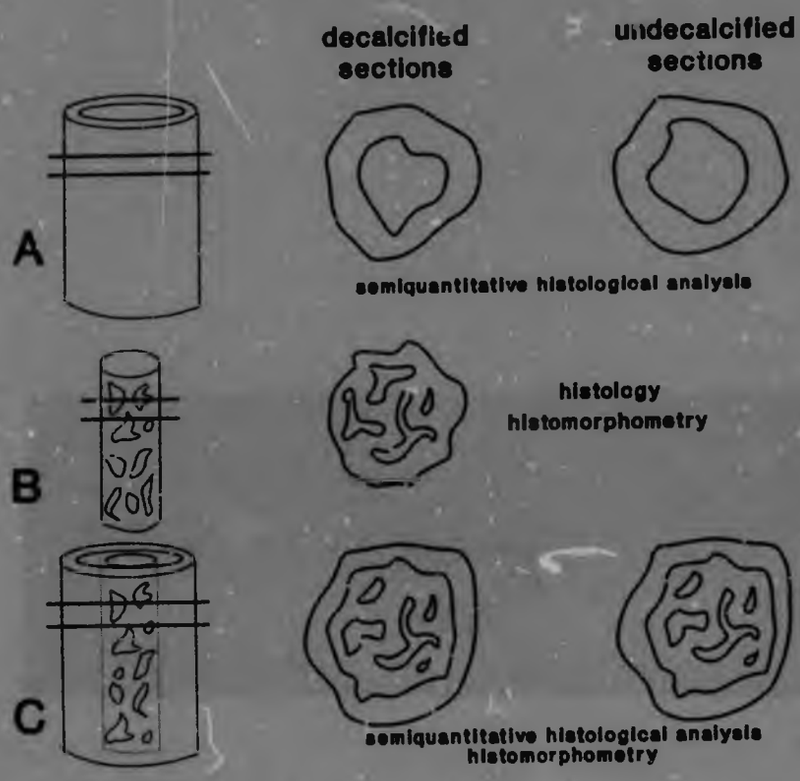


Figure 5.3

Schematic illustration of tissue processing for the preparation of decalcified and undecalcified sections for histological and histomorphometric analyses. From each specimen of AAA bone matrix (A), hydroxyapatite (B), and AA bone-hydroxyapatite composite, a minimum of four levels, approxymately 50 to 150 μm apart, were available for analysis.



Figure 5.4

Monolithic teflon blocks were macromachined for the preparation of moulds (4 x 4 x 4 cm) for processing undecalcified specimens harvested from the dorsal musculature.



Figure 5.5

Schematic illustration of a histological section cut in a plane perpendicular to the long axis of the specimen and superimposed on a star-shaped grid comprising four cross hairs arranged radially. The percentage of matrix resorption was recorded by examining each of the eight fields delineated by the intersections of the radial cross hairs with the circumference of the implanted cylinders.

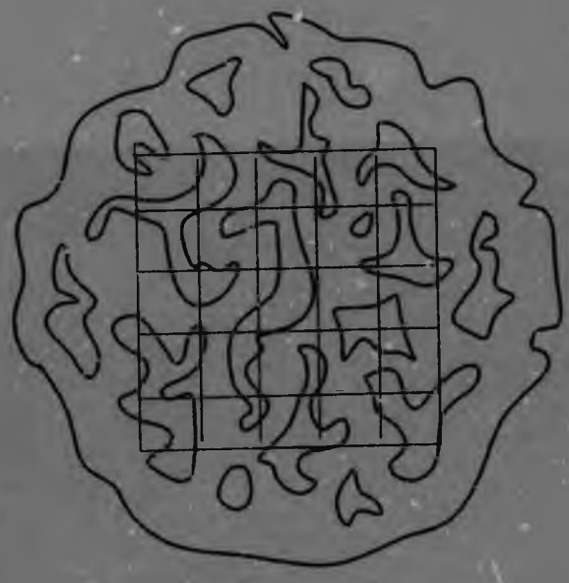


Figure 5.6

Schematic illustration of a histological section cut in a plane perpendicular to the long axis of a hydroxyapatite specimen. The calibrated square Zeiss Integration Platte II, incorporated into the Univar microscope, was projected onto the centre of the specimen, and a single central field of 7.84 mm^2 was analyzed in each section.



Figure 6.1

Photograph of the two craniotomes designed for the surgical preparation of calvarial defects of 25 mm in diameter (left), and for the harvesting of allogeneic and autogeneic bone discs (right). The craniotomes, sterilized in an autoclave, were then mounted on an electric drill (AEG, Germany) with controlled revolutions per min. The drill was sterilized in formalin vapours.



Figure 6.2

Photograph of a skull of an adult male Chacma baboon (*Papio ursinus*) showing the prominent mandibulofacial complex, and the formidable canines. Note the large temporal and infratemporal fossae which accomodate the well developed temporalis muscles.



Figure 6.3

Superior view of the skull showing the extended facial skeleton, the pronounced post-orbital constrictions, and the diverging temporalis crests. Arrows indicate the anatomical areas selected for the preparation of the four symmetrically located calvarial defects.



Figure 6.4

Preparation of a posterior right calvarial defect, 25 mm in diameter. Arrow points to the ipsilateral anterior defect.

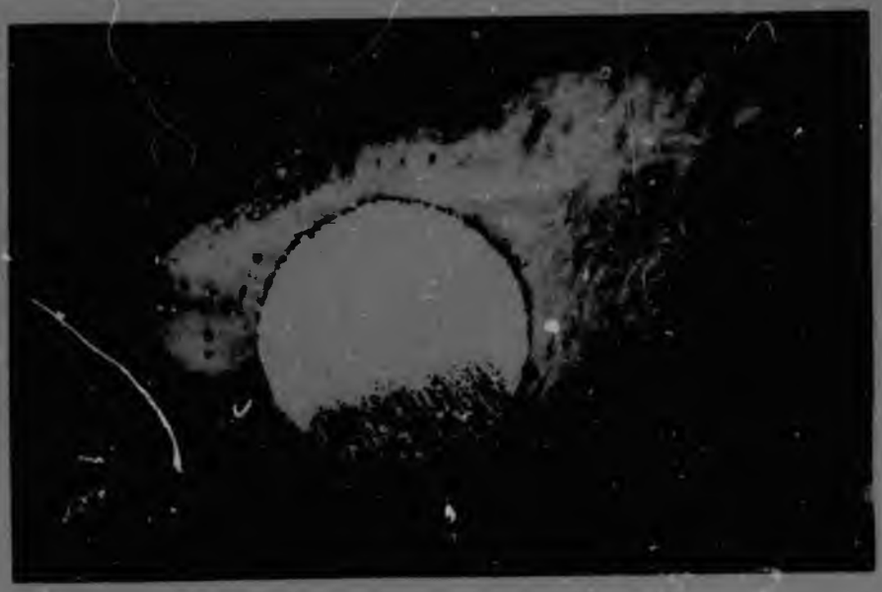


Figure 6.5

Photograph of a disc of porous hydroxyapatite positioned into a posterior right calvarial defect. The disc was inserted by friction-fit into the defect just before suturing the temporalis muscle. Arrow indicates the architecture of the hydroxyapatite framework after adsorption of blood.

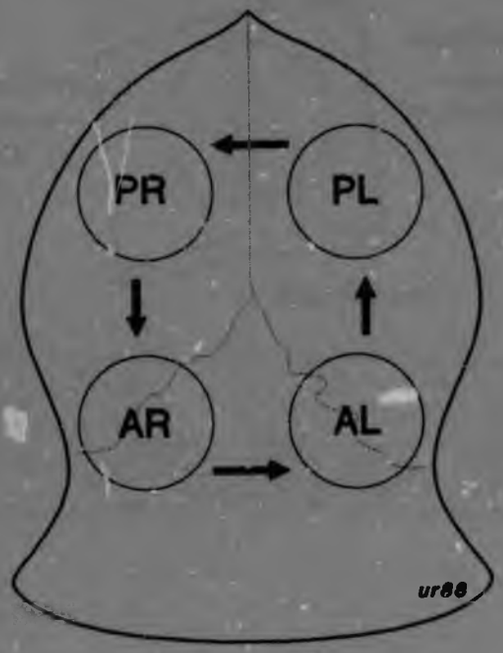


Figure 6.6

Calvarial model and implantation design in 24 adult male baboons. In each animal, a balanced Latin square block design was used to allocate the position of the implants and the ungrafted defects. This resulted in the rotational allocation of the four treatment modalities described in the text within a total of 96 defects with a balanced distribution between anterior and posterior regions of the calvaria (AR: anterior right; AL: anterior left; PL: posterior left; PR: posterior right). Arrows indicate the counterclockwise treatment rotation.

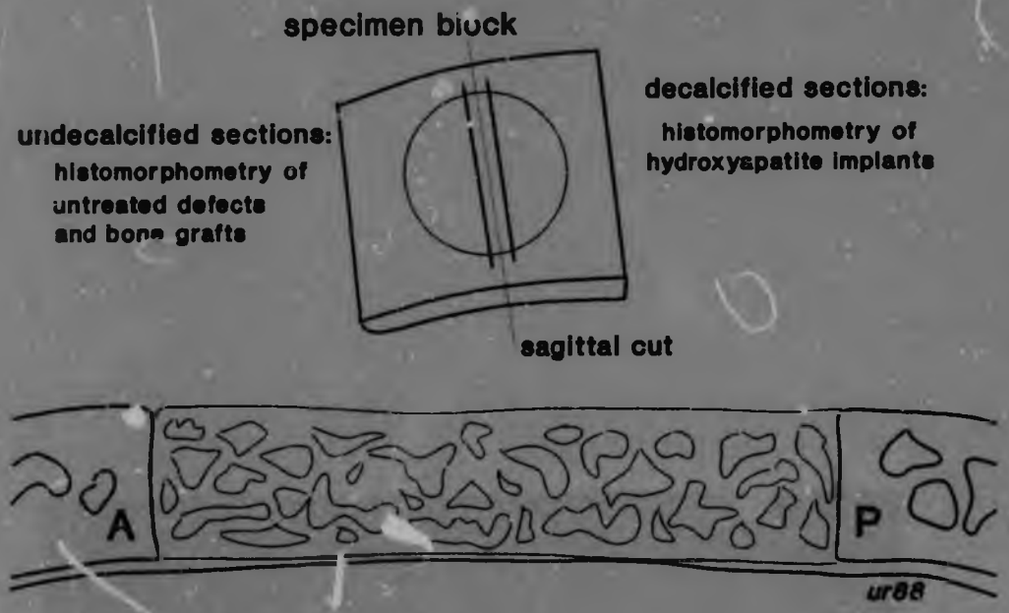


Figure 6.7

Top panel: Schematic illustration of tissue processing for the preparation of undecalcified and decalcified sections for histological and histomorphometric analyses.

Bottom panel: Schematic illustration of a sagittal calvarial section incorporating an hydroxyapatite implant. A and P: anterior and posterior recipient calvarial margins.



Figure 6.8

Rectangular teflon moulds (6 x 2 x 4 cm) for processing undecalcified specimens harvested from the calvaria.

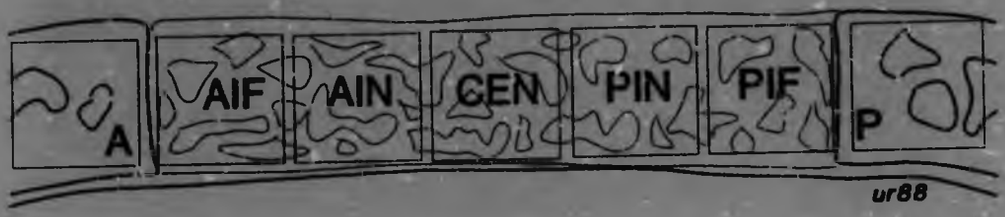


Figure 6.9

Schematic illustration of a sagittal calvarial section with an implant of hydroxyapatite showing the seven sources selected for histomorphometry. Sources, defined as the type of regions on which quantitative morphometry was performed (Parfitt et al., 1987), were anterior and posterior recipient calvarial margins (A and P), anterior and posterior interfacial regions (AIF and PIF), anterior and posterior internal regions (AIN and PIN), and a central region (CEN).

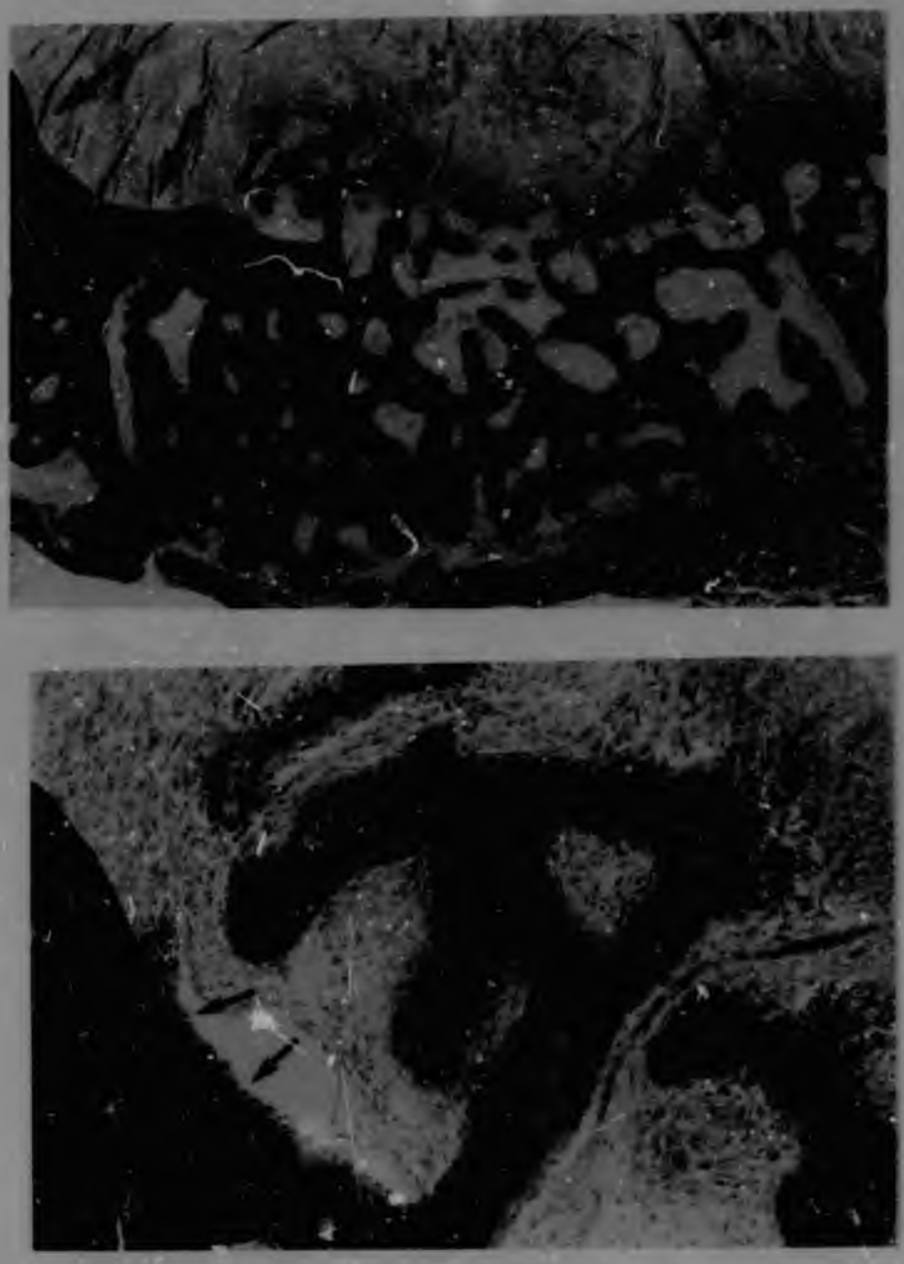


Figure 7.1

Photomicrographs of induced bone in a specimen of AAA bone matrix harvested at 3 months. **Top panel:** Low power view showing newly formed bone within the diaphyseal wall, and extending into the highly cellular connective tissue that invaded the endosteal canal. Arrows indicate the surface-demineralized matrix. **Bottom panel:** High power view showing the newly formed mineralized, and nonmineralized woven bone. Arrows indicate contiguous osteoblasts and osteoid over foci of newly mineralized matrix (undecalcified sections, Goldner's trichrome, original magnification x 10 and x 60).

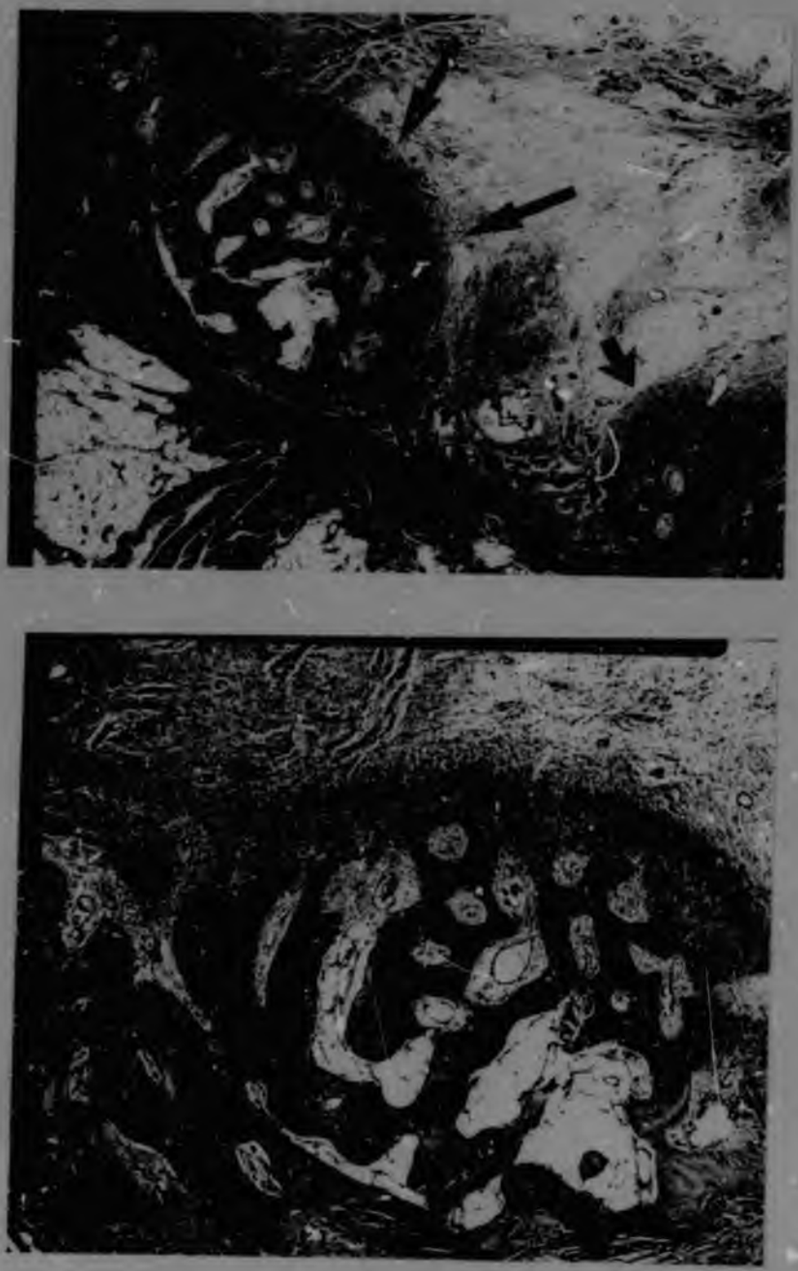


Figure 7.2

Photomicrographs of induced bone in a specimen of AAA bone matrix harvested at 6 months. **Top panel:** Low power view showing the formation of large ossicles of induced bone (arrows). **Bottom panel:** High power view showing trabeculae of newly formed bone (decalcified section, toluidine blue, original magnification x 20 and x 60).

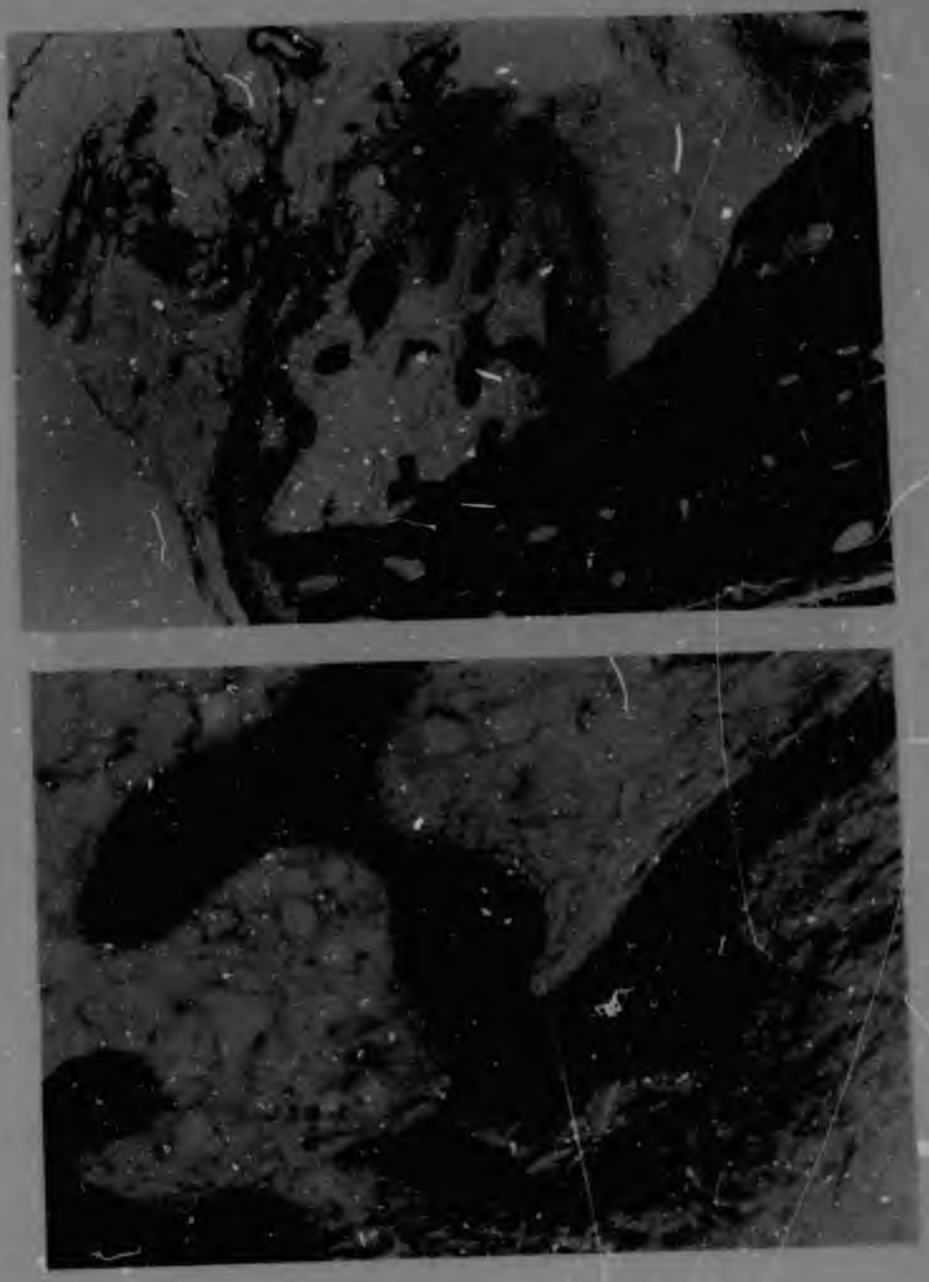


Figure 7.3

Photomicrographs of a specimen of AAA bone harvested at 9 months. **Top panel:** Low power view showing foci of mineralization within newly formed vowen bone. **Bottom panel:** High power view showing mineralization of the newly formed bone and the pronounced capillary network (undecalcified section, Goldner's trichrome, original magnification x 10 and x 80).

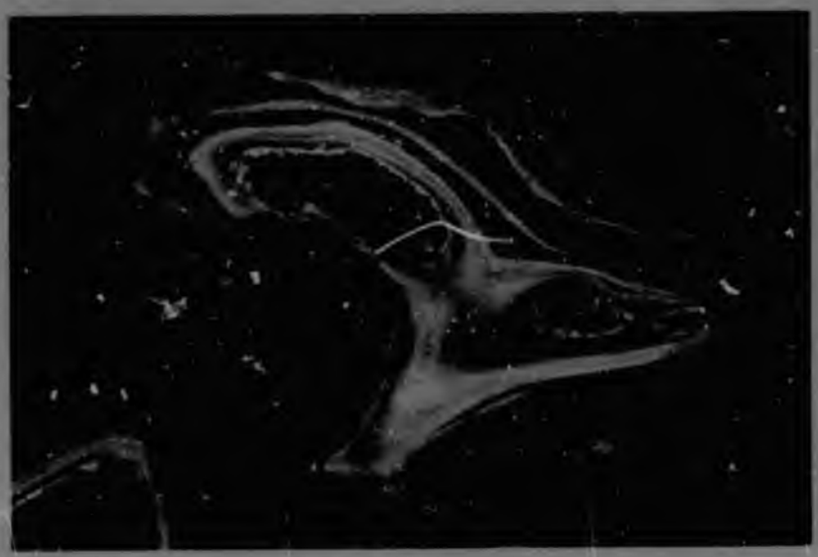


Figure 7.4

Pattern of tetracycline labelling in a specimen of AAA bone harvested at 9 months (undecalcified unstained section, UV light, original magnification x 200).

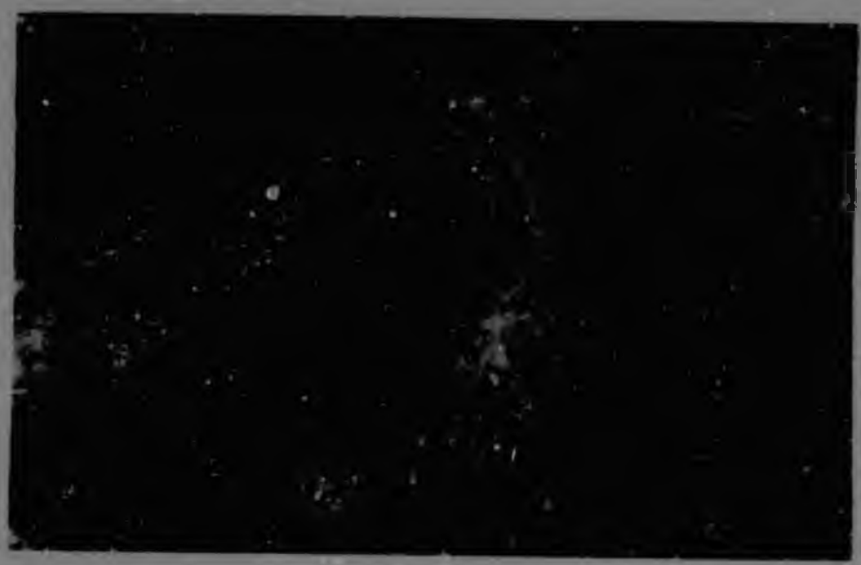


Figure 7.5

Absence of tetracycline labels in unmineralized woven bone in a specimen of AAA bone harvested [illegible] months (undecalcified unstained section, UV light, original magnification x 200).



Figure 7.6

Photomicrographs of a specimen of hydroxyapatite showing the organization of the connective tissue 3 months after implantation. **Top panel:** Condensation and organization of connective tissue fibres mainly at the hydroxyapatite interface. Empty white spaces represent the framework of the hydroxyapatite dissolved after decalcification during histological processing. **Bottom panel:** High power view of the organization of connective tissue fibres at the hydroxyapatite interface and in the porous spaces (decalcified section, toluidine blue, original magnification x 10 and x 40).

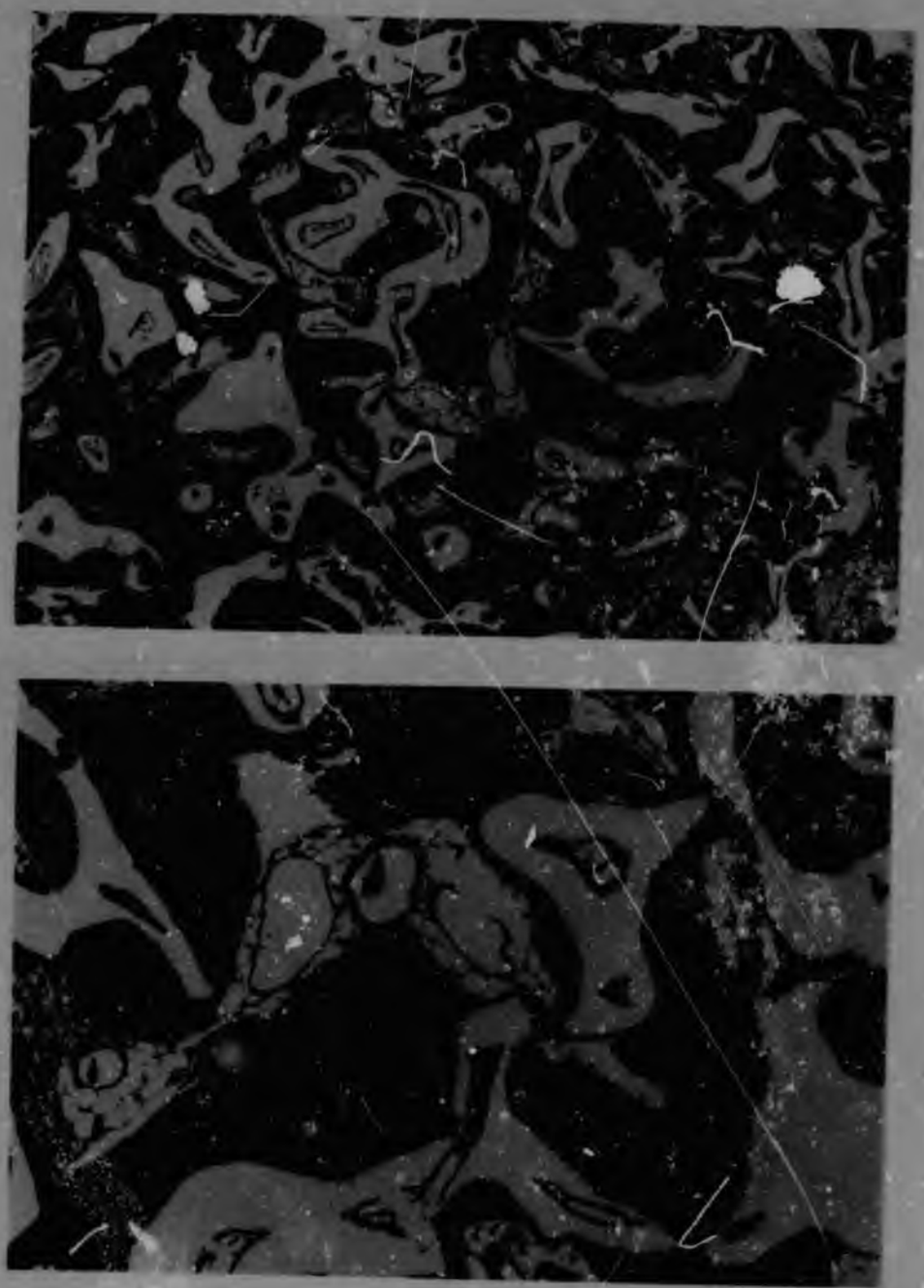


Figure 7.7

Photomicrographs of a specimen of hydroxyapatite harvested at 3 months. **Top panel:** Low power view showing extensive bone deposition within the porous spaces mainly at the centre of the specimen. **Bottom panel:** High power view showing remodelling, organization of lamellar bone and bone marrow formation (decalcified section, toluidine blue, original magnification x 10 and x 50).

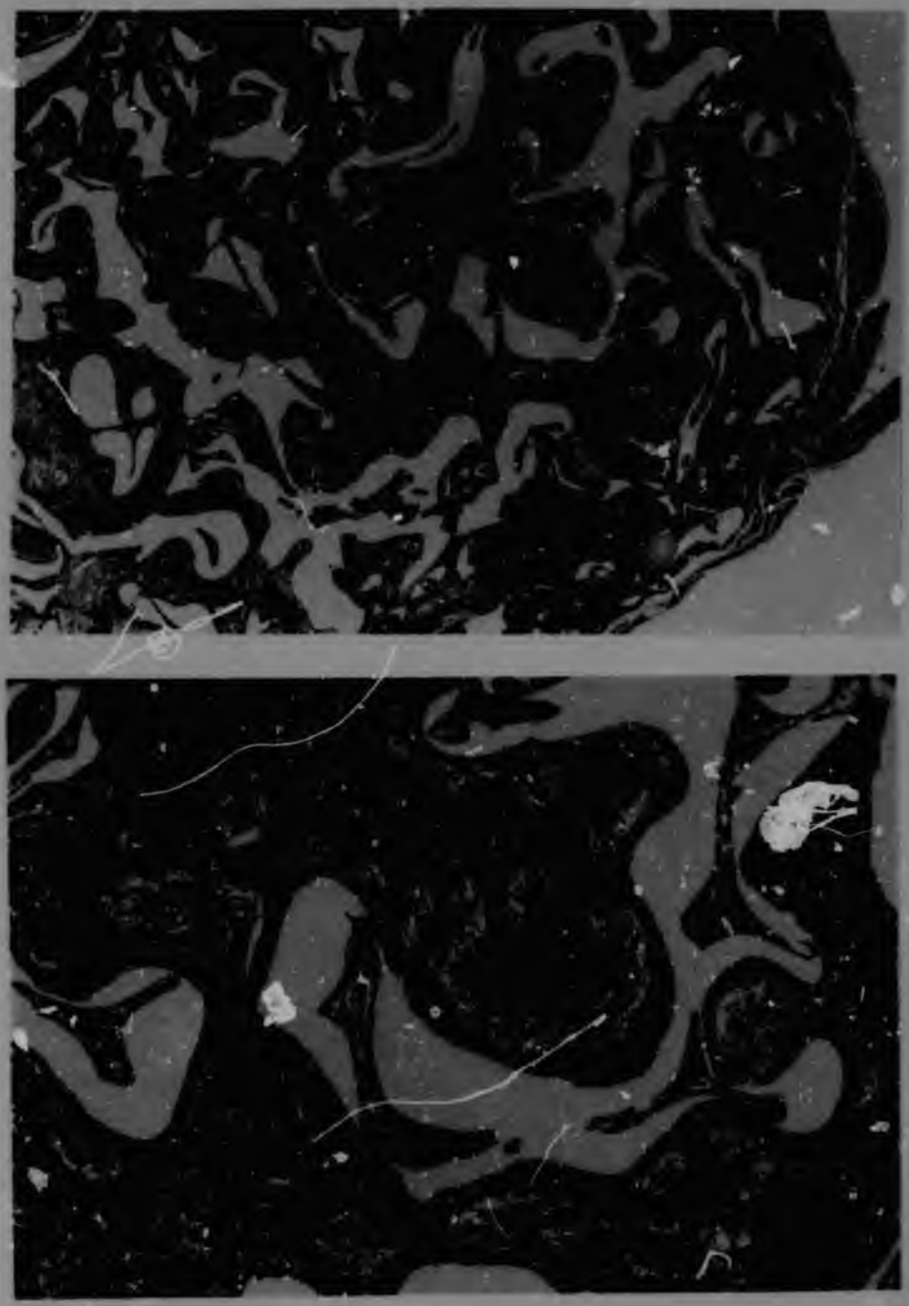


Figure 7.8

Photomicrographs of a specimen of hydroxyapatite harvested at 3 months. **Top panel:** Low power view showing delicate trabecular-like bone structures developing within localized porous spaces of the hydroxyapatite. **Bottom panel:** High power view showing the highly cellular bone matrix covered by osteoblasts, and the extensive vascular ivasion. Note the interconnections between the trabeculae of bone invading the porous spaces, and the uninterrupted bone lining the surface of the hydroxyapatite (decalcified section, toluidine blue, original magnification x 10 and x 50).

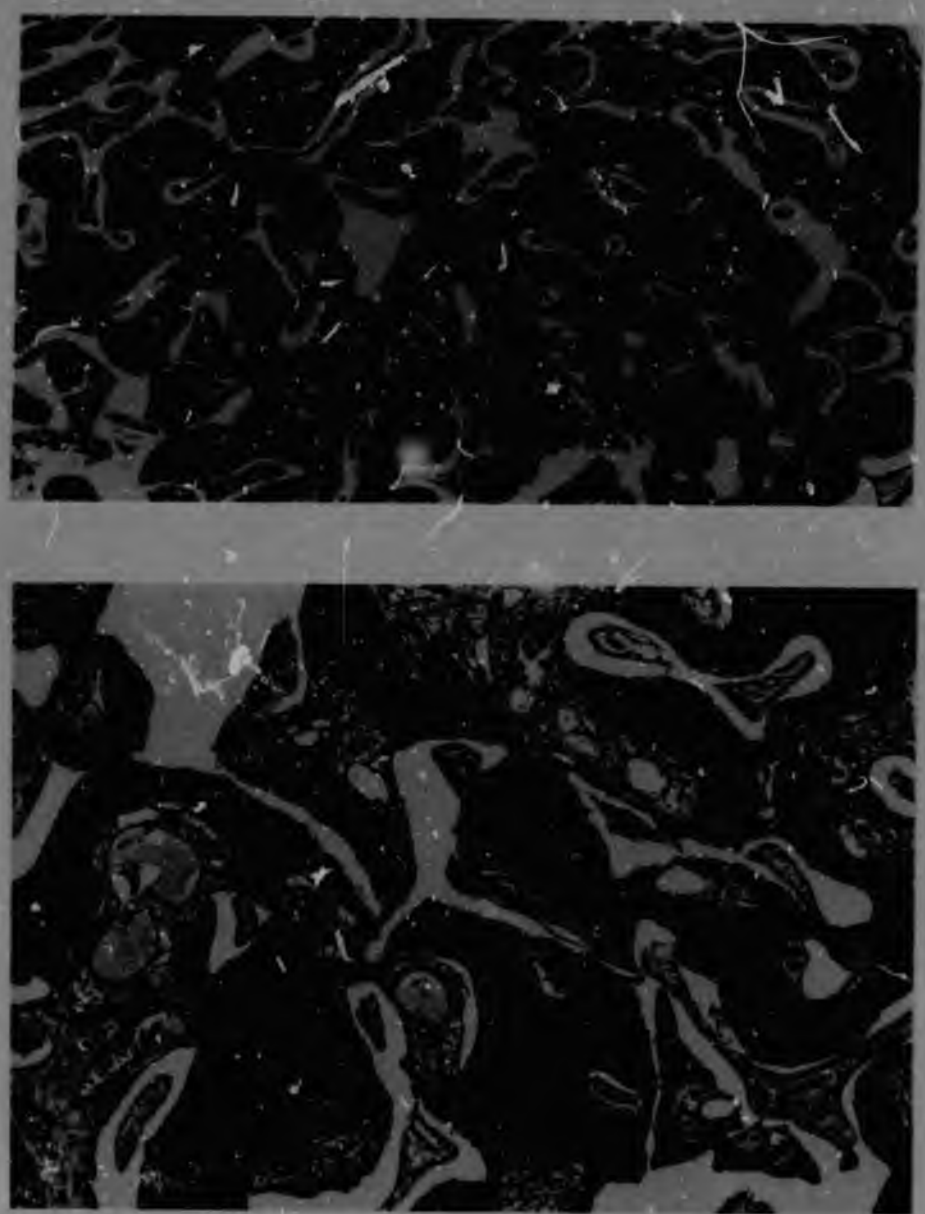


Figure 7.9

Photomicrographs of a specimen of hydroxyapatite harvested at 6 months. **Top panel:** Large areas of remodeled bone fill the porous spaces of the hydroxyapatite, particularly in the centre of the specimen. **Bottom panel:** High power view showing the structural organization of the lamellar bone (decalcified section, toluidine blue, original magnification x 10 and x 50).

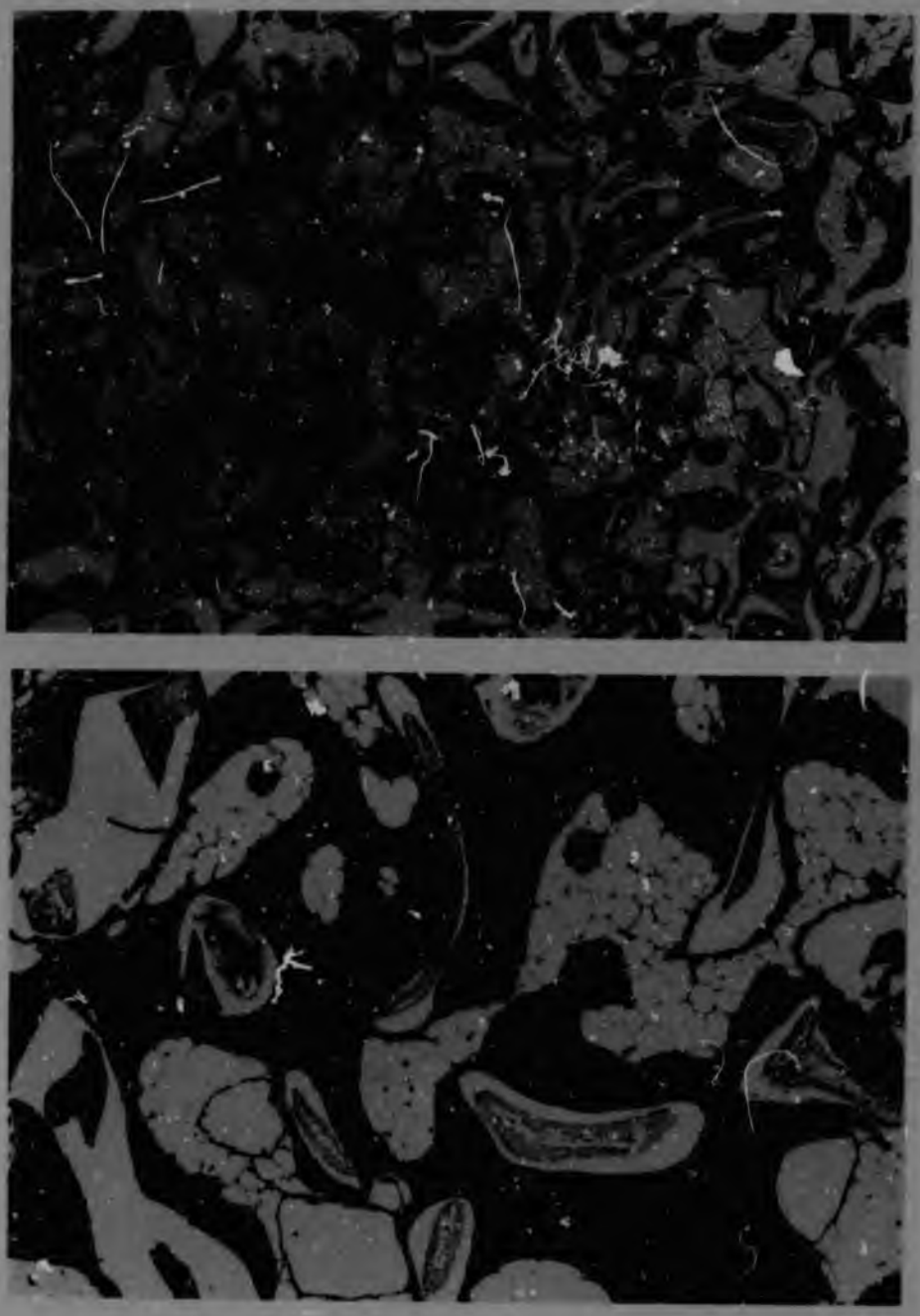


Figure 7.10

Photomicrographs of a specimen of hydroxyapatite harvested at 9 months. **Top panel:** Extensive bone formation within the porous spaces or laminating the hydroxyapatite substratum. **Bottom panel:** High power view of the remodelled lamellar bone enveloping marrow tissue (decalcified section, toluidine blue, original magnification x 10 and x 50).

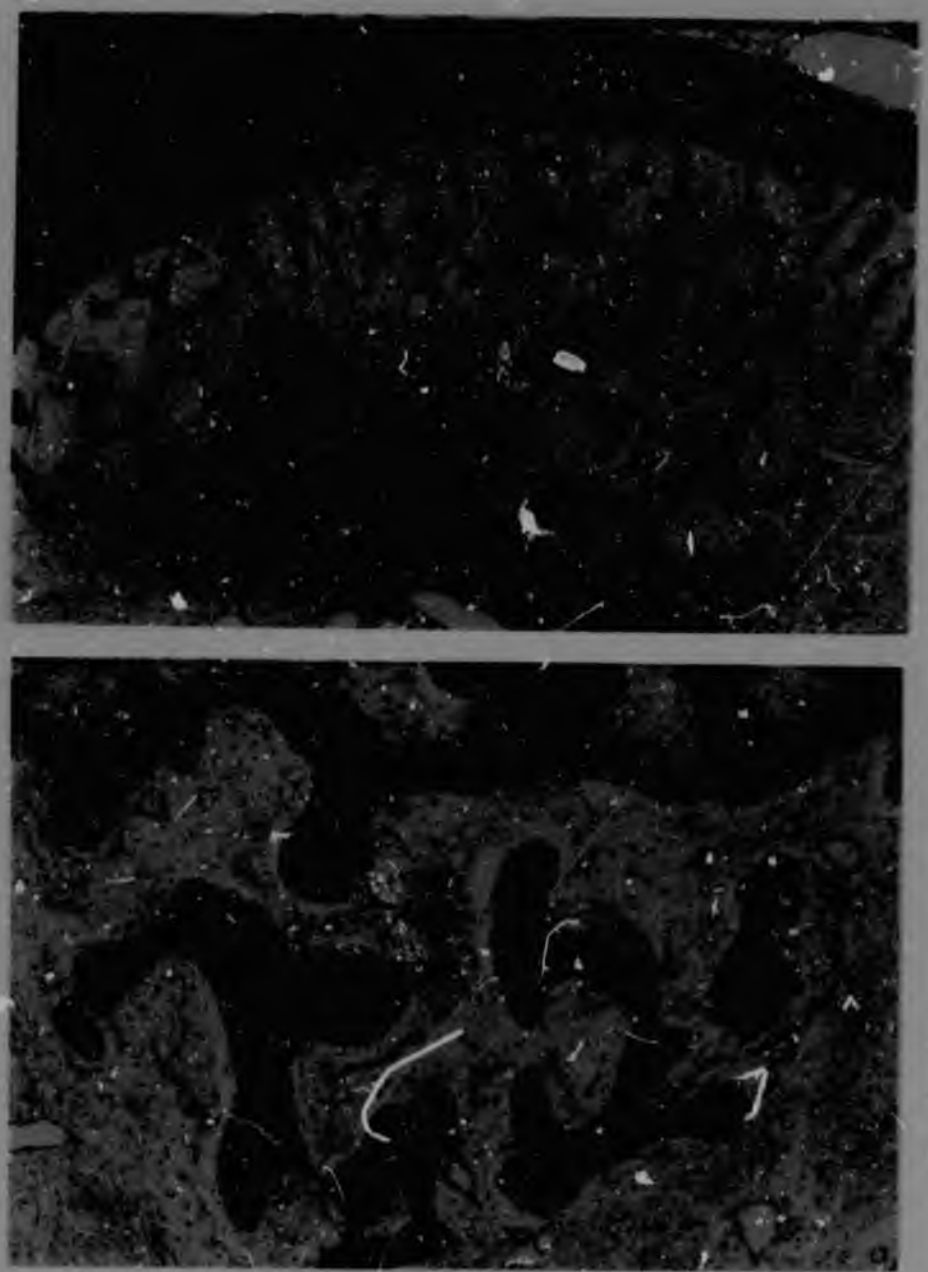


Figure 7.11

Photomicrographs of a specimen of AAA bone-hydroxyapatite composite harvested at 3 months. **Top panel:** Delicate trabeculae of newly formed woven bone had invaded the fibrovascular space between the implanted AAA bone matrix (top) and the hydroxyapatite substratum (bottom). **Bottom panel:** High power view of the newly formed bone showing multiple foci of mineralization, and contiguous osteoblasts lining the newly deposited osteoid (undecalcified section, Goldner's trichrome, original magnification x 20 and x 80).

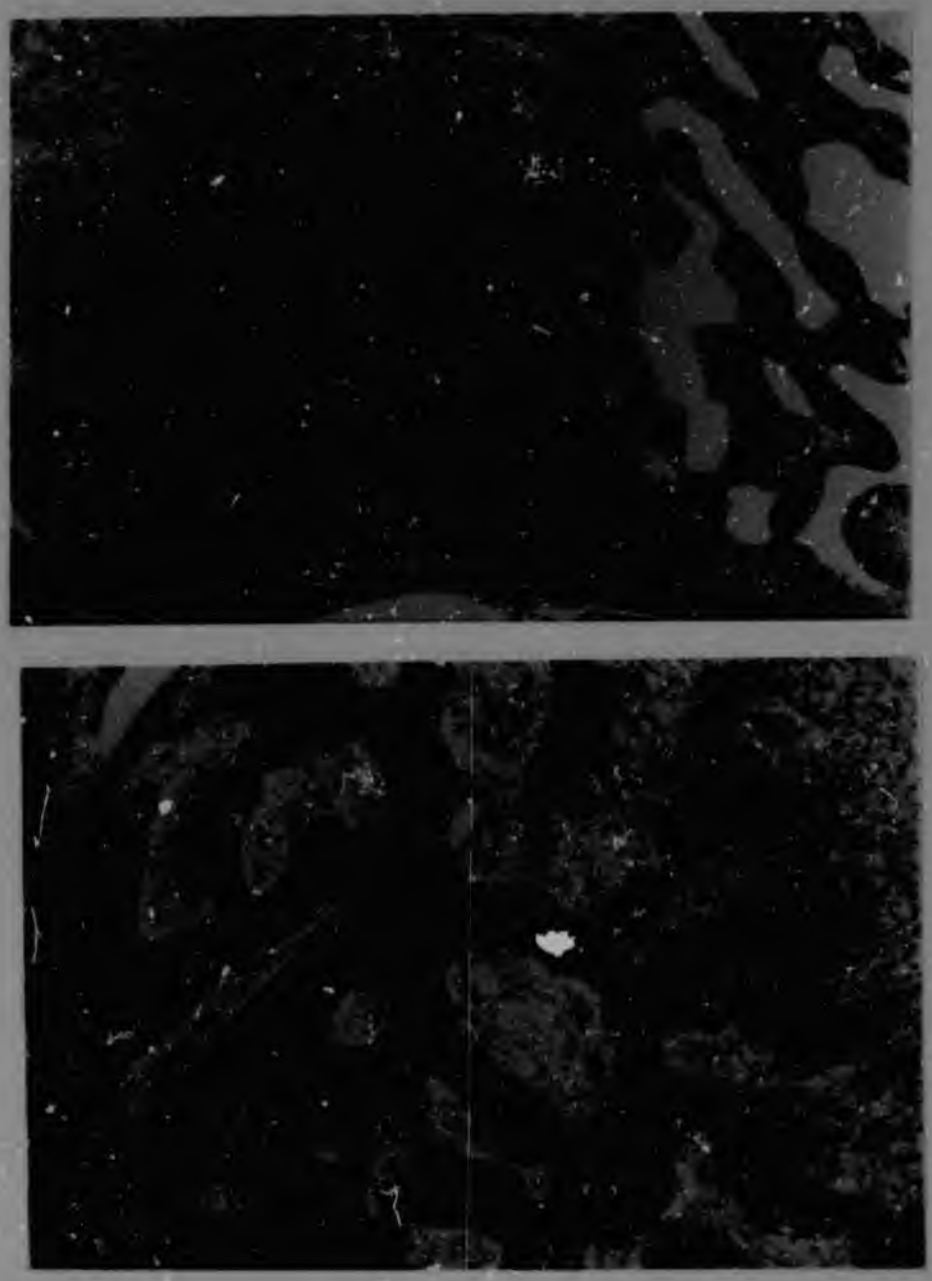


Figure 7.12

Photomicrographs of a specimen of AAA bone-hydroxyapatite composite harvested at 9 months. **Top panel:** Low power view showing the interface between matrix-induced bone (left) and the hydroxyapatite substratum (right). **Bottom panel:** High power view showing the organization of the mineralized ossicle lined by continuous osteoid seams. Newly deposited woven bone shows focal areas of mineralization (undecalcified section, Goldner's trichrome, original magnification x 20 and x 80).

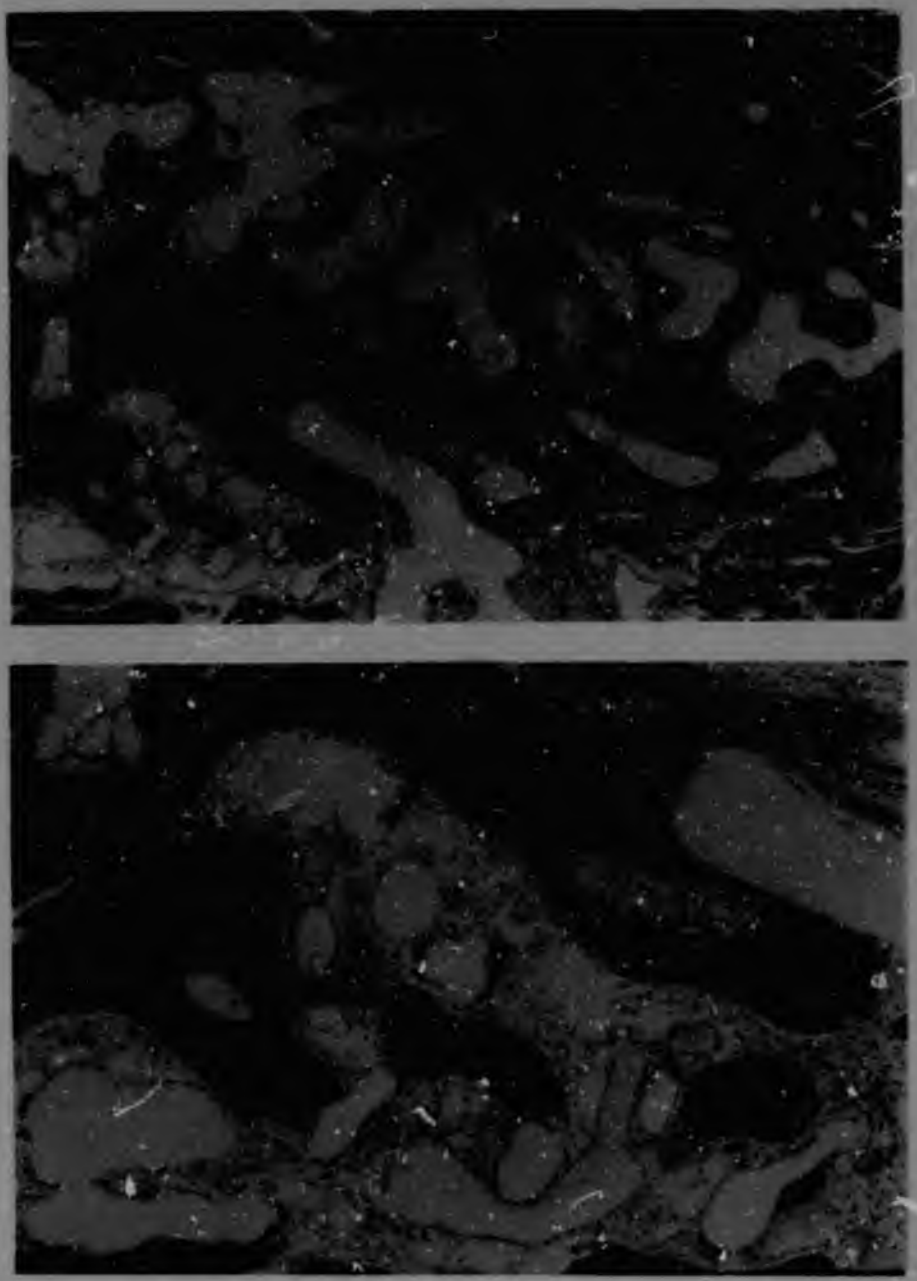


Figure 7.13

Photomicrograph of a specimen of AAA bone-hydroxyapatite composite harvested at 6 months. **Top panel:** Low power view showing the surface boundary between matrix-induced bone (top) and the hydroxyapatite substratum (bottom). Generation of marrow within newly formed bone lined by osteoid seams. **Bottom panel:** High power view of the bone forming within the porous spaces of the hydroxyapatite: wide osteoid seams and lack of mineralization (undecalcified section, Goldner's trichrome, original magnification x 20 and x 80).



Figure 7.14

Photomicrograpn of a specimen of AAA bone-hydroxyapatite composite harvested at 6 months. Extensive bone formation from both the surrounding chemosterilized AAA bone matrix (top) and within the porous spaces of the hydroxyapatite with bone marrow formation (decalcified section, toluidine blue, original magnification x 20).

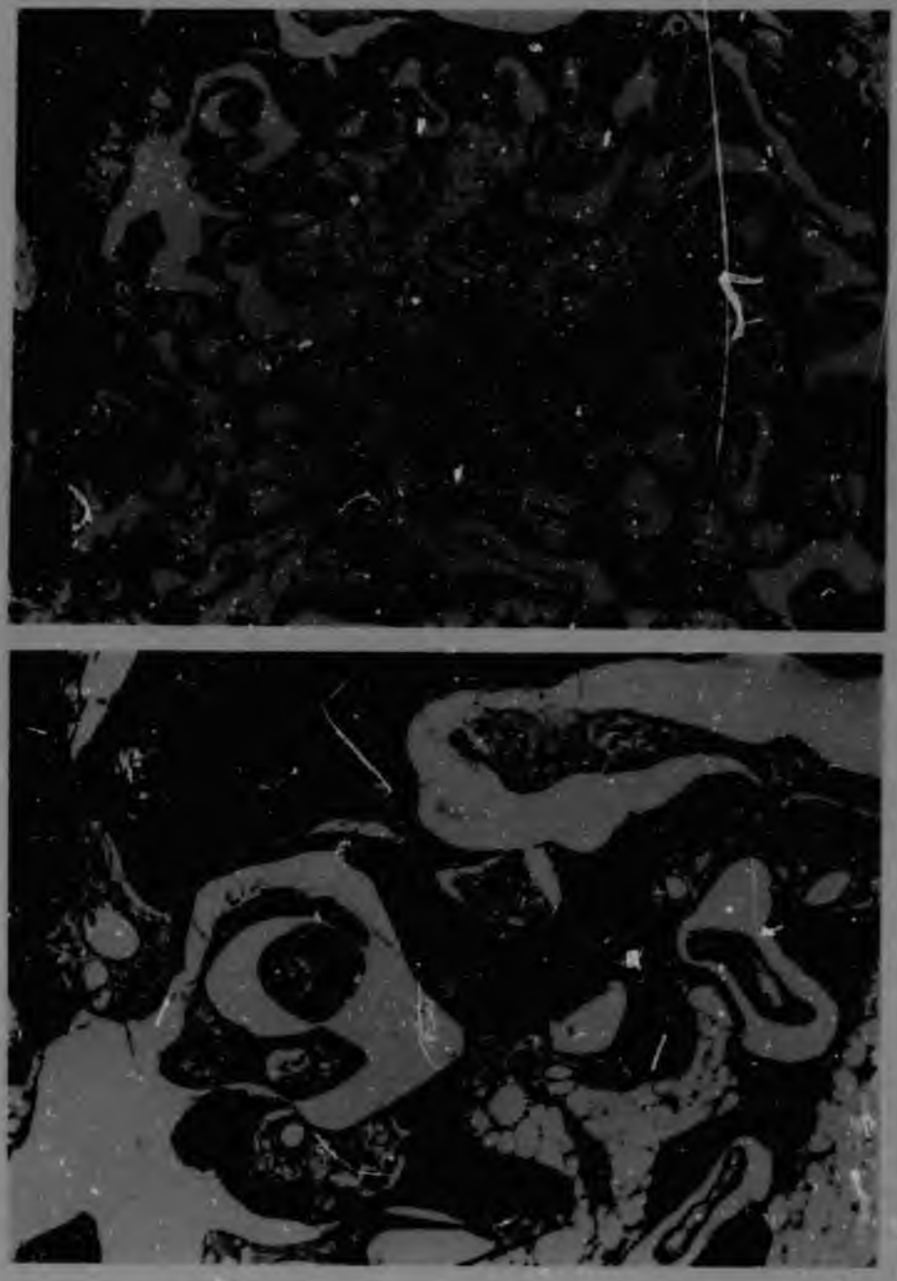


Figure 7.15

Photomicrographs of a specimen of AAA bone-hydroxyapatite composite harvested at 9 months. **Top panel:** Extensive bone and marrow formation within the porous spaces of the hydroxyapatite. Bone, originating from the AAA bone envelope (left) has fused with bone forming within the porous spaces. **Bottom panel:** High power view showing the remodeled lamellar bone and the associated marrow tissue (decalcified section, toluidine blue, original magnification x 10 and x 50).



Figure 7.16

Photomicrograph of a specimen of AAA bone-hydroxyapatite composite harvested at 6 months. Mineralized bone (appositional to the hydroxyapatite substratum) is lined by wide osteoid seams, occasionally populated by contiguous osteoblasts. Note focal areas of mineralization within the newly formed woven bone (undecalcified section, Goldner's trichrome, original magnification x 20).



Figure 8.1

Composite photomicrographs of sections from untreated calvarial defects. A: Anterior defect at 3 months showing ostegenesis confined to the calvarial margins. Note the continuous osteoid seams lining the newly formed mineralized bone, and the fusion of the temporalis muscle with the dura. B: Bone deposition in an anterior defect at 9 months, particularly at one calvarial margin (right panel). C: A minimal amount of bone is present in a posterior defect, 9 months after surgery. Note the temporalis muscle within the defect (undecalcified sections, Goldner's trichrome, original magnification x 15).

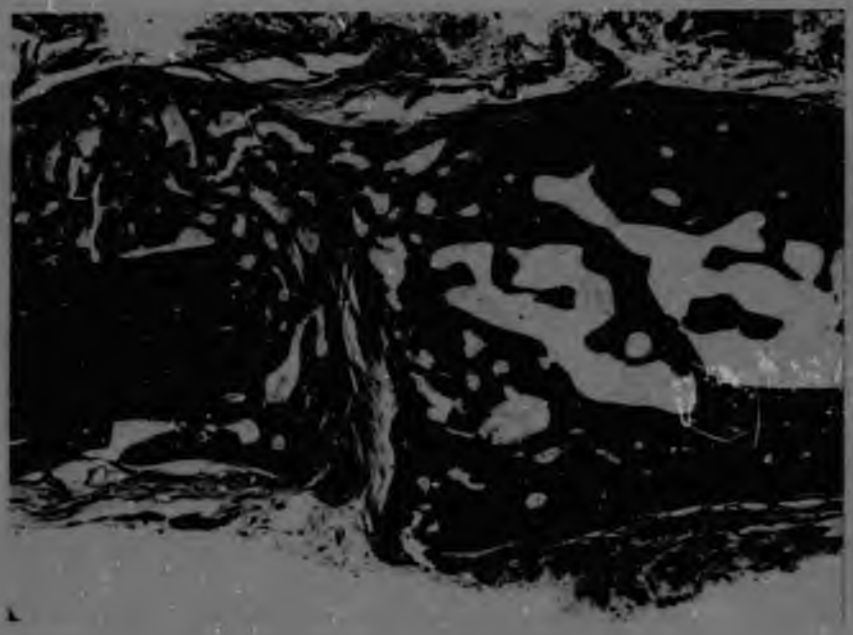


Figure 8.2

Autogenous cortico-cancellous bone, three months after grafting. Extensive pericranial bone deposition unites the graft to the recipient calvaria (closed arrows). Note the pericranial and endocranial bone deposition along the margin of the severed calvaria invading the cancellous spaces of the implanted graft (open arrows) (undecalcified section, Goldner's trichrome, original magnification, x 15).



Figure 8.3

Composite photomicrographs of specimens of autogenous bone grafted in calvarial defects. A: 6 months specimen showing the callus at the calvarial interface, and the progression of bone deposition along both the pericranial and endocranial surfaces of the grafted bone. B: 3 months specimen grafted in an anterior defect. There is an inflammatory infiltrate (arrowed). Resorption of the implanted matrix, extensive osteogenesis, and formation of trabecular bone lined by continuous osteoid seams. Nonunion at one interface (right panel). This inflammatory infiltration was only found in one specimen (undecalcified sections, Goldner's trichrome, original magnification x 15).



Figure 8.4

Photomicrograph of a specimen of AAA bone matrix harvested 3 months after calvarial implantation. Extensive bone formation at the interface after dissolution and resorption of the AAA bone matrix. Note also the prominent bone deposition at the pericranial and endocranial surfaces of the implanted matrix. White arrows outline the margins of the craniotomy preparation (left), and the mineralized remnants of the AAA bone matrix enveloped in newly formed bone. Bone is also forming within the original diploic spaces of the chemosterilized calvarial disc (undecalcified section, Goldner's trichrome, original magnification x 15).

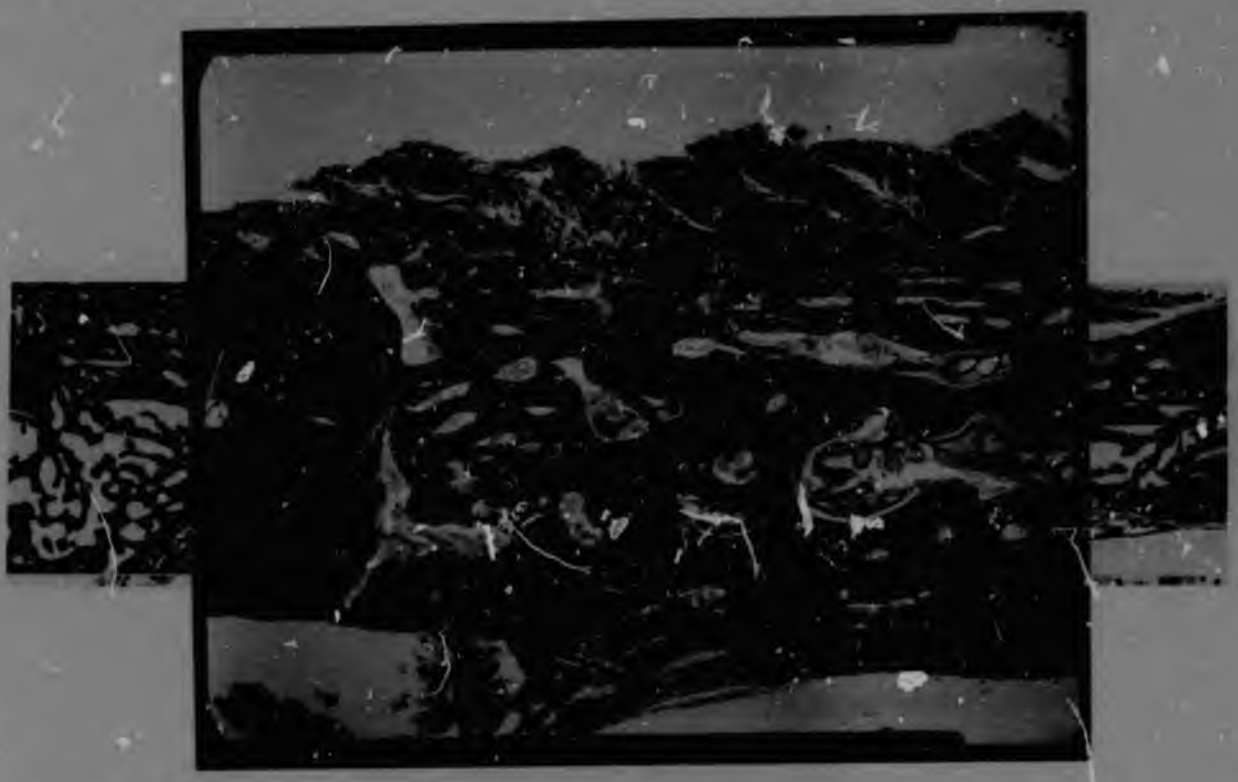


Figure 8.5

Photomicrograph of a specimen of AAA bone matrix harvested 3 months after calvarial implantation. Note the incorporation of the allogeneic implant at the recipient calvarial interface (closed arrows) and the bone deposition at the pericranial surface of the specimen uniting the implant to the recipient calvaria. Note also newly formed bone lined by osteoid seams (in black) within the original diploic spaces of the chemosterilized calvarial disc. Open arrows, at the endocranial surface, indicate remnants of demineralized matrix, which provides a substratum for bone formation after fibrovascular invasion of the matrix. The corresponding pericranial demineralized layer has been replaced by newly formed bone (undecalcified section, Goldner's trichrome, original magnification x 15).



Figure 8.6

Photomicrographs of specimens of AAA bone matrix harvested at 3 months after implantation. **Top panel:** New bone, both woven (open arrows) and lamellar (closed arrows), had formed within the open diploic spaces in the central area of a chemosterilized disc 3 months after implantation. Note the dissolution of the pericranial layer of demineralized matrix. Note also the prominent endocranial bone formation appositional to the "unmasked" mineralized implanted matrix, after complete dissolution of the external demineralized layer. **Bottom panel:** Trabecular-like pattern of woven bone in the central region of an implant of AAA bone (undecalcified sections, Goldner's trichrome, original magnification x 25 and x 120).



Figure 8.7

Trabecular pattern of pericranial bone formation appositional to the mineralized chemosterilized matrix, 3 months after implantation of an implant of AAA lone. The newly formed and mineralized bone is lined by continuous osteoid seams populated by osteoblasts (arrows) (undecalcified section, Goldner's trichrome, original magnification x 100).



Figure 8.8

Photomicrograph of a specimen of AAA bone matrix harvested at 9 months after implantation. Note bone deposition along the pericranial surface. Invasion and substitution of the implanted matrix with newly formed, remodelled, lamellar bone (arrows) (undecalcified section, Goldner's trichrome, original magnification x 15).



Figure 8.9

Composite photomicrographs of specimens of hydroxyapatite. A: 3 months specimen showing bone formation within the central and internal regions of the implant but fibrous union at the calvarial interfaces. Empty white spaces represent the hydroxyapatite framework dissolved after decalcification during histologic processing. B: Extensive and complete bone penetration in a specimen of hydroxyapatite harvested 6 months after implantation in a posterior defect. Note bone apposition directly above the dura. C: Distribution of bone in a specimen of hydroxyapatite 6 months after implantation. Note the abrupt interruption of bone at one calvarial margin (right panel) (decalcified sections, toluidine blue stain, original magnification x 15).

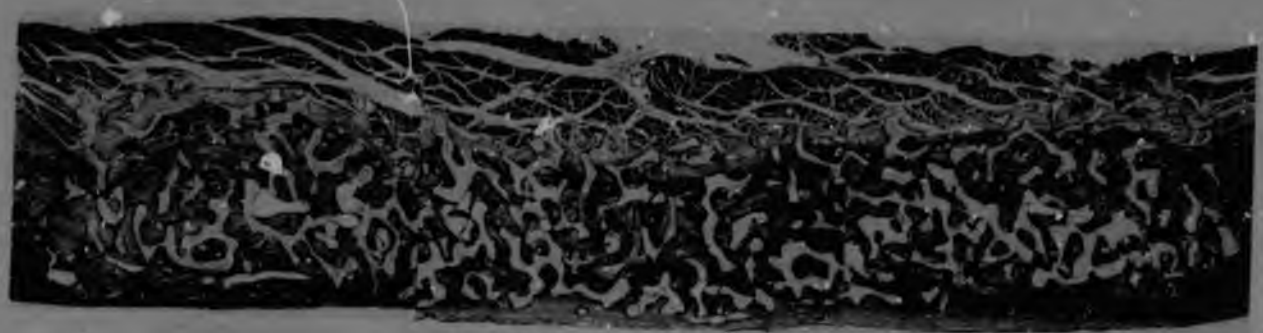


Figure 8.10

Extensive bone deposition in a hydroxyapatite specimen harvested 9 months after implantation in an anterior defect. Note the almost complete regeneration of the internal cortical layer resting directly on the dura (decalcified section, toluidine blue, original magnification x 15).

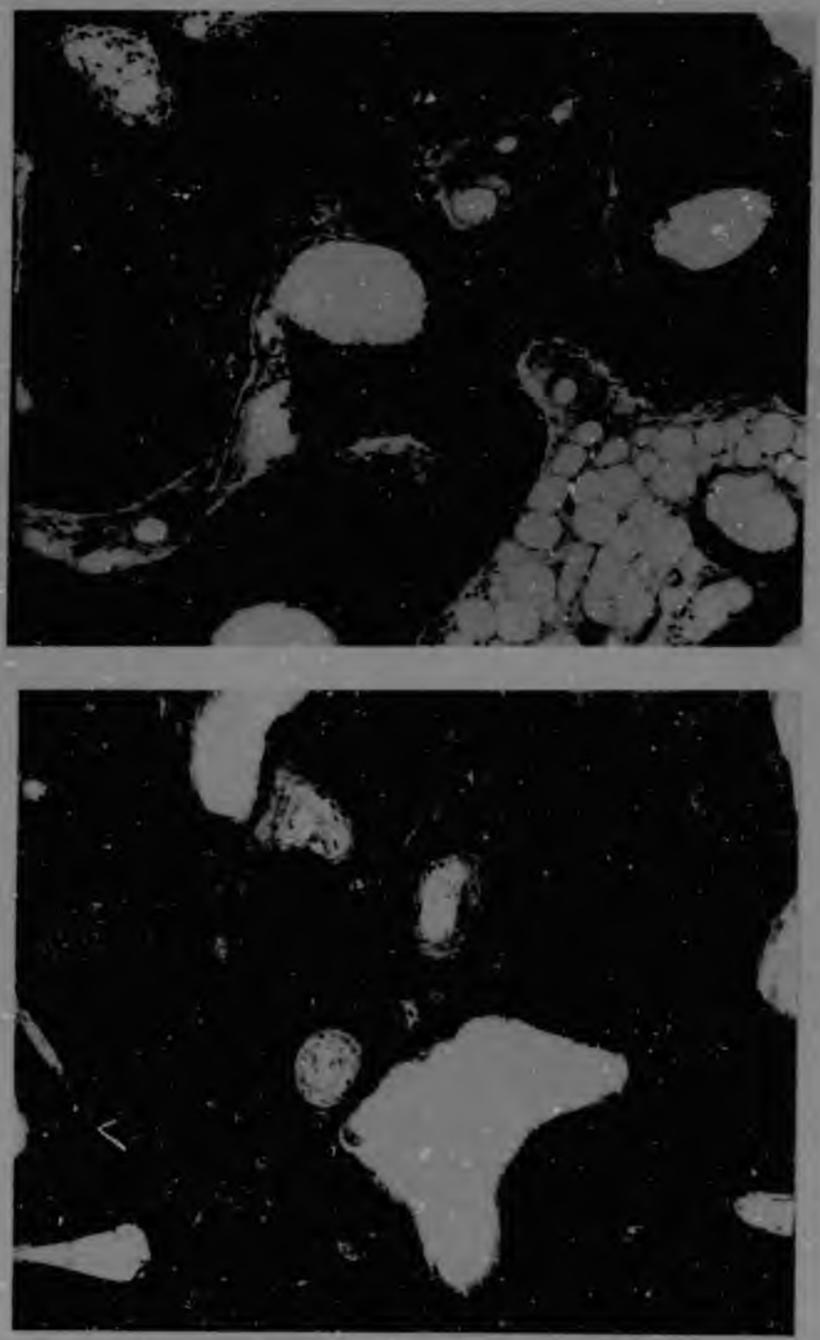


Figure 8.11

Photomicrographs of specimens of hydroxyapatite showing bone organization within the porous spaces. **Top panel:** A specimen harvested at 3 months shows osteoblasts lining continuous osteoid seams (arrowed). Note the formation of bone marrow and the direct apposition of bone to the hydroxyapatite (HA). **Bottom panel:** A specimen harvested at 9 months shows osteoid (open arrow), and lamellar and osteonic bone (closed arrows) (undecalcified sections, Goldner's trichrome, original magnification x 80).

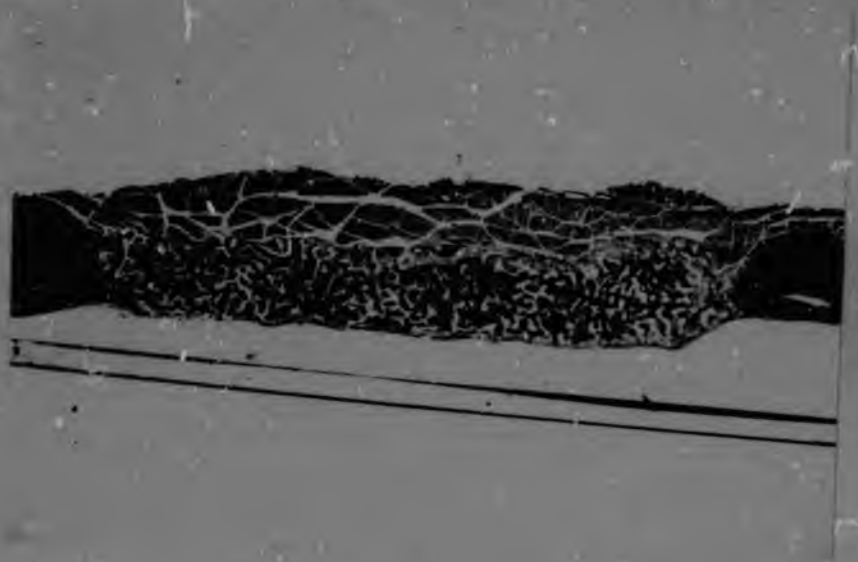


Fig. 8.12

Photomicrograph of a specimen of hydroxyapatite, 9 months after implantation. Note the fibrous union at the interfaces (arrows), but extensive bone deposition within the implant (decalcified section, toluidine blue, original magnification x 2.5).

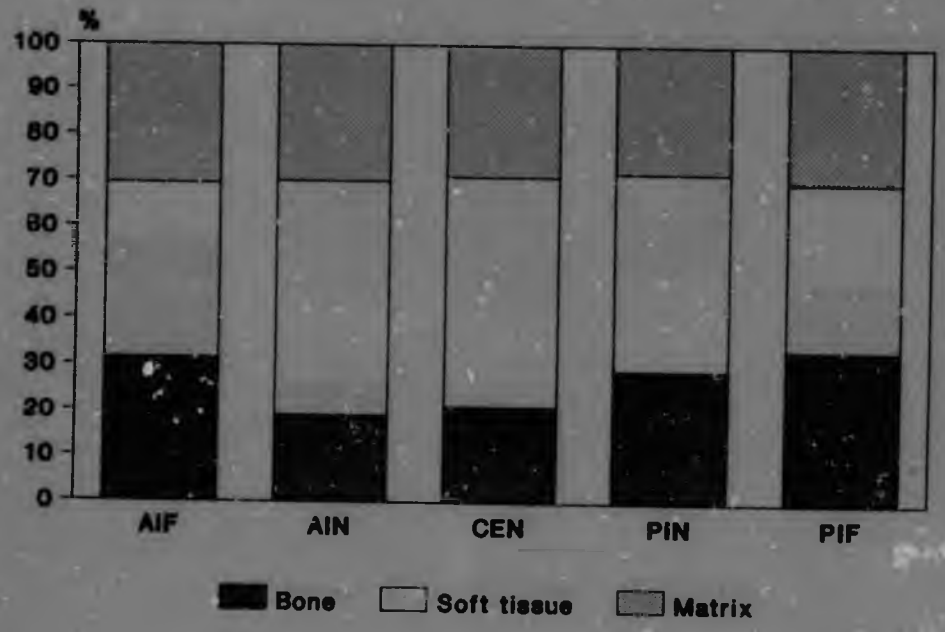


Figure 8.13

Distribution of newly formed bone and implanted matrix framework (in percent) within histomorphometric sources in autogenous bone grafts 3 months after surgery.

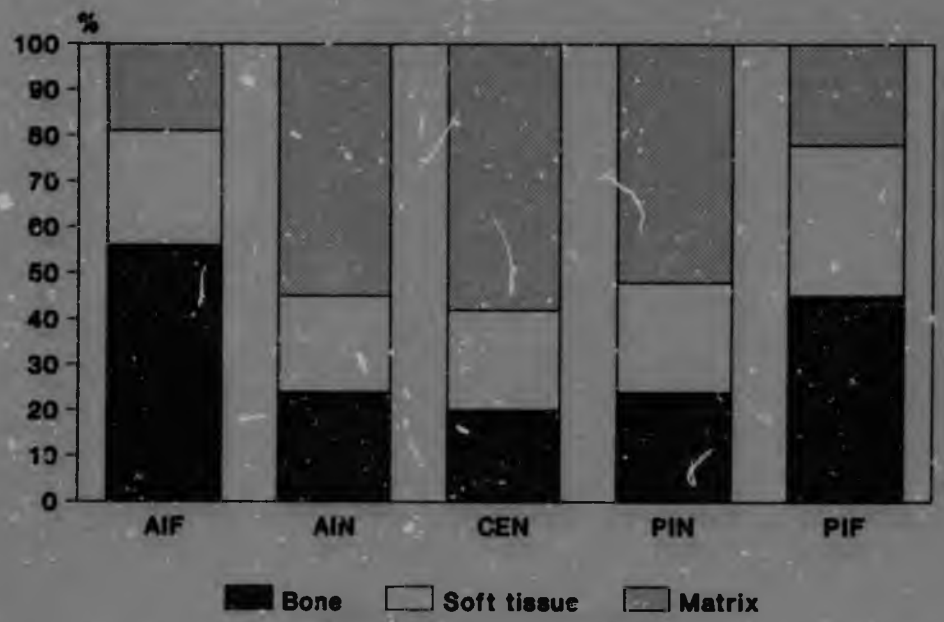


Figure 8.14

Distribution of newly formed bone and implanted chemosterilized matrix (in percent) within histomorphometric sources in autolyzed antigen-extracted allogeneic (AAA) bone implants 3 months after surgery.

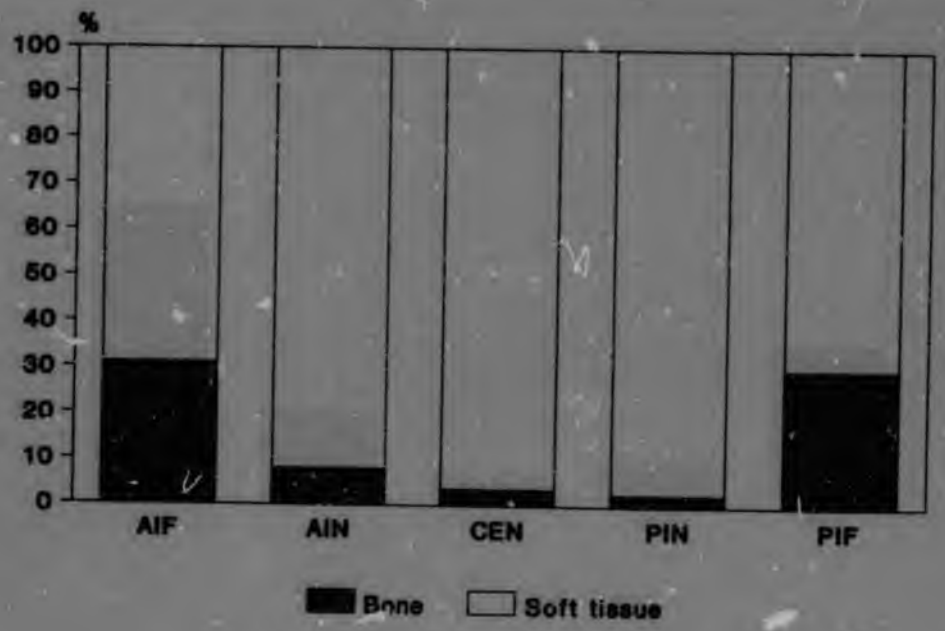


Figure 8.15

Distribution of bone and soft tissue (in percent) within histomorphometric sources in untreated calvarial defects 3 months after surgery.

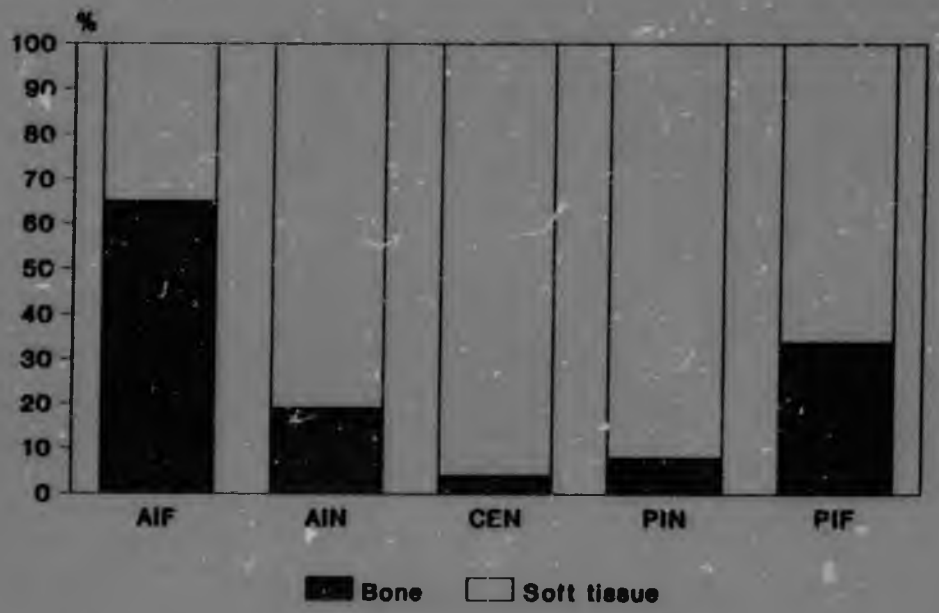


Figure 8.16

Distribution of bone and soft tissue (in percent) within histomorphometric sources in untreated calvarial defects 6 months after surgery.

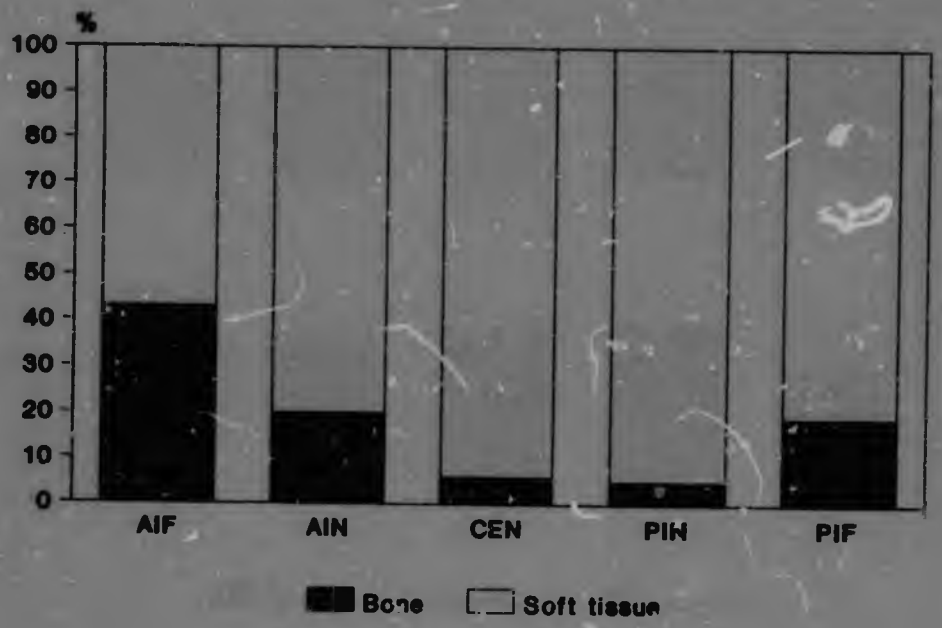


Figure 8.17

Distribution of bone and soft tissue (in percent) within histomorphometric sources in untreated calvarial defects 9 months after surgery.

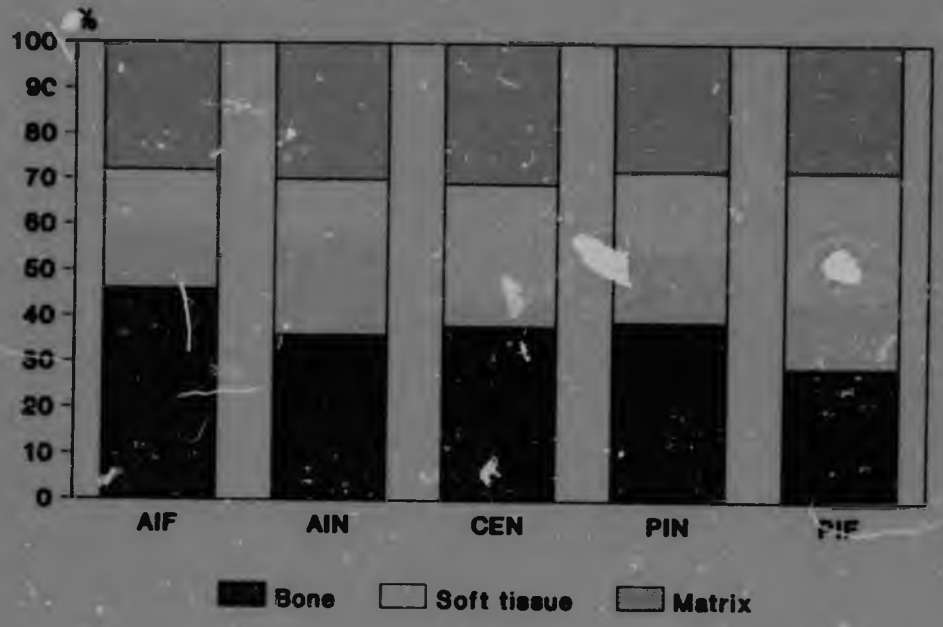


Figure 8.18

Distribution bone and implanted hydroxyapatite framework (in percent) within histomorphometric sources in hydroxyapatite specimens 3 months after surgery.

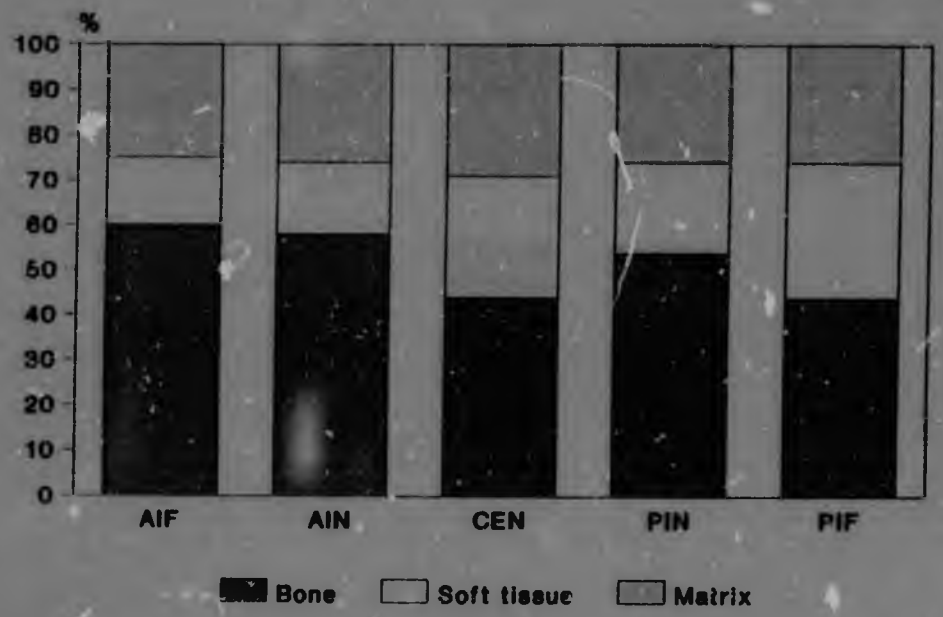


Figure 8.19

Distribution bone and implanted hydroxyapatite framework (in percent) within histomorphometric sources in hydroxyapatite specimens 6 months after surgery.

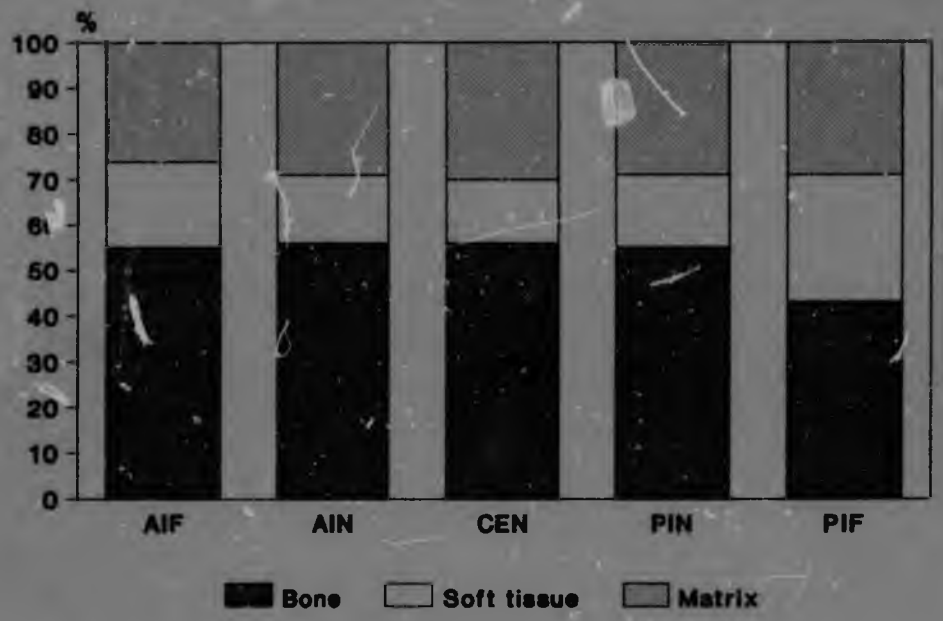


Figure 8.20

Distribution bone and implanted hydroxyapatite framework (in percent) within histomorphometric sources in hydroxyapatite specimens 9 months after surgery.

10. TABLES

Table 5.1

Sequential extraction steps for preparation of baboon chemosterilized autolyzed antigen-extracted allogeneic (AAA) bone matrix

Sequential steps	Temperature	Hours
Stirring in deionized water with 7 mM SA	4°	0.5
Extraction in 1:1 chloroform-methanol	25°	8
Surface demineralization in 0.6 N hydrochloric acid (2 acid changes)	4°	24
Autodigestion in 0.1 M PBS, pH 7.4, with 7 mM SA and 7 mM NEM	37°	48
Stirring in deionized water with 7 mM SA	4°	0.5

PBS: phosphate buffer saline; SA: sodium azide;
NEM: N-ethyl maleimide.

Table 7.1

Values of bone induced by autolyzed antigen-extracted allogeneic bone matrix in 36 AAA bone specimens and 34 AAA bone-hydroxyapatite specimens[a]

	AAA bone specimens		AAA bone-hydroxyapatite specimens	
Period (months)	Number	Induced bone	Number	Induced bone
3	14 (1)	1.6 ±0.9	15	1.3 ± 0.2
6	14 (2)	1.5 ±0.7	10 (6)	1.3 ± 0.3
9	8 (8)	1.6 ±0.6	9 (6)	1.6 ± 0.4

[a] Values are given as means ± standard deviation after semiquantitative histological analysis. The amount of induced bone was graded using values from 0 to 3 as described in Materials and Methods (5.6: Histological analysis).

In parentheses, the number of resorbed AAA bone specimens.

Table 7.2

Percentage of bone matrix resorption in 47 AAA bone specimens and 46 AAA bone-hydroxyapatite specimens[a]

	AAA bone specimens		AAA bone-hydroxyapatite specimens	
Period (months)	Number	Resorption (in percent)	Number	Resorption (in percent)
3	15	16.6 ±24.1[b]	15	20.5 ±4.7[b]
6	16	62.8 ±23.2	16	68.6 ±7.4
9	16	79.6 ±26.7	15	75.0 ±8.4

[a] Values are given as means ± standard deviation after semiquantitative histological analysis.

[b] $P<0.001$ vs 6 and 9 months.

Table 7.3

Volume fraction composition (in percent) of 46 hydroxyapatite specimens[a] and 33 AAA bone-hydroxyapatite specimens[b]

Period (months)	Treatment	Bone	Soft tissue	Matrix[c]
3	Hydroxyapatite	9.2 ±2.1	53.1 ±1.9	37.7 ±1.0
3	AAA bone-hydroxyapatite	6.1 ±2.4	54.9 ±3.3	39.0 ±2.4
6	Hydroxyapatite	25.9 ±2.2[d]	39.4 ±1.5[d]	34.7 ±1.3
6	AAA bone-hydroxyapatite	11.7 ±2.6	51.5 ±2.3	36.7 ±1.7
9	Hydroxyapatite	26.7 ±2.1	42.9 ±1.8	30.4 ±1.2[e]
9	AAA bone-hydroxyapatite	20.2 ±3.1	44.9 ±3.2	34.8 ±1.9

a Mean and standard error of the mean of 16 specimens at 3 months, 14 specimens at 6 months, and 15 specimens at 9 months.

b Mean and standard error of the mean of 8 specimens at 3 months, 14 specimens at 6 months, and 11 specimens at 9 months.

c Matrix indicates the implanted framework of the hydroxyapatite implants.

d $P<0.01$ vs AAA bone-hydroxyapatite composites

e $P<0.05$ vs AAA bone-hydroxyapatite composites

Table 8.1

Volume fraction composition (in percent) of untreated defects, autogenous bone grafts, autolyzed antigen-extracted allogeneic (AAA) bone matrix implants, and hydroxyapatite specimens[a]

Period (months)	Treatment	Bone	Osteoid	Soft Tissue	Matrix[b]
3	Untreated defects	13.0±2.6	1.85±0.4	87.0±2.6	---
3	Bone grafts	26.8±1.9[c]	3.72±0.5[c]	44.2±2.7	29.0±2.3
3	AAA bone implants	33.8±2.7[d]	4.20±0.4[d]	25.0±1.4	41.2±3.1
3	Hydroxyapatite	37.4±2.7[e]	---	33.5±2.7	29.1±0.7
6	Untreated defects	25.9±4.4	2.70±0.5	74.1±4.5	---
6	Bone grafts	---	1.80±0.3	48.1±2.3	51.9±2.3[f]
6	AAA bone implants	---	3.02±0.3[g]	26.2±1.8	73.8±1.7[f]
6	Hydroxyapatite	51.8±2.7[h]	---	22.0±2.5	26.2±0.8
9	Untreated defects	18.6±3.8	0.97±0.2	81.4±3.8	---
9	Bone grafts	---	0.65±0.2	37.6±2.5	62.4±2.5[f]
9	AAA bone implants	---	1.22±0.1[g]	17.6±1.3	82.4±1.2[f]
9	Hydroxyapatite	52.8±2.3[h]	---	18.7±2.1	28.5±0.9

[a] Mean and standard error of the mean of 8 specimens per treatment modality in 8 animals per observation period. Bone indicates mineralized bone plus osteoid.

[b] Matrix indicates the implanted matrices of bone grafts, AAA bone and hydroxyapatite implants.

[c] $P<0.01$ vs untreated defects.

[d] $P<0.05$ vs bone grafts, and $P<0.01$ vs untreated defects.

[e] $P<0.01$ vs bone grafts, and $P<0.001$ vs untreated defects.

[f] Cumulative percent of newly formed bone and implanted matrix as described in Section III, 8.2: Histomorphometry.

[g] $P<0.05$ vs bone grafts.

[h] $P<0.001$ vs untreated defects.

Table 8.2

Volume fraction composition (in percent) of anterior and posterior untreated calvarial defects[a]

	Anterior specimens		Posterior specimens	
Period (months)	Bone	Osteoid	Bone	Osteoid
3	14.6 ±4.3	2.10 ±0.65	11.5 ±2.9	1.60 ±0.44
6	34.9 ±6.5[b]	3.85 ±0.76[b]	17.0 ±5.3	1.55 ±0.57
9	27.6 ±5.7[b]	1.25 ±0.31	9.7 ±4.3	0.70 ±0.34

[a] Mean and standard error of the mean of 4 anterior and 4 posterior specimens in 8 animals per observation period.

[b] $P<0.05$ vs posterior defects.

Table 8.3

Volume fraction composition (in percent) of anterior and posterior hydroxyapatite specimens[a]

	Anterior Specimens		Posterior Specimens	
Period (months)	Bone	Matrix	Bone	Matrix[b]
3	40.1 ±3.6	27.8 ±1.1	34.7 ±4.0	30.4 ±0.9
6	46.0 ±4.3	26.3 ±1.2	57.6 ±2.6	26.1 ±0.9
9	55.1 ±3.5	27.7 ±1.6	50.5 ±3.1	29.1 ±1.1

a Mean and standard error of the mean of 4 anterior and 4 posterior specimens in 8 animals per observation period.

b Matrix indicates the implanted framework of the hydroxyapatite implants.

Table 8.4

Distribution of bone and matrix framework (in percent) within histomorphometric sources in autogenous bone grafts and autolyzed antigen-extracted allogeneic (AAA) bone matrix implants 3 months after surgery[a]

	Bone grafts		AAA bone implants	
Source	Bone	Matrix	Bone	Matrix
	P<0.05	NS	P<0.01	P<0.01
AIF	31.5±2.6	30.6±5.4	55.7±1.9	18.7±2.8
AIN	18.9±4.7	30.4±6.6	24.0±1.8	54.6±2.6
CEN	20.7±3.8	29.5±4.5	19.8±4.1	58.4±3.9
PIN	29.2±5.4	28.5±5.4	24.1±4.4	52.0±4.6
PIF	33.5±3.7	25.9±4.7	45.3±3.3	22.5±2.9

[a] Mean and standard error of the mean of 8 specimens in 8 animals per treatment modality. P values indicate levels of significance between sources.

AIF: anterior interfacial; AIN: anterior internal; CEN: central; PIN: posterior internal; PIF: posterior interfacial (see Fig. 6.9).

Table 8.5

Distribution of bone and osteoid (in percent) within histomorphometric sources in untreated calvarial defects[a]

	3 months		6 months		9 months	
Source	Bone	Osteoid	Bone	Osteoid	Bone	Osteoid
	P<0.001		P<0.001		P<0.001	
AIF	30.6±7.6	3.75±1.2	65.6±5.4	6.50±0.7	43.2±6.7	2.00±0.7
AIN	7.7±3.0	1.25±0.6	18.7±7.8	2.62±1.3	19.7±9.9	1.12±0.5
CEN	3.5±2.9	0.25±0.2	3.9±2.8	0.50±0.5	5.9±4.9	0.62±0.4
PIN	2.5±2.1	0.50±0.5	7.7±5.2	1.00±0.8	4.9±3.5	0.37±0.2
PIF	20.9±4.8	3.50±0.8	33.7±7.8	2.87±0.9	19.3±9.2	0.75±0.5

[a] Mean and standard error of the mean of 8 specimens in 8 animals per observation period. P values indicate levels of significance between sources.

AIF: anterior interfacial; AIN: anterior internal; CEN: central; PIN: posterior internal; PIF: posterior interfacial (see Fig. 6.9).

Table 8.6

Distribution of bone and matrix framework (in percent) within histomorphometric sources in hydroxyapatite specimens[a]

	3 months		6 months		9 months	
Source	Bone	Matrix	Bone	Matrix	Bone	Matrix
AIF	46.0±3.8	27.5±1.9	53.9±2.4	24.5±1.9	54.7±7.0	25.4±2.6
AIN	35.7±6.2	30.6±1.0	57.5±2.9	26.1±1.6	56.1±2.4	28.7±1.5
CEN	37.7±6.3	31.0±1.6	44.1±7.2	29.4±1.0	55.6±4.5	29.7±1.6
PIN	38.7±6.8	28.5±1.3	53.5±5.9	25.1±2.3	55.0±2.4	28.7±2.0
PIF	28.7±6.3	27.9±2.0	44.0±8.1	26.0±1.6	42.4±7.1	28.5±3.2

[a] Mean and standard error of the mean of 8 specimens in 8 animals per observation period.

AIF: anterior interfacial; AIN: anterior internal; CEN: central; PIN: posterior internal; PIF: posterior interfacial (see Fig. 6.9).

Table 8.7

Volume fraction composition (in percent) of control calvarial specimens[a]

	Anterior calvariae	Posterior calvariae
Bone	86.7 ± 1.8[b]	92.9 ± 2.8
Marrow	13.3 ± 1.8[b]	7.1 ± 2.8

[a] Mean and standard error of the mean of 10 anterior and 10 posterior specimens representing 5 adult male baboons.

[b] $P<0.01$ vs posterior calvariae.

Table 8.8

Bone volume (in per:ent) in anterior and posterior untreated and treated calvarial defects 3 months after surgery[a]

	Anterior defects		Posterior defects	
Treatment	Bone: Volume %	Bone: Volume % related to control calvariae	Bone: Volume %	Bone: Volume % related to control calvariae
Untreated defects	14.6±4.3	16.8	11.5±2.9	12.4
Bone grafts	28.1±3.1	32.4	25.4±2.6	27.3
AAA bone implants	36.1±3.6	41.6	31.4±3.9	33.8
Hydroxyapatite	40.1±3.6	46.2	34.7±4.0	37.3

[a] Mean and standard error of the mean of 4 anterior and 4 posterior specimens per treatment modality in 8 animals.

[b] Bone indicates mineralized bone plus osteoid.

SECTION IV

DISCUSSION

11. THE HETEROTOPIC INTRAMUSCULAR STUDY

11.1 The Induction of Bone with Autolysed Antigen-Extracted Allogeneic Bone Matrix

During the past three decades, a considerable research effort has been directed toward the phenomenon of bone formation by induction, and the biochemical and molecular characterization of the bone morphogenetic proteins (Celeste et al., 1990; Reddi 1981, 1985, 1992; Urist 1989, 1992, Urist et al., 1983a, 1987a, Vukicevic et al., 1993; Wozney et al., 1988). However, the vast majority of the *in vivo* experiments have been performed in rodent models, endowed with a characteristic high potential for bone regeneration (Schmitz and Hollinger, 1986; Urist, 1989). The clinical value of the phenomenon of bone formation by induction rests in its unequivocal demonstration in extraskeletal sites of primates. The results of the present heterotopic study have demonstrated that intramuscular implantation of chemosterilized

allogeneic bone matrix results in bone formation by induction in adult baboons.

The first demonstration of bone induction in nonhuman primates, albeit limited, was reported by Hosny and Sharawy (1985) after subcutaneous implantation of demineralized bone matrix in adult Rhesus monkeys. In this experiment, subcutaneous implantation of demineralized bone matrix resulted in endochondral bone formation. Intervening cartilage was seen by day 40 after matrix implantation, and by day 72 the implants showed both woven and lamellar bone and formation of marrow (Hosny and Sharawy, 1985).

The developmental cascade leading to bone differentiation by induction is the result of complex interactions between bone morphogenetic proteins released by the extracellular matrix of bone and responding recipient cells (Reddi, 1981, 1982, 1992; Urist 1965, 1989, 1992; Urist et al., 1983a). A number of reports using primate bone matrix preparations implanted intramuscularly in both primates and athymic rodents have suggested that the observed failure of bone induction in primates is related to the lack of responding cells capable of transformation and differentiation (Aspenberg and Andolf, 1989; Aspenberg

et al., 1988). The present investigation firmly establishes that the intramuscular site of adult baboons is endowed with a complement of mesenchymal cells capable of transformation under the mitogenic and differentiating stimulus of bone morphogenetic proteins released by allogeneic surface-demineralized bone. The failure of bone induction reported by Aspenberg et al. (1988) in a different nonhuman primate model is difficult to explain. Incorrect matrix preparation or the use of autogeneic rather than allogeneic bone matrix could have been responsible for the observed lack of biological activity.

In more recent studies, Aspenberg et al. (1991) have suggested that the concentration of bone morphogenetic proteins within monkey bone matrix may not be sufficient to induce bone formation in intramuscular sites of adult monkeys (Aspenberg et al., 1991). It is noteworthy that identical monkey bone matrix preparations did induce bone formation in athymic rats (Aspenberg et al., 1991). The athymic rat is a valuable model to study bone differentiation induced by xenogeneic bone matrix preparations, including human demineralized bone matrix (Aspenberg et al., 1989, 1992; Ripamonti et al., 1991). Collectively, these experiments in athymic rats have demonstrated that

T-cell functions are not a requirement for bone induction, although immunologically competent euthymic rats block the developmental cascade of bone differentiation (Ripamonti et al., 1991).

The histological analysis of the present material did not show endochondral bone formation by induction as typically described in rodent models using AAA bone (Urist, 1980; Urist et al., 1975). Cartilage was never observed in the present series, possibly due to the lack of early observation periods. An interesting feature was the presence of florid woven bone at 6 and 9 months after implantation. This suggests direct intramembranous bone differentiation without an intervening chondrogenic phase. Bone deposition during the labelling period was confirmed by fluorescence of the mineralization fronts. A continuous source of bone morphogenetic proteins released to competent responding cells might have been provided by osteoclastic resorption of the mineralized surfaces of the implanted matrices. Conceivably, a mechanism of matrix resorption and subsequent exposure and release of bone morphogenetic proteins tightly bound to the mineral phase may explain the frequent presence of induced bone lining previously resorbed areas of mineralized matrix. Alternatively, after the initial matrix-induced first

waves of bone differentiation, continuous formation of woven bone up to 9 months could have been the result of a self-sustaining mechanism. Newly forming bone might have been responsible for the local production and release of bone morphogenetic proteins and other growth factors initiating a phenomenon of autoinduction in the newly formed ossicles. Indeed, the accumulation and compartmentation of transforming growth factor-ß (TGF-ß) has been suggested to play an important role in the regulation of ossification during *in vivo* bone development by induction (Carrington et al., 1988).

The presence of induced bone in direct apposition to mineralized surfaces of the matrix was surprising, since a number of studies have shown that mineralized bone particles are unable to induce bone formation. Instead, subcutaneous implantation of mineralized bone leads to the recruitment of multinucleated giant cells (Reddi and Huggins, 1972b). This suggests that the mineral phase prevents expression of bone-inducing activity (Sampath and Reddi, 1984a), and that the differentiation of osteoclasts is related to specific factors within the bone matrix which are intimately associated with the mineral phase (Glowacki and Cox, 1986; Krukowski and Kahan, 1982; Reddi and Huggins, 1972b). The observation of induced bone forming in

apposition to mineralized matrix is, however, in agreement with previous results showing osteoinduction in mineralized bone implants treated with chemical inhibitors of endogenous matrix proteases (Urist, 1972).

The finding of several areas of newly formed woven, nonmineralized bone, seems to indicate failure or delay of the mineralization process in some animals. At the moment, no data are available on the vitamin D metabolism in baboons housed for extended periods in absence of sunlight, which might have been responsible for delayed mineralization in spite of the balanced dietary supplementation. It is also possible that the newly developing ossicles in extraskeletal sites lack a biochemical microenvironment needed for the final assembly and mineralization of newly deposited osteoid and woven bone.

The demonstration of bone induction in a large series of adult nonhuman primates indirectly supports the clinical application of the bone induction principle using bone morphogenetic protein preparations in reconstructive craniofacial and orthopaedic surgery in man (Glowacki et al., 1981b; Johnson et al., 1988). The results of the present study have been confirmed and

extended in adult baboons using increasingly purified bone morphogenetic protein preparations (Ripamonti et al., 1991; Ripamonti et al., 1992a). Other studies have demonstrated bone differentiation by induction in baboons using human bone matrix (Ripamonti et al., 1991). The induction of bone by preparations of human bone matrix is noteworthy, and suggests that intact bone matrices, as opposed to those in rodents, may not be species-specific (Ripamonti et al., 1991). Studies in other laboratories using different primate species have extended these observations in baboons showing bone formation by induction in adult squirrel monkeys (*Saimiri sciureus sciureus*) and crab-eating monkeys (*Macaca fascicularis*) (Aspenberg et al., 1992; Miyamoto et al., 1993).

11.2 The Hydroxyapatite-Induced Osteogenesis Model

Several experimental studies have been performed in orthotopic and heterotopic sites using porous hydroxyapatite replicas of calcium carbonate exoskeletons with an average porosity of 200 μm in diameter (Interpore 200) (Chiroff et al., 1975; Holmes, 1979; Holmes and Hagler, 1988a; Holmes et al., 1987; Piecuch et al., 1983). A comparatively limited material has been presented, however, using the 600 μm specification (Interpore 500) obtained from the exoskeletal microstructure of corals of the genus Goniopora (Holmes et al., 1986). The framework of the 600 μm specification appears similar to that of cancellous bone, and morphometrical comparison of its microstructure with bone harvested from human iliac crests shows a remarkable degree of morphological similarity (Holmes et al., 1986). Whilst both hydroxyapatites have clearly provided evidence of their osteoconductive potential when implanted in close apposition to viable bone, the heterotopic implantation in canine and rodent models has excluded osteoinductive properties (Piecuch, 1982; White and Shors, 1986). The present investigation, however, firmly establishes that porous hydroxyapatite obtained from calcium carbonate

exoskeletons of corals of the genus Goniopora are capable of *inducing* bone differentiation in direct contact with the hydroxyapatite when implanted extraskeletally in adult baboons. It is noteworthy that bone formation was also later observed in specimens of porous hydroxyapatite obtained from the coral of the genus Porites, with an average porosity of 200 μm in diameter when implanted intramuscularly in baboons (van Eeden and Ripamonti, 1993) and rhesus monkeys (Vargervik, 1992).

While this discovery may be important in the therapeutic initiation of bone formation as an alternative to autogenous bone grafts, the cellular and molecular signals that regulate bone differentiation in the porous hydroxyapatite are not understood. The histological analysis suggests that the differentiation of bone may be intimately associated with the morphogenesis of the connective tissue condensations at the hydroxyapatite interface. The formation of compact mesenchymal aggregates or condensations is one of the earliest morphogenetic events associated with position-dependent differentiation of skeletal structures in the developing vertebrate limb and during intramembranous ossification (Newman, 1988; Thompson et al., 1989). Similarly, the differentiation of

connective tissue condensations at the hydroxyapatite interface may be critical for the subsequent expression of the osteogenic phenotype and morphogenesis of bone.

The histological analysis indicated that the central region of the hydroxyapatite specimens was the nucleus for the initial morphogenetic events leading to bone differentiation. As early as 3 months, and mostly evident at 6 and 9 months, extensive remodelling had occurred, followed by the formation of lamellar bone. This suggests a time-related centrifugal pattern of bone growth extending to the periphery of the implants, occasionally culminating in total penetration by bone as shown in Figures 7.9 and 7.10.

While the morphological study of the histological material does not explain the morphogenesis of bone, it nevertheless suggests that the surface characteristic of the substratum may play an important role in the observed morphogenesis of bone. A role for bone morphogenetic proteins and cell-substratum interactions in the initiation of osteoblastic cell differentiation has been demonstrated both *in vitro* and *in vivo* (Reddi, 1992; Urist, 1989, 1992; Urist et al., 1983a; Vukivecic et al., 1993). The extracellular matrix of bone plays a critical role in the local control of cell

growth and differentiation by functioning as a solid substratum for anchorage of bone morphogenetic proteins and other growth factors complexed with both the organic and inorganic components of the extracellular matrix (Sampath and Reddi, 1984a). In the present material, the implanted hydroxyapatite replicates the mineralized inorganic supporting structure of the living extracellular matrix of bone. Circulating and/or locally produced bone morphogenetic proteins might have been adsorbed onto the hydroxyapatite characterized by specific surface characteristics.

Adsorption of native bone morphogenetic proteins, including osteogenin (BMP-3) on hydroxyapatite is a fundamental chromatographic step for their purification (Luyten et al., 1989; Sampath et al., 1987; Ripamonti et al., 1992a; Urist et al., 1984a, 1987a). Bone differentiation in hydroxyapatite substrata may be the result of adsorption of endogenously-produced BMPs and induction of bone as a secondary response. Indirectly, this is supported by the *in vitro* binding of one of the recombinant human BMPs (BMP-4) on the porous hydroxyapatite substratum (Ripamonti et al., 1992b; Ripamonti, Paralkar and Reddi, unpublished results), and by the generation of bone in porous hydroxyapatites pretreated with osteogenin (BMP-3) in extraskeletal

sites of both rodents and primates (Ripamonti et al., 1992b, 1992c, 1993a).

The correlation between the magnitude of induced bone and a specific range of values of the hydroxyapatite suggests that the geometrical configuration of the substratum may have an influence on the extent of bone formation, perhaps by providing porous spaces architecturally more conducive to bone deposition. However, measurement of the internal surface area of the porous spaces and correlation with bone deposition should be required to establish more specifically which aspect of the implant geometry is important for optimal bone deposition.

The critical importance of the geometry of the substratum on cell shape and cell differentiation has been previously demonstrated (Bissell and Barcellos-Hoff, 1987; Brunette, 1988; Folkman and Greenspan, 1975; Gospodarowicz et al., 1978; Reddi, 1974). The geometry of the substratum has been shown to profoundly influence the expression of the osteogenic phenotype *in vivo* (Reddi and Huggins, 1973; Reddi, 1974; Ripamonti et al., 1992b; Sampath and Reddi, 1984b).

In the present material, the volume fraction composition of the hydroxyapatite framework is in agreement with the data reported by Holmes et al. (1986) (34.6 versus 35.1 per cent respectively). The significant difference between the values of the hydroxyapatite at 6 and 9 months clearly indicate biodegradation of the substratum over time, suggesting an incomplete carbonate to apatite conversion. Variation in the amount of bone formation within different specimens may be the result of subtle differences in surface characteristics of the porous hydroxyapatite, and time-related release of putative adsorbed bone morphogenetic proteins interacting with a variable source of responding mesenchymal cells in different animals.

This apparently unique endogenously-regulated mechanism initiating bone differentiation in porous hydroxyapatites in baboons has been investigated extensively in this laboratory. Sequential time studies using the hydroxyapatite-induced osteogenesis model have included the histologic examination of the porous hydroxyapatite harvested at 1 month (Ripamonti et al., 1992c, 1993b), 2 months (Ripamonti et al., 1993b, van Eeden and Ripamonti, 1993), 3 months (Ripamonti et al., 1992c, 1993b; van Eeden and

Ripamonti, 1993, and this study), and 6 and 9 months (this study). The results have shown that bone differentiation in porous hydroxyapatite occurs by day 60 after intramuscular implantation in baboons. This observation, combined with the observed lack of bone differentiation in specimens harvested at day 30 after implantation (Ripamonti et al., 1992c, 1993b), suggests that the initiation of bone formation may depend on a critical concentration of endogenously produced bone morphogenetic proteins adsorbed onto the hydroxyapatite. Moreover, it is noteworthy that bone differentiation in porous hydroxyapatite occurs without an intervening chondrogenic phase. This may have important therapeutic implications when generation of cartilage is not desirable.

This experimental model has the potential to explore certain morphologic and biochemical aspects of postfetal bone differentiation which may be difficult to study in embryonic membranous bone development in primates. Although this model of hydroxyapatite-induced osteogenesis is useful to synchronize the onset of connective tissue condensations, cellular differentiation and morphogenesis of bone, there are overlaps in the temporal sequence of differentiation. There are, however, clear temporally and spatially

related phenotype transitions ultimately culminating in the differentiation of bone (Ripamonti et al., 1993b). These studies using porous hydroxyapatites have focused on the possible correlation between the developmental changes during vascularization (angiogenesis) and bone differentiation using histochemical markers of the osteogenic phenotype (Ripamonti et al., 1993b). The results of these studies, by including the analysis of early periods of observation (i.e. days 30 and 60), have indicated that the differentiation of large, hyperchromatic and intensely alkaline phosphatase positive cells at the hydroxyapatite interface is a critical morphogenetic event preceding the differentiation of bone. Interestingly, alkaline phosphatase expression, an enzyme marker prominently associated with the differentiation of the osteogenic phenotype (Wlodarski and Reddi, 1986), was also localized in the invading vasculature, and subsequently found in capillaries in close relationship with differentiating cells at the hydroxyapatite interface (Ripamonti et al., 1993b).

The angiogenic response surrounding and penetrating the porous substrata was a prominent histologic feature. It is likely that the specific geometry and surface characteristics of the substratum are conducive to

rapid vessel ingrowth and capillary sprouting within the early mesenchyme penetrating the porous spaces. In recent studies, the rich capillary network invading the porous spaces was investigated by immunolocalization of laminin, a prominent vascular basement membrane component (Foidart et al., 1980). Laminin, in the context of developing bone, is a useful marker for vascular endothelial cells prior to and during bone formation (Foidart and Reddi, 1980). Previous studies have monitored by immunofluorescence the distribution of laminin and type IV collagen during vascular invasion in endochondral bone differentiation in a rat bioassay model (Foidart and Reddi, 1980). The results demonstrated a close relationship between vascular invasion and subsequent bone differentiation (Foidart and Reddi, 1980). Interestingly, laminin staining was demonstrated around capillaries in close proximity to the hydroxyapatite as well as around individual cells that seemed to migrate out of the vascular compartment (Ripamonti et al., 1993b).

Angiogenesis and vascular invasion are prerequisite for osteogenesis (Trueta, 1963; Foidart and Reddi, 1980; Reddi and Kuettner, 1981). During capillary ingrowth into the zone of hypertrophic chondrocytes in the endochondral growth plate and during intramembranous

ossification, osteoprogenitor cells and osteoblasts are in contact with basement membrane components of invading blood vessels (Rhodin, 1974). Angiogenesis is also of critical importance in fracture healing (Trueta, 1963; Simmons, 1980). Trueta has stressed the importance of the blood vessels in osteogenesis, and defined the vascular invasion during bone formation as *osteogenetic vessels*, suggesting that the endothelium may be capable of osteoblastic differentiation (Trueta, 1963). While circumstantial evidence is lacking, it is tempting to suggest that *osteogenetic vessels*, penetrating the porous spaces of the hydroxyapatite, might have provided a temporally regulated flow of cell populations capable of expression of the osteogenic phenotype, as previously suggested in the course of endochondral bone differentiation (Foidart and Reddi, 1980) and bone remodelling (Burkhardt et al., 1984). Urist et al. (1983a) in a series of studies of matrix-induced endochondral bone differentiation have suggested that perivascular mesenchymal cells (pericytes) may be the target of bone morphogenetic proteins. More recently, it has been suggested that the capillary or microvessel pericyte may be an osteoblastic precursor cell (Brighton et al., 1992), and a supplementary source of osteoblasts in periosteal osteogenesis (Diaz-Flores et

al., 1992). The recent discovery of the affinity of osteogenin (BMP-3) and BMP-4 for type IV collagen (Paralkar et al., 1990) may link angiogenesis to osteogenesis, since type IV collagen is a major constituent of vascular basement membranes. Thus, type IV collagen and other basement membrane components (Vlodavsky et al., 1987; Paralkar et al., 1990; Paralkar et al., 1991) may function as a delivery system by sequestering both angiogenic and bone morphogenetic proteins. This may promote the observed angiogenic response and the formation of the extensive vascular network in the porous spaces. It is noteworthy that specific domains of laminin have been shown to play a role in the phenotypic differentiation and modulation of endothelial (Grant et al., 1989) and osteoblastic cells (Vukicevic et al., 1990).

The extraskeletal morphogenesis of bone in porous hydroxyapatite substrata is a new observation which may have important biomedical implications, particularly because obtained in a large series of adult primates. Whatever the mechanisms responsible for the remarkable morphogenesis of bone are, the results of the present study strongly support the use of hydroxyapatites with an average porosity of 600 μm as a biological alternative to autogenous bone grafts for the controlled initiation of bone formation in man.

The hydroxyapatite substratum may act as a solid state matrix for adsorption, storage and controlled release of bone morphogenetic proteins which locally initiate bone formation. A crucial step in this postulated developmental sequence is the vascular invasion and the attachment of responding mesenchymal cells, perhaps migrating endothelial or perivascular cells, to the substratum, and their differentiation into functional osteoblasts under the stimulus of matrix-released morphogenetic proteins. Final proof that endogenously-produced bone morphogenetic proteins are in fact adsorbed onto the substratum will require their localization by radioimmunoassay and immuno-histochemical methods.

Finally, the reproducibility of bone differentiation using the porous hydroxyapatite in intramuscular sites of baboons (Ripamonti et al., 1992c, 1993b; van Eeden and Ripamonti, 1993, and this study), indicates that the surface characteristics of porous bone substitutes may be manipulated to exploit endogenously-regulated mechanisms initiating bone differentiation in primates. In future, the requirements of porous bone substitutes to be used for skeletal replacement therapies may not be confined to a merely passive osteoconductive

scaffold, but should include osteoinductive properties as well, which may be achieved by altering the surface characteristics and geometry of the substratum. Thus, a variety of porous metals and alloys could be conveniently coated with hydroxyapatite or with other extracellular matrix components with binding affinity for bone morphogenetic proteins (Paralkar et al., 1990), and bioassayed for osteogenic activity in this extraskeletal primate model. This may have important implications in reconstructive craniofacial and orthopaedic surgery: these data in primates may help tissue engineers to construct substrata and delivery systems with defined geometries and surface characteristics for replacement therapies that are conducive to the initiation and promotion of therapeutic osteogenesis.

11.3 The Induction of Bone in Osteogenic Composites of Bone Matrix and Porous Hydroxyapatite

The association of an inductive organic substratum with a porous hydroxyapatite can be exploited to construct osteogenic composites for the controlled initiation of bone formation. The present study confirms that chemosterilized allogeneic bone matrix induces bone differentiation in heterotopic sites of adult recipient baboons, and that porous hydroxyapatites obtained from calcium carbonate coral exoskeletons of the genus Goniopora initiate bone differentiation by an unique mechanism. In the present material, and on the basis of previous observation, bone differentiation seems to have occurred by two distinct osteogenic mechanisms sustained by their complementary organic and inorganic substrata.

Recruitment of mesenchymal cells, direct transformation into osteoblasts and deposition of woven bone were the features of bone differentiation by induction regulated by the chemosterilized AAA bone matrix. Differentiation of bone within the porous spaces of the hydroxyapatite might have been the result of adsorption of endogenously-produced bone morphogenetic proteins and

induction of bone as a secondary response. A possible morphogenetic sequence in the porous hydroxyapatite may be summarized as follws: after penetration of a highly cellular and vascularized connective tissue matrix, there is morphogenesis of connective tissue condensations at the hydroxyapatite interface, followed by osteoblast differentiation, deposition of bone matrix, remodeling of the newly formed bone with organization of lamellar bone, and finally, generation of bone marrow in the hydroxyapatite-integrated ossicle. As previously discussed, the analysis of the histological material suggests that the differentiation of bone is intimately associated with the morphogenesis of the connective tissue condensations at the hydroxyapatite interface. It is noteworthy that mineralization occurred within connective tissue condensations, as demonstrated by Goldner's trichrome stain for undecalcified bone.

As previously commented upon, the initiation of bone formation seems to have occurred within the central regions of the hydroxyapatite substratum. Interestingly, bone never differentiated at the level of the most external surfaces of the implanted hydroxyapatites. There was, however, bone deposition along the external porous spaces when newly formed bone

generated by the chemosterilized bone matrix had grown into the porous spaces, occasionally merging with the bone forming within the central region of the porous hydroxyapatite.

The formation of bone within the central porous spaces of the hydroxyapatite implants is noteworthy. This contrasted markedly with previous results obtained using partially purified bone morphogenetic protein preparations delivered into sintered porous hydroxyapatites (Kawamura et al., 1987; Takaoka et al., 1988). In these experiments, after extraskeletal implantation bone formed only at the periphery of the hydroxyapatite implants. Furthermore, bone formed only when the partially purified protein fractions were delivered in conjunction with purified collagen (Takaoka et al., 1988). In more recent experiments, however, adsorption of bone morphogenetic protein fractions, including osteogenin (BMP-3) onto porous hydroxyapatite induced bone formation within the porous spaces of hydroxyapatite, and in direct apposition to the hydroxyapatite substratum in rodent and baboon extraskeletal sites (Ripamonti et al., 1992b, 1993a). The most likely explanation for these observed differences may be related to the purification level of the bone morphogenetic protein fractions used, as well

as the surface and chemical characteristics and interconnectivity of the hydroxyapatites used for the creation of the osteogenic composites.

The heterotopic initiation of bone formation in porous hydroxyapatites may have an important clinical application, particularly because it could be obtained in a large series of adult primates. However, the inherent fragility of the porous hydroxyapatite still limits its utilization in load-bearing orthotopic sites. Mechanical strength and biological integration is achieved by surrounding the porous hydroxyapatite with surface-demineralized allogeneic bone matrix, creating osteogenic composite implants. Large bone defects, lack of periosteum as a consequence of resective oncologic surgery and extensive traumatic avulsions are formidable challenges to skeletal reconstructionists; in such instances, the possibility of restoring continuity solely by conventional autotransplantation or osteoconductive means is minimal. In this perspective, osteogenic composites hold realistic potential in reconstructive craniofacial and orthopaedic surgery, initiating bone differentiation and growth in recipient beds that lack viable bone.

The results obtained in this primate model contrast markedly with a previous study in rodents using a similar composite configuration (Ripamonti et al., 1989). In the rodent model, bone failed to form within the porous spaces of the hydroxyapatite and along the internal surface of the AAA bone matrix enveloping the hydroxyapatite rods (Ripamonti et al., 1989).

Collectively, the results of the present heterotopic experiments in a primate underscore the crucial role of a proper animal model when evaluating the osteogenic potential of porous biomaterials and composite implants as alternatives to autogenous bone grafts in humans (Ripamonti, 1990). A full understanding of the interactions between bone morphogenetic proteins, hydroxyapatite substrata and responding cells in primates will afford the potential for rapid and controlled initiation of therapeutic osteogenesis.

12. THE ORTHOTOPIC CALVARIAL STUDY

Numerous studies on the healing of cranial defects in different animals have shown the limited regenerative capacity of the adult calvaria (Hollinger and Kleinschmidt, 1990; Schmitz and Hollinger, 1986, for reviews). Thus, there has been a growing interest in the use of nonhealing calvarial defects to test bone morphogenetic preparations for craniofacial and orthopaedic applications in an effort to initiate and promote bone formation as a biological alternative to autogenous bone grafts (Ferguson et al., 1987; Mulliken and Glowacki, 1980; Oklund et al., 1986; Prolo et al., 1982; Sato and Urist, 1985; Takagi and Urist, 1982).

The present experiments of bone regeneration have been generated in an effort (1) to develop a reproducible primate model that would closely approximate calvarial repair in man; (2) to evaluate the spontaneous regenerative potential of the adult baboon calvaria; (3) to study the biology of incorporation and the morphogenetic properties of antigen-extracted autolysed allogeneic bone implants compared to autogenous bone grafts; (4) to evaluate the growth of bone into a porous hydroxyapatite as an alternative to autogenous

bone grafts; and (5) to devise quantitative methods of evaluation of osteogenesis in untreated and treated calvarial defects.

The comparatively large size of the adult male baboon calvaria allows the surgical preparation of four symmetrically located defects of 25 mm in diameter, with sufficient remaining intervening calvarial bone to limit the possible reduction of blood flow and vascular penetration within treated and untreated defects. In the present study, the use of the Latin block design for the distribution of treatments permitted to analyze separately the anterior and posterior regions of the adult baboon calvaria. The introduction of the Latin block design overcomes the possible effect of vascular disturbances in specific regions of the calvaria. The osteogenic response was controlled in each animal by the simultaneous comparison of spontaneous repair in control defects versus autogenous grafts, chemosterilized AAA bone implants, and porous hydroxyapatites, thus reducing animal to animal variation since systemic factors are likely to affect healing (Urist, 1989). The identification of five sources for histomorphometry within each section allowed evaluation and analysis of the distribution of newly formed bone across the treated and untreated defects and the 3 observation periods.

Calvarial repair has been mainly investigated in rodent and canine models (Hollinger and Kleinschmidt, 1990; Schmitz and Hollinger, 1986), and comparatively limited material has been presented using nonhuman primate species (Ferguson et al., 1987; Hollinger et al., 1989b; Hollinger et al., 1990). The therapeutic application of bone substitutes rests on their osteogenic potential in adult primates (Hollinger et al., 1990; Ripamonti, 1990). The present model, by using a large series of adult baboons, may closely approximate calvarial repair in man. It is noteworthy that comparative histomorphometric studies between iliac crest bone biopsies of humans and baboons showed a remarkable degree of similarity (Schnitzler et al., 1993). More significantly, bone turnover tended to be lower than in humans, making the adult baboon an ideal model for comparative bone physiology and repair.

The validity of a calvarial defect as a model for evaluating bone substitutes for craniofacial and orthopaedic reconstruction is subjected to the defect limited capacity of spontaneous repair (Schmitz and Hollinger, 1986). The results of the present study demonstrate that a defect of 25 mm in diameter is a critical size defect of the adult male baboon calvaria.

Interestingly, a defect of 15 mm in diameter was found not to be a critical size defect of the baboon calvaria (Hollinger e al., 1989; Hollinger and Kleinschmidt, 1990). While there is no mention of the species selected, and male and female baboons were used in their experiment, Hollinger et al. (1989b) reported that substantial bone often formed in untreated defects, as evaluated histomorphometrically 60 days after surgical preparation. On average, in the present material, osteogenesis in untreated defects was limited, and essentially confined to the edges of the craniotomies. The histologic analysis suggests that the penetration of the temporalis muscle into the defects mechanically contained centripetal osteogenesis. While on average the amount of bone in control defects at 9 months was less than 20 percent, separate analysis for the site of surgical preparation demonstrated a superior healing in the anterior regions of the calvaria. This may be related to the observed significant difference in marrow spaces between anterior and posterior calvarial regions. In addition, variation in the extent of muscle penetration may account for the difference in the amount of bone in anterior versus posterior defects.

Numerous studies on the healing of cranial defects in different animal species have consistantly reported the limited regenerative potential of the adult calvaria (Hollinger and Kleinschmidt, 1990; Schmitz and Hollinger, 1986). The results of the present study indicated that, at least in the anterior regions of the adult baboon calvaria, spontaneous regeneration is greater than previously suspected. Inhibition of osteogenesis may be related to the fusion of the pericranium with the dura, after penetration of the temporalis muscle into the defect, sealing the previously open diploic and endosteal spaces of the craniotomy site.

The normal adult calvaria has identifiable boundaries between contiguous tissues: the membranous bone, the pericranium with its temporalis muscle, and the endocranium with its dural layer. Segregation with identifiable boundaries between contiguous tissues is a well recognized phenomenon in developmental processes (Armstrong and Armstrong, 1990). The alternative situation to tissue segregation is invasion, or the intrusion of one tissue into space occupied by a second tissue (Abercrombie, 1970; Armstrong and Armstrong, 1990). Experiments using the concept of mechanically guided tissue regeneration (Dahlin et al., 1988;

Gottlow et al., 1984; Nyman et al., 1982) were performed in this laboratory to demonstrate that the fusion of the pericranium with the dura may be responsible for the observed limited osteogenesis in calvarial defects of adult baboons (Petit and Ripamonti, 1993).

Calvarial defects treated with a rigid template positioned over the margins of the defects so as to re-establish tissue segregation between the calvarial tissues during healing showed superior osteogenesis when compared with untreated defects. These findings in a primate are in agreement with other studies that suggests that the intrusion of cell populations of the nonosteogenic lineage may inhibit osteogenesis (Dahlin et al., 1988, 1991; Gottlow et al., 1984). Fibroblasts have been shown to inhibit bone formation by producing factors that depress the differentiation and proliferation of osteoprogenitor cell populations (Ogiso et al., 1989). The effects of different cell populations upon one another and their respective extracellular matrix products on the final assembly of osseous wounds during healing are still poorly understood. Moreover, the mechanisms regulating segregational patterns in embryonic development and regenerative processes are also poorly understood

(Armstrong, 1989). In general, the final assembly of multiple tissues participating in the regeneration and repair processes appear to depend on the production of a scaffolding of extracellular matrix that is enriched with a number of attachment proteins, growth and morphogenetic factors (Reddi, 1984). Failure to provide an adequate scaffolding may result in the loss of the capacity to regenerate, in its complexity, the original structure with identifiable boundaries. The concept that invasion of nonosteogenic tissue is a factor in the genesis of pathologic nonunions has been proposed decades ago (Heiple and Herndon, 1965; Urist and McLean, 1963; Urist et al., 1954). Previous studies have indicated that the integrity of the periosteum may act as a protective sheath against tissue invasion from the surrounding nonosteogenic soft tissue (Dos Santos Neto and Volpon, 1984). Interposition of muscular or neurogenic tissue within osseous defects has been shown to inhibit healing of ulnar and mandibular defects respectively (Altner et al., 1975; Retief and Dreyer, 1967). It is noteworthy however, that the strategy of guided tissue regeneration did not result in osseous healing when applied to a long bone defect model in rabbits (Nielsen et al., 1992).

In the present primate model, AAA bone matrix implants achieved superior incorporation and osteogenesis, at least at 3 months, when compared with autogenous cortico-cancellous bone grafts, the *gold standard* in reconstructive craniofacial and orthopaedic surgery (Habal, 1992; Lance, 1985; Prolo and Rodrigo, 1986). While no significant difference was found at 3 months with regard to osteoid volume, it is noteworthy that at 6 and 9 months, AAA bone implants showed superior osteogenesis when compared with autogenous grafts as evaluated morphometrically by the amount of osteoid volume. Biologically, autogenous bone grafts are the best material available for craniofacial and orthopaedic application, since the grafted nonimmunogenic bone partially retains viability of its cellular and molecular components (Bassett, 1972; Burchardt, 1983, 1987; Habal, 1992; Heiple et al., 1983; Prolo and Rodrigo, 1985). Yet, at no time did the AAA bone matrix appear to elicit an adverse tissue response, and there was no histological evidence of implant rejection or dural reaction. These results in adult primates demonstrate that the chemosterilization procedure devised by Urist (1972, 1980, 1983) and Urist et al. (1975) is effective in extracting lipid soluble antigenic components (Mikulski and Urist, 1975), thereby greatly lowering the alloantigenic load of

cadaveric bone tissue, in spite of the presence of residual marrow tissue. Preservation of bone morphogenetic protein activity within the chemosterilized matrix is ensured by extraction and inactivation of putative BMPase(s) in the presence of sulphydryl enzyme inhibitors (Urist, 1972, 1980; Urist and Iwata, 1973; Urist et al., 1972, 1974, 1975). The ambiguities of the orthotopic site make it difficult to unequivocally demonstrate bone morphogenetic protein activity in the present material. Particulate demineralized bone matrix prepared from allogeneic calvariae has been shown to induce bone differentiation in the subcutaneous space of rodent species (Reddi, 1975; Reddi and Huggins, 1972a). The finding of delicate trabecular-like bone structures, appositional to the central areas of the chemosterilized matrix, suggests that AAA bone implants prepared from donor calvariae might also have acted as inductive substratum for bone differentiation by induction. This interpretation is further supported by the heterotopic study which showed bone formation by induction using AAA bone matrix implants.

As previously discussed, the histomorphometric analysis demonstrated greater amounts of bone in anterior than in posterior untreated defects. It is noteworthy,

however, that the extent of bone formation in AAA bone specimens appeared to be independent of the site of surgical implantation. This indicates that bone deposition was a function of the implanted matrix rather than the spontaneous healing potential of specific anatomical regions within the calvaria.

Bone morphogenetic protein preparations have been shown to regenerate nonhealing calvarial defects in rats, dogs, sheep, monkeys and baboons (Ferguson et al., 1987; Hollinger et al., 1989b; Lindholm et al., 1988; Ripamonti et al., 1992a, 1993c; Takagi and Urist, 1982; Sato and Urist, 1985). Osteogenin (BMP-3) fractions, in conjunction with an insoluble collagenous matrix carrier, induced complete regeneration of calvarial defects in baboons 90 days after implantation (Ripamonti et al., 1992a, 1993c). It was noteworthy that on day 30, in implants of demineralized bone matrix, bone formed with an intervening phase of cartilage development. This provided the phenotypic evidence of endochondral bone differentiation by induction in defects of membranous calvarial bone in adult primates (Ripamonti et al., 1993c). Partial healing using particulate human AA bone matrix has been reported using primates of the genus Macaca (Hollinger et al., 1990). However, the same study showed minimal

Indeed, in 10 operations performed with the use of surface-demineralized allogeneic bone (SDAB) implants, which were compared with 25 comparable cases treated with other forms of allogeneic implants, it was shown that the bone induction principle could be used in adult humans to repair large bone defects (Urist, 1968).

bone regeneration using a BMP-copolymer composite, possibly owing to residual antigenicity of the xenogeneic BMP preparation (Hollinger et al., 1990). In a canine model, AAA bone failed to regenerate calvarial defects of adult dogs (Oklund et al., 1986). In the present study, AAA bone implants, processed as described here, showed superior osteogenesis when compared with autogenous cortico-cancellous bone grafts. The most likely explanation for these differences may be attributed to different animal models as well as variation in the extraction procedures.

The observed superior osteogenesis in chemosterilized bone alloimplants in an orthotopic site indicates that AAA bone matrix may be a valid alternative to autogenous bone grafts in reconstructive craniofacial surgery, and supports the therapeutic application of the bone induction principle (Urist, 1965) using AAA bone matrix (Urist and Dawson, 1981), or human BMP preparations (Johnson et al., 1988; Urist, 1989; 1992). While the allogeneic collagenous matrix may carry a potential risk of viral contamination, the recent isolation, purification, and molecular cloning of bone morphogenetic proteins will help to construct appropriate osteogenic delivery systems for the rapid

and controlled therapeutic initiation of bone formation.

In this primate model, substantial bone deposition had occurred in the implants of porous hydroxyapatite, culminating in complete penetration of the porous spaces by bone. The close apposition to viable bone indicates that ingrowth of bone had occurred *via* osteoconduction from the calvarial margins. In addition, however, the combined histologic and morphometric analyses indicate that other osteogenic mechanisms might have occurred during the incorporation of the porous hydroxyapatite. The heterotopic study has established that porous hydroxyapatites obtained from the coral of the genus Goniopora are capable of inducing bone differentiation when implanted intramuscularly in this primate model. The contribution of an osteoinductive mechanism to the cranial incorporation of the porous hydroxyapatite is further substantiated by the histologic evidence on serial sections of apparently isolated islands of bone within the central regions of the specimens, and by the histomorphometric evidence of uniformity of bone deposition across the implants as early as 3 months. This suggests a centripetal osteoconductive pattern of bone ingrowth coupled with an osteoinductive mechanism

of bone deposition, mainly within the central regions of the implants. As previously discussed, porous hydroxyapatite may selectively adsorbs bone morphogenetic proteins, since these proteins are partially purified by adsorption chromatography on hydroxyapatite gels (Luyten et al., 1989; Ripamonti et al., 1992a; Urist et al., 1984a; Wang et al., 1988). Thus, it is possible that circulating or locally produced bone morphogenetic proteins adsorbed onto the hydroxyapatite may additionally regulate the morphogenesis of bone in orthotopic sites.

One of the recombinant human bone morphogenetic proteins (BMP-4, previously known as BMP-2b) binds to porous hydroxyapatites *in vitro* (Ripamonti et al., 1992b). This observation has resulted in the construction of delivery systems using porous hydroxyapatite activated by bone morphogenetic proteins with osteogenic activity in heterotopic sites of rodents and baboons (Ripamonti et al., 1992b, 1993a). In recent experiments, composites of porous hydroxyapatite and osteogenin (BMP-3) fractions, adsorbed onto the hydroxyapatite, induced rapid bone differentiation in calvarial defects of adult baboons (Ripamonti et al., 1992d). Moreover, approximately 2 μg of osteogenin purified to apparent homogeneity after

electroendosmotic elution induced copious amounts of bone as early as 30 days when adsorbed onto the porous hydroxyapatite implanted in an identical baboon calvarial model (Ripamonti et al., 1992a). The finding that the biological activity of electroeluted native osteogenin (BMP-3) could be restored and delivered by a nonimmunogenic inorganic porous substratum represented a significant advance over the reconstitution with the allogeneic insoluble collagenous carrier (Ripamonti et al., 1992a). By exploiting the principle of centripetal mesenchymal ingrowth (Hulbert et al., 1970), porous hydroxyapatites appear to be well suited for the formulation of delivery systems for bone morphogenetic proteins. The porous substratum of the hydroxyapatite allows a spatially controlled osteogenesis, restricting bone differentiation locally to surgical sites (Ripamonti et al., 1992, 1992).

Interestingly, in these studies of bone regeneration in calvarial defects of primates, resorbable porous substrata of calcium carbonate, with a remaining surface *coating* of hydroxyapatite of 2 μm, performed poorly when compared with nonresorbable hydroxyapatite implants, even when pretreated with BMP fractions (Ripamonti et al., 1992d). Other resorbable compositions, however, have been found to effectively

deliver bone morphogenetic protein activity in heterotopic and orthotopic sites of mice and dogs (Urist et al., 1984b, 1987b; Wu et al., 1992).

In the present material, a point of concern was the morphologic evidence of nonunions at the calvaria-hydroxyapatite interfaces confirmed by serial sections on selected specimens, in spite of the often extensive bone deposition within the implants. The presence of bone in nonunited specimens is in agreement with previous results obtained with the 200 μm porous hydroxyapatite in a canine calvarial model (Holmes and Hagler, 1988b). In the present study, as in others (Holmes and Hagler, 1988b), fixation of the implants was not performed. Thus, it is possible that the occasional fibrous unions at the interfaces could be the result of motion generated by the underlying brain. The results of the regression analysis are in agreement with the data obtained with the porous hydroxyapatites implanted intramuscularly. This suggests that the extent of bone formation may be additionally regulated by the geometric configuration of the porous spaces of the implanted hydroxyapatite, perhaps by providing porous spaces that are architecturally more conducive to deposition of bone. The geometry of the substratum has been shown to profoundly influence the expression

of the osteogenic phenotype *in vivo* using both collagenous matrix and porous hydroxyapatite (Ripamonti et al., 1992b; Sampath and Reddi, 1984b).

Specimens of autogenous bone grafts showed less bone, at least at 3 months, when compared to specimens of hydroxyapatite. Comparative data of bone grafts versus hydroxyapatite implants at 6 and 9 months are not available, owing to the technical difficulty in differentiating newly formed bone from the original grafted matrix, as encountered in other studies (Holmes and Hagler, 1988b). The major source of osteogenesis within the grafted specimens seemed to be the pericranial and endosteal surfaces of the adjacent calvaria, translating into greater amounts of bone at the graft-calvarial interface than near the central region of the graft. While this pattern of repair is consistent with osteoconduction, it is likely that pericranial bone deposition over the central areas of the grafts was also the result of local osteogenesis from viable osteoblasts which survived the transplantation injury (Bassett, 1972; Lance, 1985; Prolo and Rodrigo, 1986).

As in AAA bone matrix implants, it is noteworthy that the extent of bone formation in specimens of hydroxyapatite appeared to be independent of the site of surgical implantation. This indicates that bone deposition within the porous spaces was a function of the implanted porous hydroxyapatite rather than the healing potential of specific regions within the calvaria.

The remarkable degree of bone growth in implants of hydroxyapatite suggests that the porous substratum is a valid alternative to autogenous bone grafts in craniofacial reconstruction in man. The limitations of the material have been previously discussed, and include a weak mechanical performance and brittleness which requires special care during manipulation and fixation (Holmes and Hagler, 1988b; Holmes et al., 1986; White and Shors, 1986). Additional studies are required to evaluate the mechanical performance of the bone-porous matrix complex of such specimens at different observation periods. Further experiments are also required to identify the reasons for nonunion to promote optimal bone ingrowth for therapeutic osseous reconstruction in humans.

Finally, while longer observation periods may be required to evaluate the long term incorporation and remodeling of bone that formed in AAA bone matrix and hydroxyapatite implants, and in autogenous bone grafts, the histomorphometric data have indicated that maximal bone and osteoid deposition were achieved within 3 and 6 months after surgery. This establishes baseline data as to the healing potential of the adult baboon calvaria. Thus, future experiments using the same model should focus on shorter time periods after altering the experimental conditions in an effort to stimulate the regenerative capacity and the controlled initiation of bone formation (Ripamonti et al., 1992a; 1992d; 1993c).

LIST OF REFERENCES

Abercrombie M. Contact inhibition in tissue culture. In Vitro 6: 128, 1970

Altner PC, Grana N, Grodon M. An experimental study on the significance of muscle tissue interposition on fracture healing. Clin Orthop 111: 269, 1975

Armstrong PB, Armstrong MT. An instructive role for the interstitial matrix in tissue patterning: Tissue segregation and intercellular invasion. J Cell Biol 110: 1439, 1990

Aspenberg P, Andolf E. Bone induction by fetal and adult human bone matrix in athymic rats. Acta Orthop Scand 60: 195, 1989

Aspenberg P, Lohmander LS, Thorngren KG. Failure of bone induction by bone matrix in adult monkeys. J Bone Joint Surg 70B: 625, 1988

Aspenberg P, Lohmander S, Thorngren K-G. Monkey bone matrix induces bone formation in the athymic rat, but not in adult monkeys. J Orthop Res 9: 20, 1991

Aspenberg P, Wang E, Thorngren K-G. Bone morphogenetic

protein induces bone in the squirrel monkey, but bone matrix does not. Acta Orthop Scand 63: 619, 1992

Bassett CAL. Clinical implications of cell function in bone grafting. Clin Orthop 87: 49, 1972

Brighton CT, Lorich DG, Kupcha R, Reilly TM, Jones AR, Woodbury RA. The pericyte as a possible osteoblast progenitor cell. Clin Orthop 275: 287, 1992

Burchardt H. The biology of bone graft repair. Clin Orthop 174: 28, 1983

Burchardt H. Biology of bone transplantation. Orthop Clin North Am 18: 187, 1987

Burchardt R, Bartl R, Frisch B, Jager K, Mahl C, Hill W and Kettner, G. The structural relationship of bone forming and endothelial cells of the bone marrow. In: Bone Circulation. Arlet J, Ficat RP, Hungerford DS, eds. Williams & Wilkins: Baltimore, p 2, 1984

Burger M, Sherman BS, Sobel AE. Observations of the influence of chondroitin sulfate on the rate of bone repair. J Bone Joint Surg 44B: 675, 1962

Burwell RG. Studies in the transplantation of bone. 8. Treated composite homograft-autografts of cancellous bone: An analysis of inductive mechanisms in bone transplantation. J Bone Joint Surg 48B: 532, 1966

Bruce JA. Time and order of appearance of ossification centers and their development in the skull of the rabbit. Am J Anat 68: 41 1941

Carrington JL, Roberts AB, Flanders KC, Roche NS, AH Reddi. Accumulation, localization, and compartmentation of transforming growth factor ß during endochondral bone development. J Cell Biol 107: 1969, 1988

Celeste AJ, Iannazzi JM, Taylor, RC, Hewick RM, Rosen V, Wang EA, Wozney JM. Identification of transforming growth factor ß family members present in bone-inductive protein purified from bovine bone. Proc Natl Acad Sci USA 87: 9843, 1990

Chiroff RT, White EW, Weber JN, Roy DM. Tissue ingrowth of replamineform implants. J Biomed Mater Res 9: 29, 1975

Dahlin C, Linde A, Gottlow J, Nyman, S. Healing of bone defects by guided tissue regeneration. Plast Reconstr

Surg 81: 672, 1988

Dahlin C, Alberius P, Linde A. Osteopromotion for cranioplasty: An experimental study in rats using a membrane technique. J Neurosurg 47: 487, 1991

Deatherage JR, Miller EJ. Packaging and delivery of bone induction factors in a collagenous implant. Collagen Rel Res 7: 225, 1987

Deporter DA, Komori N, Howley TP, Shiga A, Ghent A, Hansel P, Parisien K. Reconstituted bovine skin collagen enhances healing of bone wounds in the rat calvaria. Calcif Tissue Int 42: 321, 1988

Diaz-Flores L, Gutierrez R, Lopez-Alonso A, Gonzales R, Varela H. Pericytes as a supplementary source of osteoblasts in periosteal osteogenesis. Clin Orthop 275: 280, 1992

Dos Santos Neto FL, Volpon JB. Experimental nonunion in dogs. Clin Orthop 187: 260, 1984

Dreyer JJ, Du Bruyn DB. Composition of a food mixture developed at the NNRI for supplementation of predominantly cereal diets. South Afr Med J 42: 600,

1968

Enneking WF, Burchardt H, Puhl JJ, Poitrowski G. Physical and biological aspects of repair in dog cortical-bone transplants. J Bone Joint Surg 57A: 237, 1975

Ferguson D, Davis WL, Urist MR, Hurt WC, Allen EP. Bovine bone morphogenetic protein (bBMP) fraction-induced repair of craniotomy defects in the rhesus monkey (*Macaca speciosa*). Clin Orthop 219: 251, 1987

Foidart JM, Reddi AH. Immunofluorescent localization of type IV collagen and laminin during endochondral bone differentiation and regulation by pituitary growth hormone. Dev Biol 75: 130, 1980

Friedenberg ZB, Lawrence RR. The regeneration of bone in defects of varying size. Surg Gynecol Obstet 114: 721, 1962

Friedlaender GE. Bone grafts. The basic science rationale for clinical applications. J Bone Joint Surg 69A: 786, 1987

Friedlaender GE, Mankin HJ, Sell KW. Osteochondral Allografts: Biology, Banking, and Clinical Applications. Boston: Little, Brown and Company, 1983

Frost HM. Bone Remodeling and its Relationship to Metabolic Bone Diseases. Springfield, Illinois: Charles C Thomas Publisher, p 50, 1973

Glowacki J, Cox KA. Osteoclastic features of cells that resorb bone implants in rats. Calcif Tissue Int 39: 97, 1986

Glowacki J, Altobelli D, Mulliken JB. Fate of mineralized and demineralized osseous implants in cranial defects. Calcif Tissue Int 33: 71, 1981a

Glowaki J, Kaban LB, Murray JE, Folkman J, Mulliken JB. Application of the biological principle of induced osteogenesis for craniofacial defects, Lancet 1: 959 1981b

Goldner J. A modification of the Masson trichrome technique for routine laboratory purposes. Am J Path 14: 237, 1938

Gottlow J, Nyman S, Karring T, Lindhe J. New attachment

formation as the result of controlled tissue regeneration. J Clin Periodontol 11: 494, 1984

Grant DS, Tashiro KI, Segui-Real B, Yamada Y, Martin GR, Kleinman HK. Two different laminin domains mediate the differentiation of human endothelial cells into capillary-like structures *in vitro*. Cell 58: 933, 1989

Habal MB. Craniofacial surgery. In: Bone Grafts & Bone Substitutes. Habal MB, Reddi AH, eds. Philadelphia: WB Saunders, p 316, 1992

Habal MB, Reddi AH. An update on bone grafts and bone substitutes. Adv Plast Reconstr Surg 3: 147, 1987

Habal MB. Reddi AH. Bone Grafts & Bone Substitutes. Philadelphia: WB Saunders, 1992

Hammonds RG, Schwall R, Dudley A, Berkemeier L, Lai C, Lee J, Cunningham N, Reddi AH, Wood WI, Mason AJ. Bone inducing activity of mature BMP-2b produced from a hybrid BMP-2a/2b precursor. Mol Endocrinol 5: 149, 1991

Heiple GK, Herndon CH. The pathologic physiology of nonunion. Clin Orthop 43: 11, 1965

Heiple GK, Goldberg VM, Powell AE, Bos GD, Zika JM. Biology of Cancellous Bone Graft Repair. In: Osteochondral Allografts: Biology, Banking, and Clinical Applications. Friedlaender GE, Mankin HJ, Sell KW, eds. Boston: Little, Brown and Company, p 37, 1983

Heine UI, Munoz EF, Flanders KC, Ellingsworth LR, Sporn MB, Roberts AB. Role of transforming growth factor-β in the development of the mouse embryo, J Cell Biol 105: 2861, 1989

Hollinger JO, Schmitz JP, Mizgala JW, Hassler C. An evaluation of two configurations of tricalcium phosphate for treating craniotomies. J Biomed Mater res 23: 17, 1989a

Hollinger JO, Mark DE, Bach DE, Reddi AH, Seyfer AE. Calvarial bone regeneration using osteogenin. J Oral Maxillofac Surg 47: 1182, 1989b

Hollinger JO, Kleinschmidt JC. The critical size defect as an experimental model to test bone repair materials. J Craniofac Surg 1: 60, 1990

Hollinger JF, Schmitz JP, Mark DE, Seyfer AE. Osseous

wound healing with xenogeneic bone implants with a biodegradable carrier. Surgery 107: 50, 1990

Holmes RE. Bone regeneration within a coralline hydroxyapatite implant. Plast Reconstr Surg 63: 626, 1979

Holmes RE, Hagler HK. Porous hydroxyapatite as a bone graft substitute in mandibular contour augmentation: A histometric study. J Oral Maxillofac Surg 45: 421, 1987

Holmes R, Hagler H. Porous hydroxyapatite as a bone graft substitute in maxillary augmentation. A histometric study. J Cranio-Max-Fac Surg 16: 199, 1988a

Holmes RE, Hagler HK. Porous hydroxyapatite as a bone substitute in cranial reconstruction: A histometric study. Plast Reconstr Surg 81: 662, 1988b

Holmes RE, Bucholz RW, Mooney V. Porous hydroxyapatite as a bone-graft substitute in methaphyseal defects. J Bone and Joint Surg 68A: 904, 1986

Holmes RE, Bucholz RW, Mooney V. Porous hydroxyapatite as bone graft substitute in diaphyseal defects: A histometric study. J Orthop Res 5: 114, 1987

Hosny M, Sharawy M. Osteoinduction in Rhesus monkeys using demineralized bone powder allografts. J Oral Maxillofac Surg 43: 837, 1985

Hulbert SF, Young FA, Mathews RS, Klawitter JJ, Talbert CD, Stelling FH. Potential of ceramics materials as permanently implantable skeletal prosthesis. J Biomed Mater Res 4: 433, 1970

Huggins CB. The formation of bone under the influence of the epithelium of the urinary tract. Arch Surg 22: 377, 1931

Johnson EE, Urist MR, Finerman GAM. Bone morphogenetic protein augmentation grafting of resistant femoral nonunions. A preliminary report. Clin Orthop 230: 257, 1988

Kawamura M, Iwata H, Sato K, Miura T. Chondroosteogenic response to crude bone matrix proteins bound to hydroxyapatite. Clin Orthop 217: 281, 1987

Klawitter JJ, Bagwell JG, Weinstein AM, Sauer BW, Pruitt JR. An evaluation of bone growth into porous high density polyethylene. J Biomed Mater Res 10: 311,

1976

Kramer IRH, Killey HC, Wright HC. A histological and radiological comparison of the healing of defects in the rabbit calvarium with and without implanted heterogeneous anorganic bone. Archs Oral Biol 13: 1095, 1968

Krukowski M, Kahan AJ. Inductive specificity of mineralized bone matrix in ectopic osteoclast differentiation. Calcif Tissue Int 34: 474, 1982

Lance EM. Some observations on bone graft technology. Clin Orthop 200: 114, 1985

Lindholm TC, Lindholm TS, Alitalo I, Urist MR. Bovine bone morphogenetic protein (bBMP) induced repair of skull trephine defects in sheep. Clin Orthop 227: 265, 1988

Luyten FP, Cunningham NS, Ma S, Muthukumaran N, Hammonds RG, Nevins WB, Wood WI, Reddi AH. Purification and partial amino acid sequence of osteogenin, a protein initiating bone differentiation. J Biol Chem 264: 13377, 1989

Lyons KM, Pelton RW, Hogan BLM. Patterns of expression of murine Vgr-1 and BMP-2a RNA suggest that transforming growth factor-ß-like genes coordinately regulate aspects of embryonic development. Genes Dev 3: 1657, 1989a

Lyons KM, Graycar JL, Lee A, Hashmi S, Lindquist PB, Chen EY, Hogan BLM, Derynck R. Vgr-1, a mammalian gene related to *Xenopus* Vg-1 and a new member of the transforming growth factor ß superfamily. Proc Natl Acad Sci USA. 86: 4554, 1989b

Mark DE, Hollinger JO, Hastings C, Chen G, Marden LJ, Reddi AH. Repair of calvarial nonunions by osteogenin, a bone inductive protein. Plast Reconstr Surg 86: 623, 1990

Marks SC, Popoff SN. Bone cell biology: The regulation of development, structure, and function in the skeleton. Am J Anat 183: 1, 1988

Melton DA, Melton CL. Blood parameters of the wild Chacma baboon, *Papio ursinus*. South Afr J Zool 17: 85, 1982

Mikulski AJ, Urist MR. An antigenic antimorphogenetic

bone hydrophobic glycopeptide. Prep Biochem 5: 21, 1975

Mizutani H, Urist MR. The nature of bone morphogenetic protein (BMP) fractions derived from bovine bone matrix gelatin. Clin Orthop 171: 213, 1982

Miyamoto S, Takaoka K, Ono K. Bone induction in monkeys by bone morphogenetic protein. A trans-filter technique. J Bone Joint Surg 75B: 107, 1993

Molnar LM. Decalcifying solution for hard or soft tissue. Histo-Logic 4: 72, 1975

Moore JC, Matukas VJ, Deatherage JR, Miller EJ. Craniofacial osseous restoration with osteoinductive proteins in a collagenous delivery system. Int J Oral Maxillofac Surg 19: 172, 1990

Moss ML. Growth of the calvaria in the rat. The determination of osseous morphology. Am J Anat 94: 333, 1954

Mulliken JB, Glowacki J. Induced osteogenesis for repair and construction in the craniofacial region. Plast Reconstr Surg 65: 553, 1980

Napier JR, Napier PH. The natural history of the primates. British Museum (Natural History), Cambridge University Press, 1985

Nathan RM, Bentz H, Armstrong RM, Piez KA, Smestad TM, Ellingsworth LR, McPherson JM, Seyedin SM. Osteogenesis in rats with an inductive bovine composite. J Orthop Res 6: 324, 1988

Newman SA. Lineage and pattern in the developing vertebrate limbs. Trends Gen 4: 329, 1988

Nielsen FF, Karring T, Gogolewski S. Biodegradable guide for bone regeneration. Polyurethane membranes tested in rabbit radius defects. Acta Orthop Scand 63: 66, 1992

Nyman S, Gottlow J, Karring T, Lindhe J. The regenerative potential of the periodontal ligament. An experimental study in the monkey. J Clin Periodontol 9: 257: 1982

Oklund SA, Prolo DJ, Gutierrez RV, King SE. Quantitative comparisons of healing in cranial fresh autografts, frozen autografts and processed autografts, and allografts in canine skull defects. Clin Orthop

205: 269, 1986

Ozkaynak E, Rueger DC, Drier EA, Corbett C, Ridge RJ, Sampath TK, Oppermann H. OP-1 cDNA encodes an osteogenic protein in the TGF-ß family. EMBO J. 9: 2085, 1990

Paralkar VM, Nandedkar AKN, Pointer RH, Kleinman HK, Reddi AH. Interaction of osteogenin, a heparin binding bone morphogenetic protein, with type IV collagen. J Biol Chem 265: 17281, 1990

Paralkar VM, Vukicevic S, Reddi AH. Transforming growth factor ß type 1 binds to collagen IV of basement membrane matrix: Implications for development. Dev Biol 143: 303, 1991

Padgett RW, St Johnston RD, Gelbart WM. A transcript from a Drosophila pattern gene predicts a protein homologous to the transforming growth factor-beta family. Nature 325: 81, 1987

Parfitt AM. Stereologic basis of bone histomorphometry: Theory of quantitative microscopy and reconstruction of the third dimension. In: Bone Histomorphometry: Techniques and Interpretation. Recker RR, ed. Boca

Raton: CRC Press, p 53, 1983

Parfitt AM, Drezner MK, Glorieux FH, Kanis JA, Malluche H, Meunier PJ, Ott SM, Recker RR. Bone histomorphometry: Standardization of nomenclature, symbols, and units. Report of the ASBMR Histomorphometry Nomenclature Committee. J Bone Min Res 2: 595, 1987

Piecuch JF. Extraskeletal implantation of a porous hydroxyapatite ceramic. J Dent Res 61: 1458, 1982

Piecuch JF, Topazian RG, Skoly S, Wolfe S. Experimental ridge augmentation with porous hydroxyapatite implants. J Dent Res 62: 148, 1983

Prolo DJ, Rodrigo JJ. Contemporary bone graft physiology and surgery. Clin Orthop 200: 322, 1985

Prolo DJ, Pedrotti PW, Burres KP, Oklund S. Superior osteogenesis in transplanted allogeneic canine skull following chemical sterilization. Clin Orthop 168: 230, 1982

Rath NC, Reddi AH. Collagenous bone matrix is a local mitogen. Nature 278: 855, 1979

Ray RD, Holloway JA. Bone implants. Preliminary report of an experimental study. J Bone Joint Surg 39A: 1119, 1957

Reddi AH. The matrix of the rat calvarium as transformant of fibroblasts. Proc Soc Biol Med 150: 324, 1975

Reddi AH. Cell biology and biochemistry of endochondral bone development. Collagen Relat Res 1: 209, 1981

Reddi AH. Regulation of local differentiation of cartilage and bone by extracellular matrix: A cascade type mechanism. In: Limb Development and Regeneration. Kelly RO, Goetinck PF, MacCabe JA, eds. New York: Alan R Liss, p 261, 1982

Reddi AH. Extracellular matrix and development. In: Extracellular Matrix Biochemistry. Piez KA, Reddi AH, eds. New York: Elsevier, p 375, 1984

Reddi AH. Regulation of bone differentiation by local and systemic factors. In: Bone and Mineral Research. Vol. 3. Peck WA, ed. Amsterdam: Elsevier Science Publisher, p 27, 1985

Reddi AH. Regulation of cartilage and bone differentiation by bone morphogenetic proteins. Curr Opin Cell Biol 4: 850, 1992

Reddi AH, Huggins CB. Biochemical sequences in the transformation of normal fibroblasts in adolescent rats. Proc Natl Acad Sci USA 69: 1601, 1972a

Reddi AH, Huggins CB. Citrate and alkaline phosphatase during transformation of fibroblasts by the matrix and minerals of bone. Proc Soc Exp Biol Med 140: 807, 1972b

Reddi AH, Huggins CB. The formation of bone marrow in fibroblast-transformation ossicles. Proc Natl Acad Sci USA 72: 2212, 1975

Reddi AH, Anderson WA. Collagenous bone matrix-induced endochondral ossification and hemopoiesis. J Cell Biol 69: 557, 1976

Reddi AH, Huggins CB. Hormone-dependent hematopoiesis in fibroblast-transformation ossicles. Nature 263: 514, 1976

Reddi AH, Gay R, Gay S, Miller EJ. Transitions in

collagen types during matrix-induced cartilage, bone and bone marrow formation. Proc Natl Acad Sci USA 74: 5589, 1977

Reddi AH, Hascall VC, Hascall GK. Changes in proteoglycan types during matrix-induced cartilage, bone and bone marrow formation. Biochem Biophys Res Commun 81: 106, 1978

Reddi AH, Sullivan NS. Matrix induced endochondral bone differentiation. Influence of hypophysectomy, growth hormone and thyroid stimulating hormone. Endocrinology 107: 1291, 1980

Reddi AH, Kuettner KE. Vascular invasion of cartilage: Correlation of morphology with lysozyme, glycosaminoglycans, protease, and protease-inhibitory activity during endochondral bone development. Dev Biol 82: 217, 1981

Reddi AH, Muthukumaran N, Ma S, Carrington JL, Luyten F, Paralkar VM, Cunningham NS. Initiation of bone development by osteogenin and promotion by growth factors. Connect Tissue Res 20: 303, 1989

Retief DH, Dreyer CJ. Effects of neural damage on the

repair of bony defects in the rat. Arch Oral Biol 12: 1035, 1967

Rhodin JAG. Histology. London: Oxford University Press, p 212, 1974

Ripamonti U. Inductive bone matrix and porous hydroxyapatite composites in rodents and nonhuman primates. In: Handbook of Bioactive Ceramics. Vol. 2: Calcium Phosphate and Hydroxylapatite Ceramics. Yamamuro T, Wilson-Hench J, Hench LL, eds. Boca Raton: CRC Press, p 245, 1990

Ripamonti U, Schnitzler CM, Cleaton-Jones PE. Bone induction in a composite allogeneic bone/alloplastic implant. J Oral Maxillofac Surg 47: 963, 1989

Ripamonti U, Magan A, Ma S, van den Heever B. Moehl T, Reddi AH. Xenogeneic osteogenin, a bone morphogenetic protein, and demineralized bone matrices, including human, induce bone differentiation in athymic rats and baboons. Matrix 11: 404, 1991

Ripamonti U, Ma S, Cunningham N, Yeates L, Reddi AH. Initiation of bone regeneration in adult baboons by osteogenin, a bone morphogenetic protein. Matrix 12:

369, 1992a

Ripamonti U, Ma S, Reddi AH. The critical role of geometry of porous hydroxyapatite delivery system in induction of bone by osteogenin, a bone morphogenetic protein. Matrix 12: 202, 1992b

Ripamonti U, Ma S, Reddi AH. Induction of bone in composites of osteogenin and porous hydroxyapatite in baboons. Plast Reconstr Surg 89: 731, 1992c

Ripamonti U, Ma S, van den Heever B, Reddi AH. Osteogenin, a bone morphogenetic protein, adsorbed on porous hydroxyapatite substrata induces rapid bone differentiation in calvarial defects of adult primates. Plast Reconstr Surg 90: 382, 1992d

Ripamonti U, Ma S, Cunningham N, Yeates L, Reddi AH. Reconstruction of the bone-bone marrow organ by osteogenin, a bone morhogenetic protein, and demineralized bone matrix in calvarial defects of adult primates. Plast Reconstr Surg 91: 27, 1993a

Ripamonti U, van den Heever B, van Wyk J. Expression of the osteogenic phenotype in porous hydroxyapatite implanted extraskeletally in baboons. Matrix 1993b, in

press

Ripamonti U, Yeates L, van den Heever B. Initiation of heterotopic osteogenesis after chromatographic adsorption of osteogenin, a bone morphogenetic protein, onto porous hydroxyapatite. Biochem Biophys Res Commun 193: 509, 1993c

Roy DM, Linnehan SK. Hydroxyapatite formed from coral skeletal carbonate by hydrothermal exchange. Nature 247: 220, 1974

Rosa F, Roberts AB, Danielpour D, Dart LL, Sporn MB, Dawid IB. Mesoderm induction in amphibians: the role of TGF-ß2-like factors Science 239: 783, 1988

Sampath TK, Reddi AH. Dissociative extraction and reconstitution of extracellular matrix components involved in local bone differentiation. Proc Natl Acad Sci USA 78: 7599, 1981

Sampath TK, Reddi AH. Homology of bone-inductive proteins from human, monkey, bovine and rat extracellular matrix. Proc Natl Acad Sci USA 80: 6591, 1983

Sampath TK, Reddi AH. Distribution of bone inductive proteins in mineralized and demineralized extracellular matrix. Biochem Biophys Res Commun 119: 949, 1984a

Sampath TK, Reddi AH. Importance of geometry of the extracellular matrix in endochondral bone differentiation. J Cell Biol 98: 2192, 1984b

Sampath TK, Muthukumaran N, Reddi AH. Isolation of osteogenin, an extracellular matrix-associated, bone inductive protein, by heparin affinity chromatography. Proc Natl Acad Sci USA 84: 7109, 1987

Sampath TK, Coughlin JE, Whetstone RM, Banach D, Corbett C, Ridge RJ, Ozkaynak E, Oppermann H, Rueger DC. Bovine osteogenic protein is composed of dimers of OP-1 and BMP-2A, two members of the transforming growth factor ß superfamily. J Biol Chem 265: 13198, 1990

Sampath TK, Maliakal JC, Hauschka PV, Jones WK, Sasak A, Tucker RF, White KH, Coughlin JE, Tucker MM, Pang RHL, Corbett C, Ozkaynak E, Oppermann E, Rueger DC. Recombinant human osteogenic protein-1 (hOP-1) induces new bone formation in vivo with a specific activity comparable with natural bovine osteogenic protein and stimulates osteoblast proliferation and differentiation

in vivo. J Biol Chem 267: 20352, 1992

Sato K, Urist MR. Induced regeneration of calvaria by bone morphogenetic protein (BMP) in dogs. Clin Orthop 197: 301, 1985

Schmitz JP, Hollinger JO. The critical size defect as an experimental model for craniomandibulofacial nonunions. Clin Orthop 205: 299, 1986

Schmitz JP, Hollinger JO. A preliminary study of the osteogenic potential of a biodegradable alloplastic-osteoinductive alloimplant. Clin Orthop 237: 245, 1988

Schnitzler CM, Pettifor JM, Mesquita JM, Bird MDT, Schaid E, Smyth AE. Histomorphometry of iliac crest bone in 346 normal black and white South African adults. Bone and Mineral 10: 183, 1990

Schnitzler CM, Ripamonti U, Mesquita JM. Histomorphometry of iliac crest trabecular bone in adult male baboons in captivity. Calcif Tissue Int 52: 447, 1993

Seyedin SM, Segarini PR, Rosen DM, Thompson AY, Bentz H, Graycar J. Cartilage-inducing factor-β is an unique

protein structurally and functionally related to transforming growth factor-ß. J Biol Chem 262: 1946, 1987

Simmons DJ. Fracture healing. In: Fundamental Clinical and Bone Physiology. Urist MR, ed. Philadelphia: Lippincott, p 283, 1980

Solheim E, Pinholt EM, Bang G, Sudman E. Regeneration of calvarial defects by a composite of bioerodible polyorthoester and demineralized bone in rats. J Neurosurg 76: 275, 1992

Spector M, Flemming WR, Kreutner A, Sauer BW. Bone growth into porous high-density polyethylene. J Biomed Mater Res, Symp No 7: 595, 1976

Sporn MB, Roberts AB. The transforming growth factor-ßs. In: Peptide Growth Factors and their Receptors. Sporn MB, Roberts AB, Eds. Berlin: Springer-Verlag, p 419, 1990

Statistical Analysis System. Statistics Version, 5th ed. Cary, North Carolina: SAS Institute, p 433, 1985

Takaoka K, Nakahara H, Yoshikawa H, Masuhara K, Tsuda

Urist MR. Surface-decalcified allogeneic bone (SDAB) implants. A preliminary report of 10 cases and 25 comparable operations with undecalcified lyophilized bone implants. Clin Orthop 56: 37, 1968

T, Ono K. Ectopic bone induction on and in porous hydroxyapatite combined with collagen and bone morphogenetic protein. Clin Orthop 234: 250, 1988

Tencer AF, Shors EC, Woodard PL, Holmes RE. Mechanical and biological properties of a porous polymer-coated coralline ceramics. In: Handbook of Bioactive Ceramics. Vol. 2: Calcium Phosphate and Hydroxylapatite Ceramics. Yamamuro T, Wilson-Hench J, Hench LL, eds. Boca Raton: CRC Press, p 209, 1990

Thompson TJ, Owens PDA, Wilson DJ. Intramembranous osteogenesis and angiogenesis in the chick embryo. J Anat 166: 55, 1989

Trueta J. The role of the vessels in osteogenesis. J Bone Joint Surg 45B: 402, 1963

Takagi K, Urist MR. The reaction of the dura to bone morphogenetic protein (BMP) in repair of skull defects. Ann Surg 196: 100, 1982

Urist MR. Bone: Formation by autoinduction. Science 159: 893, 1965

Urist MR. Osteoinduction in undemineralized bone

implants modified by chemical inhibitors of endogenous matrix enzymes. Clin Ortop 87: 132, 1972

Urist MR. Bone transplants and implants. In: Fundamental and Clinical Bone Physiology. Urist MR, ed. Philadelphia: JB Lippincott, p 331: 1980

Urist MR. Chemosterilized antigen-extracted surface-demineralized autolysed allogeneic (AAA) bone for arthrodesis. In: Osteochondral Allografts: Biology, Banking and Clinical Applications. Friedlaender GE, Mankin, HJ, Sell KW, eds. Boston: Little, Brown and Company, p 193, 1983

Urist MR. Bone morphogenetic protein, bone regeneration, heterotopic ossification and the bone-bone marrow consortium. In: Bone and Mineral Research. Vol. 6. Peck WA, ed. Amsterdam: Elsevier Science Publisher, p 27, 1989

Urist MR. Bone morphogenetic protein. In: Bone Grafts & Bone Substitutes. Habal MB, Reddi AH, eds. Philadelphia: WB Saunders, p 70, 1992

Urist MR, McLean FC. Recent advances in physiology of bone. J Bone Joint Surg 45A: 1304, 1963

implants modified by chemical inhibitors of endogenous matrix enzymes. Clin Ortop 87: 132, 1972

Urist MR. Bone transplants and implants. In: Fundamental and Clinical Bone Physiology. Urist MR, ed. Philadelphia: JB Lippincott, p 331: 1980

Urist MR. Chemosterilized antigen-extracted surface-demineralized autolysed allogeneic (AAA) bone for arthrodesis. In: Osteochondral Allografts: Biology, Banking and Clinical Applications. Friedlaender GE, Mankin, HJ, Sell KW, eds. Boston: Little, Brown and Company, p 193, 1983

Urist MR. Bone morphogenetic protein, bone regeneration, heterotopic ossification and the bone-bone marrow consortium. In: Bone and Mineral Research. Vol. 6. Peck WA, ed. Amsterdam: Elsevier Science Publisher, p 27, 1989

Urist MR. Bone morphogenetic protein. In: Bone Grafts & Bone Substitutes. Habal MB, Reddi AH, eds. Philadelphia: WB Saunders, p 70, 1992

Urist MR, McLean FC. Recent advances in physiology of bone. J Bone Joint Surg 45A: 1304, 1963

Urist MR, Strates BS. Bone morphogenetic protein. J Dent Res (suppl 6) 50: 1392, 1971

Urist MR, Iwata H. Preservation and biodegradation of the morphogenetic property of bone matrix. J Theor Biol 38: 155, 1973

Urist MR, Dawson E. Intertransverse process fusion with the aid of chemosterilized autolysed antigen-extracted allogeneic (AAA) bone. Clin Orthop 154: 97, 1981

Urist MR, Mazet R, McLean FC. The pathogenesis and treatment of delayed union and non-union: A survey of 85 ununited fractures of the shaft of the tibia ans 100 control cases with similar injuries. J Bone Joint Surg 36A: 931, 1954

Urist MR, Silverman BF, Buring K, Dubuc FL, Rosenberg JM. The bone induction principle. Clin Orthop 53: 243, 1967

Urist MR, Dowell TA, hay PH, Strates BS. Inductive substrates for bone formation. Clin Orthop 59: 59, 1968

Urist MR, Hay PH, Dubuc F, Buring K. Osteogenetic

competence. Clin Orthop 64: 194, 1969

Urist MR, Jurist JM, Dubuc FL, Strates BS. Quantitation of new bone formation in intramuscular implants of bone matrix in rabbits. Clin Orthop 68: 279, 1970

Urist MR, Iwata H, Strates BS. Bone morphogenetic protein and proteinase in the guinea pig. Clin Orthop 85: 275, 1972

Urist MR, Iwata H, Boyd S, Ceccotti PL. Observations implicating an extracellular enzymic mechanism of control of bone morphogenesis. J Histochem Cytochem 22: 88, 1974

Urist MR, Mikulski AM, Boyd SD. A chemosterilized antigen-extracted autodigested alloimplant for bone banks. Arch Surg 110: 416, 1975

Urist MR, Mikulski A, Lietze A. Solubilized and insolubilized bone morphogenetic protein. Proc Natl Acad Sci USA 76: 1828, 1979

Urist MR, Lietze A, Mizutani H, Takagi K, Triffitt JT, Amstutz J, DeLange R, Termine J, Finerman GAM. A bovine low molecular weight bone morphogenetic protein (BMP)

fraction. Clin Orthop 162: 219, 1982

Urist, MR, DeLange RJ, Finerman GAM. Bone cell differentiation and growth factors: Induced activity of chondro-osteogenetic DNA. Science 220: 680, 1983a

Urist MR, Sato K, Brownell AG, Malinin TI, Lietze A, Huo Y-K, Prolo DT, Oklund S, Finerman GAM, DeLange RJ. Human bone morphogenetic protein (hBMP). Proc Soc Exp Biol Med 173: 194, 1983b

Urist MR, Huo Y-K, Brownell AG, Hohl WM, Buyske J, Lietze A, Tempst P, Hunkapiller M, DeLange RJ. Purification of bone morphogenetic protein by hydroxyapatite chromatography. Proc Natl Acad Sci USA 81: 371, 1984a

Urist MR, Lietze A, Dawson E. ß-tricalcium phosphate delivery system for bone morphogenetic protein. Clin Orthop 187: 277, 1984b

Urist MR, Nilsson O, Rasmussen J, Hirota W, Lovell T, Schmalzreid T, Finerman GAM. Bone regeneration under the influence of a bone morphogenetic protein (BMP) beta tricalcium phosphate (TCP) composite in skull trephine defects in dogs. Clin Orthop 214: 295, 1987a

Urist MR, Chang JJ, Lietze A, Huo YK, Brownell AG, DeLange RJ. Preparation and bioassay of bone morphogenetic protein and polypeptide fragments. Methods Enzymol 146: 294, 1987b

Vandersteenhoven JJ, Spector M. Osteoinduction within porous polysulfone implants at extraosseous sites using demineralized allogeneic bone matrix. J Biomed Mater Res 17: 793, 1983

van Eeden S, Ripamonti U. Bone differentiation in porous hydroxyapatite in baboons is regulated by the geometry of the substratum: Implications for reconstructive craniofacial surgery. Plast Reconstr Surg 1993, in press

Vargervik K. Critical sites for new bone formation. In: Bone Grafts & Bone Substitutes. Habal MB, Reddi AH, eds. Philadelphia: WB Saunders, p 112, 1992

Vlodavsky I, Folkman J, Sullivan R, Fridman R, Ishai-Michaeli R, Sasse J, Klagsbrun M. Endothelial cell-derived basic fibroblast growth factor: Synthesis and deposition into subendothelial extracellular matrix. Proc Natl Acad Sci USA 84: 2292, 1987

Vukicevic S, Luyten P, Kleinman HK, Reddi AH. Differentiation of canalicular cell processes in bone cells by basement membrane matrix components: Regulation by discrete domains of laminin. Cell 63: 437, 1990

Vukicevic S, Paralkar WM, Reddi AH. Extracellular matrix and bone morphogenetic proteins in cartilage and bone development and repair. Adv Mol Cell Biol 6: 207, 1993

Wang EA, Rosen V, Cordes P, Hewick RM, Kriz MJ, Luxenberg DP, Sibley BS, Wozney JM. Purification and characterization of other distinct bone-inducing factors. Proc Natl Acad Sci USA 85: 9484, 1988

Wang EA, Rosen V, D'Alessandro JS, Bauduy M, Cordes P, Harada T, Israel D, Hewick RM, Kerns K, LaPan P, Luxenberg DP, McQuaid D, Moutsatsos I, Nove J, Wozney JM. Recombinant human bone morphogenetic protein induces bone formation. Proc Natl Acad Sci USA 87: 2220, 1990

Weeks DL, Melton DA. A maternal mRNA localized to the vegetal hemisphere in Xenopus eggs codes for a growth

factor related to TGF-ß. Cell 51: 861, 1987

Weiss RE, Reddi AH. Synthesis and localization of fibronectin during collagenous matrix mesenchymal cell interaction and differentiation of cartilage and bone *in vivo*. Proc Natl Acad Sci USA 77: 2074, 1980

Weiss RE, Reddi AH. Appearance of fibronectin during the differentiation of cartilage, bone and bone marrow. J Cell Biol 88: 630, 1981a

Weiss RE, Reddi AH. Role of fibronectin in collagenous matrix-induced mesenchymal cell proliferation and differentiation *in vivo*. Exp Cell Res 133. 247, 1981b

Wells JW. Scleractinia. In: Treatise on Invertebrate Paleontology. Moore RC, ed. Kansas City: University of Kansas Press, p 328, 1956

Wharton KA, Thomsen GH, Gelbart WM. Drosophila 60A gene, another transforming growth factor ß family member, is closely related to human bone morphogenetic proteins. Proc Natl Acad Sci USA 88: 9214, 1991

White E, Weber JN, Roy DM, Owen EL Replamineform

porous biomaterials for hard tissue implant applications. J Biomed Mater Res 9: 23, 1975

White E, Shors EC. Biomaterial aspects of Interpore-200 porous hydroxyapatite. Dent Clin North Am 30: 49, 1986

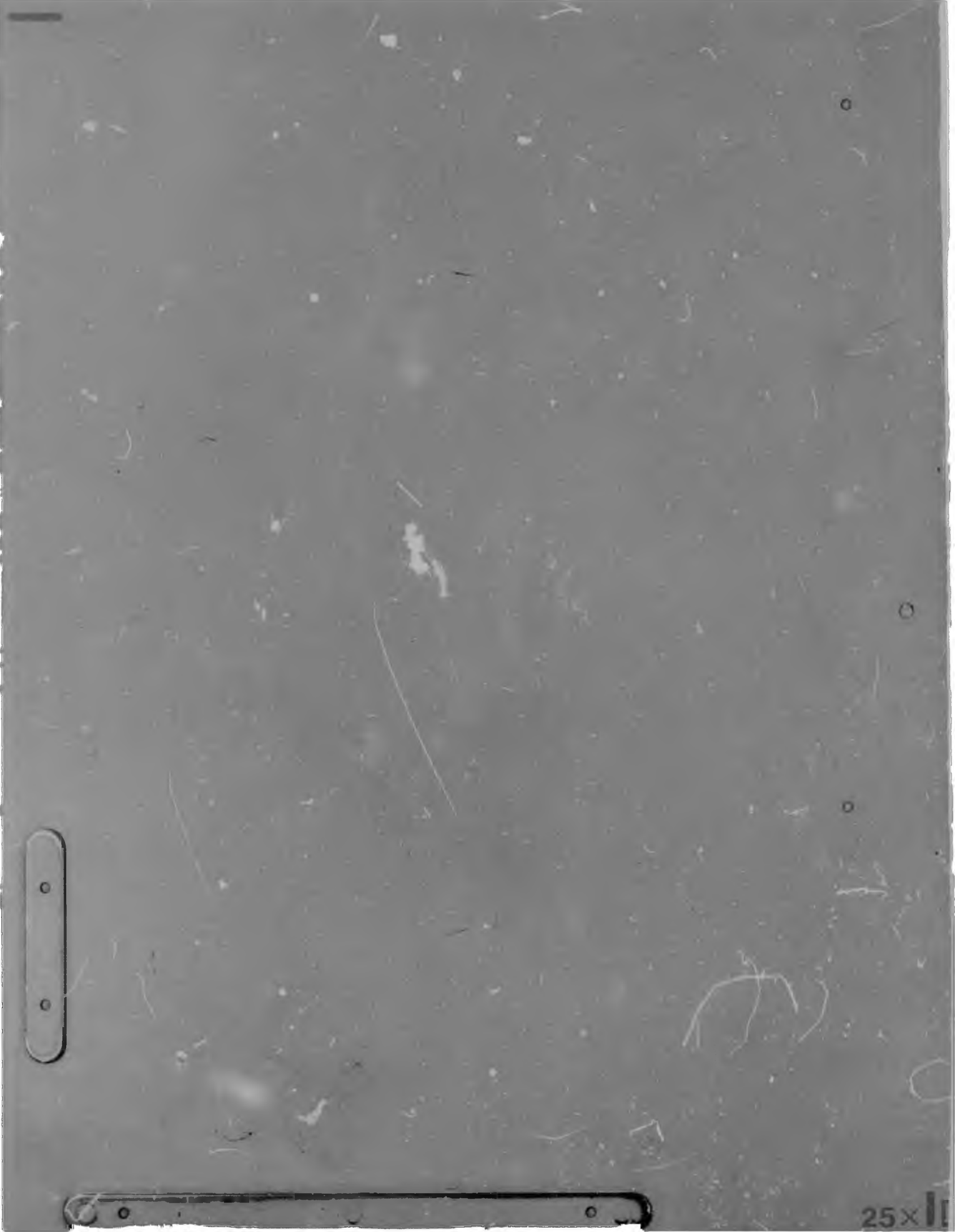
Wlodarski KH, Reddi AH. Alkaline phosphatase as a marker of osteoinductive cells. Calcif Tissue Int 38: 382, 1986

Wozney JM, Rosen V, Celeste AJ, Mitsock LM, Whitters, MJ, Kriz RW, Hewick RM, Wang EA. Novel regulators of bone formation: Molecular clones and activities. Science 242: 1528, 1988

Wu C-H, Hara K, Ozawa H. Enhanced osteoinduction by intramuscular grafting of BMP-ß-TCP compound pellets into murine models. Arch Histol Cytol 55: 97, 1992

Young MH. The repair of experimental defects in rabbit skulls. Observations after implantation with decalcified, deproteinised and deep frozen homogenous whole bone. J Bone Joint Surg 46B: 329, 1964





Author Ripamount U
Name of thesis The Generation of bone in Nonhuman Primates. Experimental studies on the Baboon (Papio Ursinus) 1993

PUBLISHER:
University of the Witwatersrand, Johannesburg
©2013

LEGAL NOTICES:

Copyright Notice: All materials on the University of the Witwatersrand, Johannesburg Library website are protected by South African copyright law and may not be distributed, transmitted, displayed, or otherwise published in any format, without the prior written permission of the copyright owner.

Disclaimer and Terms of Use: Provided that you maintain all copyright and other notices contained therein, you may download material (one machine readable copy and one print copy per page) for your personal and/or educational non-commercial use only.

The University of the Witwatersrand, Johannesburg, is not responsible for any errors or omissions and excludes any and all liability for any errors in or omissions from the information on the Library website.